Modelling the subglacial drainage system of Petermann Glacier, north-west Greenland

Grant Macdonald

MPhil Polar Studies
June 2013

Scott Polar Research Institute
University of Cambridge

UNIVERSITY OF CAMBRIDGE

Abstract

Studies suggest that much of the Greenland Ice Sheet is accelerating as temperatures increase. Increased temperatures can raise the pressure in the subglacial drainage system as meltwater input increases and the system fails to efficiently evacuate it. Some studies suggest that increased temperatures and meltwater input will slow glaciers down by causing earlier channelization, allowing stable conduit expansion and efficient drainage of input. However, studies also suggest that even channelized systems fail to evacuate meltwater when input is rapid. This study's modelling of the subglacial drainage system of Petermann Glacier suggests that conduits cannot quickly accommodate rapid changes in meltwater input, such as from lake drainages or warm phases, causing subglacial water pressure to reach ice overburden pressure for as long as 5 days. High ice thickness at Petermann Glacier causes rapid conduit closure, making the sustaining of a sustainable conduit system especially difficult. Along with other research, this study suggests that the subglacial drainage system of Petermann Glacier is key to its dynamics. Lake drainages play a large role in perturbing the system, but their role is limited by the short melt season which means many lakes freeze-over before draining. Warming is expected to cause lake drainage at higher elevations, causing more frequent basal pressure spikes and over a larger area. Petermann Glacier is therefore expected to contribute more to sea-level as temperatures increase.

Acknowledgements

Firstly, I must thank Dr Neil Arnold, my supervisor, for his kind support at all stages of the project. Without my regular visits to his office, and his quick feedback on drafts, completion of this study would not have been possible. I also thank Dr Alison Banwell for introducing me to the SWMM model and for e-mail support from Chicago. I thank Dr Steve Palmer for processing the newly-released bed DEM for me.

Again, I thank Dr Pete Nienow and his Edinburgh disciples for their support that got me here and introducing me to the excitement and beauty of glaciology,

I thank my fellow MPhils: TJ, Mia, Johnny, Ed and Dave for making coming into SPRI every morning such a pleasure. The fact my thesis marks the end of my time with them makes hand-in more sad than relieving. I wish them luck and look forward to encountering them in their various exciting new positions. I also specifically thank TJ for help projecting the DEMs and Johnny for creating a map of Greenland.

Of course, I thank my family, whose support got me to Cambridge. I'd like to thank everyone at SPRI for making it such a lovely place to work.

I declare that this thesis is my own work, except where acknowledged. The thesis does not exclude 20 000 words, excluding figures, captions, contents, acknowledgements, abstract, references and appendix.

Grant Macdonald

Table of Contents

Figures

Tables

Equations

After drain, are moulin
Mention two channels in k

Chapter 1: Introduction

1.1 Aims

This project aims to investigate the subglacial hydrology of an outlet glacier in the north west of the Greenland Ice Sheet (GrIS). The results should prove useful for assessing the impact that variations in temperature and meltwater generation will have on Petermann Glacier, as well as other marine-terminating and high-latitude glaciers, particularly in the context of climate change. It will also help inform the discussion on the extent to which subglacial water pressures govern the motion of such marine-terminating and high-latitude glaciers. Specifically, the primary aims are to:

[1.] Assess spatial and temporal variations in the subglacial drainage system in response to changing melt input.

[2.] Evaluate the presence, evolution and implications of supraglacial lakes

[3.]. Assess performance of the model on a high-latitude, marine-terminating glacier with a floating ice tongue.

[4.] Assess the implications of the results for the glacier in the present and future, particularly in relation to dynamics.

To accomplish these aims, the objectives were to:

- Model melting on the surface and subsequent supraglacial routing to depressions that form lakes.
- Model the drainage of the lakes and input after moulin formation to produce hydrographs for the subglacial system.
- Model the subglacial drainage system configuration and analyse how subglacial water pressure, cross-sectional area (CSA) and discharge of conduits varies with meltwater input from the surface based on modelling of the 2004 melt season.
- Model supraglacial lake area and depth based on satellite imagery and compare with model results based on routing over the surface.

The remainder of this chapter will justify and provide the context for the study. In chapter 2 the study site and data used will be discussed. Chapter 3 will cover the methods. Chapter 4 will present the results gathered. In chapter 5 the results of the study and their implications for the subglacial hydrology and dynamics will be discussed. Chapter 6 will present the conclusions.

1.2 Climate Change and Greenland

1.2.1 Global significance

The IPCC (IPCC, 2007) predicts that global temperature will rise by at least 1.8°C by the end of the century. This is expected to be accompanied by an associated rise in sea-level of up to 0.59m by 2099, due to runoff from melting glaciers, ice-caps and the GrIS and from thermal expansion of sea water. Many (e.g. Parizek and Alley, 2004) consider this estimate conservative, particularly because it does not account for ice dynamic feedback effects, which play a critical role in the ablation of glaciers (e.g. Zwally et al, 2002). This means that the potential sea-level contribution from the poles was not properly accounted for.
Understanding the potential contribution of the GrIS is essential for constraining predictions, as the GrIS stores 7.3m worth of potential sea-level (Bamber et al., 2001), compared to ~0.5m from melting all non-ice sheet glaciers and ice caps (Church et al., 2001). Sea-level rise could have devastating effects for millions of people due to lost land and increased risk from tidal surges, highlighting the importance of understanding the factors governing sea-level rise (IPCC, 2007).

1.2.2 Greenland climatology

The GrIS experiences significant interannual climatic variability (Hanna et al., 2008). This is largely due to the island's climate's relationship with the North Atlantic Oscillation (NAO) (Hall et al., 2008). A positive NAO index is associated with colder on the GrIS and a negative index is associated with warmer winters. Studies show that the NAO exhibits a significant correlation with melt extent on

the GrIS (Mote, 1998; Johannessen et al., 2005; Fettweis et al., 2011) and regional scale relationships between NAO and precipitation have been shown, Fettweis (2007) showing a negative NAO index tends to be associated with greater precipitation in the south-west GrIS due to the presence of strong southerly moisture-bearing winds.

Although there is significant interannual climatic variability, this is superimposed on an overall trend of increasing temperatures (IPCC, 2007). Indeed, the GrIS has been subject to an even greater increase than the global average in the context of climate change, with the 2005-2007 average annual temperature anomaly more than double the global value, at 1.5°C compared to 0.7°C (compared to the reference temperature of 1951-1980) (AMAP, 2009).

Mass gain at the interior of the GrIS through accumulation from snowfall (Johannessen et al., 2005) is being more than offset by an approximately equal loss between meltwater runoff (Hanna et al., 2008; van den Broeke et al., 2009) and accelerated glacier flow (Rignot and Kanagaratnam, 2006). Observations suggest that mass loss is rapidly increasing, with estimates for 2010-2011 at $430Gta^{-1}$ (Box et al., 2011), 150% of a 2007-2009 estimate of $286Gta^{-1}$ (Velicogna, 2009) and 314% of a 2002-2003 estimate of $137Gta^{-1}$ (Velicogna and Wahr, 2006). This is associated with an estimated contribution to sea-level rise of $0.59\pm0.200mma^{-1}$ over the period 1992-2012 (Shepherd et al., 2012). Rignot et al. (2011) found that if acceleration of ice sheet loss is maintained in the coming decades, cumulative ice sheet loss will raise global sea-level by 15±2cm by 2050. With surface melt rates predicted to double this century (Mernild et al., 2010) and dynamical perturbations also contributing to mass loss, ice sheets are on course to surpass the contribution of mountain glaciers and ice caps to sea-level within several decades, much sooner than previously thought (IPCC, 2007; Rignot et al., 2011)). The acceleration of mass loss from the GrIS and Antarctic Ice Sheets between 1993 and 2011 ($36\pm2Gta^{-2}$) was three times larger than for mountain glaciers and ice caps ($12\pm6Gta^{-2}$) (Rignot et al., 2011). In the longer term, Parizek and Alley (2004) predict the GrIS to contribute up to 3.60m to sea-level by 2500.

1.3 Subglacial hydrology

As the previous section showed, melting is increasing on the GrIS. This means that more water will be entering the subglacial hydrological system and it will be expanding its area. To understand the behaviour of glaciers, it is fundamental to understand the subglacial hydrology.

Early in the melt season, when meltwater input is low, an inefficient, distributed subglacial drainage system is thought to exist. This exists following a winter of very low volumes of meltwater leading to the system almost closing down through creep closure (Nye, 1953). Distributed systems are thought to exist in the configuration of a thin, distributed film of water (Weertman, 1972; Walder and Hallet, 1979) or more likely in a linked-cavity network (Walder, 1986; Kamb, 1987). A linked-cavity system is favoured by rapid sliding and high bed roughness. The water flowing through the 'links' between the cavities dissipates heat that preferentially enlarges the links (Walder, 1986). Importantly, an inefficient system exhibits a positive relationship between discharge and hydraulic pressure, because water flows over a larger area, spreading frictional heat over a wider area, reducing the capacity of the system to accommodate increased discharge by wall-melting, thus increasing hydraulic head and pressure (Rothlisberger, 1972).

During the melt season, the distributed, subglacial system adjusts from a configuration of multiple links and a large total CSA to an efficient system with fewer links and a smaller CSA (Nienow et al., 1998). As discharge increases in the small conduits, the walls melt and expansion takes place due to frictional heating of the flowing water (Mair et al., 2002; Colgan et al., 2011). Particular conduits grow preferentially, as viscous heat dissipation and thus melting is greater in larger conduits with higher discharge, which further increases their size and redirects discharge there at the expense of smaller conduits (Shreve, 1972). This encourages the development of an aboresscent system, with tributary conduits flowing into successively larger primary conduits flowing at

lower pressure. Once an efficient, channelized system is established, continued high discharge maintains wall-melting by heat dissipation, compensating for inward creep motion in the surrounding ice. In contrast to an inefficient, distributed system, efficient, channelized systems exhibit an inverse relationship between discharge and subglacial water pressure, as higher discharge causes more heat dissipation and wall melting which allows water to be evacuated more quickly, reducing pressure (Rothlisberger, 1972; Iken et al., 1983). As discharge in the channelized system drops below a certain level towards the end of the melt season, channels cannot be kept open and the system contracts and reverts to an inefficient system (Schoof, 2010).

It is important, however, not to rely on a crude binary categorisation of steady-state drainage systems. The system is not uniform and both types may exist simultaneously in different parts of glaciers. For example, Hubbard et al. (1995) observed a 'variable pressure axis' aligned approximately parallel to the direction of ice flow, its orientation consistent with the location of a hydraulically efficient subglacial channel at its centre. A hydraulically-linked, distributed system was observed beneath adjacent parts of the bed. During high pressures in the early-afternoon, water was driven out of the channel into the surrounding area and returned overnight. Additionally, the assumed steady-state conditions on which the stable discharge-pressure relationships are based are unlikely to exist in reality (Schoof, 2010; Bartholomew et al., 2011a). Indeed Rothlisberger (1972) claimed that the actual channel pressure would fluctuate about the value calculated under steady-state conditions. This highlights the complexity of the system and need to better understand it.

1.3.1. Subglacial routing

Water flow along the base of a glacier can be determined by water pressure potential:

$$\Phi_b = \rho_w g Z_b + k \rho_i g (Z_s - Z_b)$$

(Equation 1)

Where ρ_W is water density (1000kgm^{-3}); ρ_i is ice density (917kgm^{-3}); g is acceleration due to gravity (9.81ms^{-1}); Z_b is the bed elevation (m); Z_S is surface elevation (m); k is a factor indicating the subglacial water pressure, ranging from 0 (subglacial drainage system at atmospheric pressure) to 1 (subglacial drainage system at ice overburden pressure).

Ice overburden pressure can play a significant role in affecting subglacial drainage, with water at the base potentially almost matching overburden pressure, i.e. exhibiting a K-value close to 1 (Colgan et al. 2011). While water ultimately flows downglacier, water drains perpendicular to the equipotential of the hydraulic potential, and subglacial passages will follow the steepest rate of decrease of hydraulic potential on the bed. The equipotential will slope downward in an upglacier direction, with a gradient ~11 times that of the surface. This means that water can flow upglacier into local depressions (Shreve, 1972; Sharp, 2005). Studies have shown (e.g. Sharp et al., 1993; Flowers and Clarke, 1999; Rippin et al., 2003) that a decrease in basal water pressure increases the significance of basal topography in water routing, resulting in a less efficient, more dispersed drainage system.

K-values have been seen to vary significantly both spatially and temporally. Variation in k-value has been shown to substantially affect the extent and configuration of drainage basins by affecting the flow of water. Values as low as 0.5 have been calculated for summer conditions (e.g. Flowers et al., 1999; Rippin et al., 2003; Willis et al., 2009), while Thomsen and Olesen (1990) measured values between 0.79 and 1.05 within 10km of the ice margin. K-values close to 1 are supported by modelling (Colgan et al., 2011) and observations of hydraulic head close to the ice surface (Cowton et al., 2013).

Rothlisberger (1972) assumed water is routed at the base in channels at the base in semi-circular ('R-') channels, but alternatives have been proposed. Hooke et al. (1984), for example, proposed broad ('H-') channels, which allow application

of Glen's flow law of deformation with reasonable viscosity parameter values. Analysis based on Shreve (1974) does not account for the different subglacial physics associated with R-, N- or H- channels as proposed by Walder and Fowler (1994). It also does not account for the likely non-uniform distribution of water pressure (Flowers et al, 2003; Hubbard et al., 1995) or feedbacks within the system, such as with dynamics. However, Shreve's (1974) analysis remains fundamental to understanding subglacial routing (Schoof 2010; Banwell, 2012).

1.4 Subglacial Hydrology in Greenland

Few observational studies of subglacial hydrology on the GrIS currently exist, and those that do are concentrated in west Greenland. There are not yet any direct observations of the subglacial drainage system (Cowton et al., 2013). However, measurements of hydrological parameters in proglacial stream outlets at Leverett Glacier, a land-terminating glacier around 67°N have provided useful information on the hydrology of the GrIS's margins.

Observations of GrIS hydrology suggest that the drainage system and its morphological evolution are analogous to Alpine hydrology (Bartholomew et al., 2011a; Chandler et al., 2013; Cowton et al., 2013). Bartholomew et al. (2011a) noted four distinct pulses of water superimposed onto the rising limb of the seasonal hydrograph. The beginning of the season was characterised by a small amount of runoff and small amount of proglacial output with high electrical conductivity, suggesting leakage of basal meltwater from an inefficient drainage system remaining from winter (Collins, 1979; Skidmore and Sharp, 1999). High discharge from the base lagged above-zero temperatures at the surface by ~20 days, due to observed ponding and refreezing of initial meltwater (Pfeffer et al., 1991). Therefore, the first pulse is interpreted as being the establishment of a hydrological connection between the surface and base at lower elevations, delivering significant meltwater to the base for the first time. Solute measurements (Bartholomew et al., 2011a) and ice velocity measurements (Bartholomew et al., 2011b) suggest that this input was into an inefficient drainage system. This early period is characterised by high englacial water

levels as the system lacks the capacity to evacuate the rapidly rising discharge, with moulins filling up almost to the surface level (Fountain, 1993; Rothlisberger and Lang, 1987; Cowton et al., 2013).

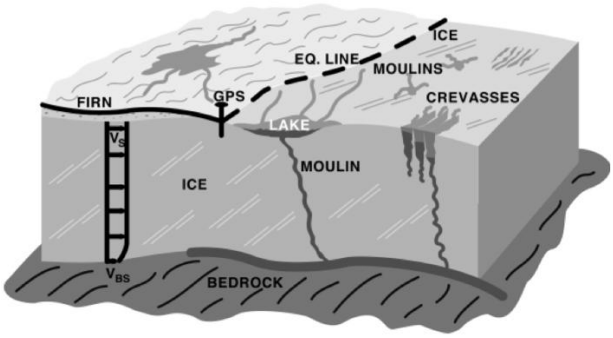

Figure 1.1: *A schematic of glaciological features, including meltwater sources and potential routes to the base (Zwally et al., 2002)*

Only one of the three subsequent bulk discharge pulses observed by Bartholomew et al. (2011a) are associated with heightened temperatures. Instead, pulses 2 and 4, superimposed on the rising limb of upglacier expansion of hydrological connectivity between the glacier's surface and base. The upglacier expansion of hydrological connectivity is as observed in alpine glaciers and results in the upglacial expansion of subglacial channelization (Nienow et al., 1998; Bartholomew et al., 2011a). Cowton et al.'s (2013) observations show that channelization does not occur immediately, with melt cessation leading to a draining of high englacial water levels over two days, and another four days of melting raised levels again before channelization occurred. Additionally, observations suggest two stages to channelization. At first (early June), tracing results suggest that while some water was rapidly drained down a preferred pathway, some was diverted down anabranching slower routes (Seaberg et al., 1988), indicating structural inefficiencies in the early summer channelized drainage. During this period, for 2-4 weeks following channel formation, water continued to back-up during high input, as observed by high englacial water levels. This likely represents a period of continual readjustment of channel CSA to rising melt input as bulk discharge continued to increase. Therefore, Cowton et al. (2013) assert that drainage morphology continues to significantly evolve

after initial channel formation, and influence the relationship between subglacial discharge and pressure. By the time the rise in bulk discharge slowed down, in early July, the system reached a relatively stable configuration, at least in the lower ~6.6km, and englacial water level remained stable and low as water was efficiently evacuated (Cowton et al., 2013). For the system to return to a distributed condition, it is proposed that discharge must drop below a critical level, lower than the critical level for initiating channelization (Schoof, 2010).

Modelling work by Schoof (2010) on the GrIS suggested that discharge and pressure re-couple in a channelized drainage system under conditions of rapid melt input. Conduit sizes adjust to meltwater input slowly over several days, meaning that the system does not have the capacity to deal with sudden and rapid increases in discharge under a steady-state, and must increase the hydraulic gradient, which requires raised basal pressure. This supports Bartholomew et al.'s (2011a) observations and further highlights the significance of rapid meltwater delivery on the subglacial system.

This section has shown that the subglacial hydrology of the GrIS's outlet glaciers behaves in a similar manner to Alpine glaciers. This includes the exhibition of high spatial and temporal variability, and high pressures even after channelization. Such behaviour highlights the need for further study and suggests the suitability of applying a model originally developed for Alpine glaciers, as in the present study, to the GrIS margin. Furthermore, the importance of upglacier expansion of hydrological connectivity in forcing expansion of channelization emphasises the significance of supraglacial lakes, which facilitate the creation of the connection and the discharge pulses that promote channel extension.

1.5 Supraglacial lake evolution

Supraglacial lakes play a fundamental role in subglacial hydrology, by storing the large quantities of water necessary to initiate hydrofracture to the base of thick ice, creating a hydrological connection between the surface and base, and to rapidly deliver melt that can pressurize and channelize the system (Bartholomew et al., 2010; 2011a; Shepherd et al., 2009). Hence, to understand subglacial hydrology it is essential to understand the formation and evolution of supraglacial lakes.

Surface topography predominantly determines the location and geometry of supraglacial lake formation. This is indicated by observations of lakes forming in the same spots interannually (Thomsen et al., 1988; Echelmeyer et al., 1991) and images showing them not advecting with ice-flow over a ten-year period (Selmes et al., 2011). Lakes form in surface depressions and especially in areas with backslopes (Nienow and Hubbard, 2005), which are less likely to occur in steep areas. This is likely responsible for the dearth of lakes in the especially steep south-east GrIS, with a strong negative correlation existing between average ice surface slope and percentage lake area (Sundal et al., 2009). It follows that lake formation is also controlled the basal topography and ice thickness, which predominantly determine the surface topography (Lampkin and Vanderberg, 2011). Lampkin and Vanderberg (2011) suggest that a window of basal roughness components of wavelengths between 3 and 8 times the ice thickness are transferred to the surface, with the transfer of wavelengths less than 3 and more than 8 times ice thickness being attenuated to a level of negligible impact. The 10-11km frequency component dominates over thicker ice (1200-1400m) and 5-6km over thinner ice (500-700m). Variations in drag can also affect transfer of undulations to the surface (Gudmundsson, 2003). Additionally, bed topography influences the stress regime, with lakes more likely to form in compressive stress regimes (Krawczynski et al., 2009). Compressive stress regimes tend to be present in depressions that promote ponding and deter crevasse formation (and thus likely drainage) (Catania et al., 2008). Lakes tend

not to form around margins, where heavy crevassing is likely though crevasses may become water-filled (Lampkin, 2011).

Other factors may also influence lake formation. Surface depressions may form due to variations in accumulation, ablation and factors such as wind-blown snow (Smith, 2005). Elevation, latitude and time-of-year are also hugely significant as all affect temperature and thus the availability of water for ponding (McMillan et al., 2007). The higher frequency of lakes in the south-west compared to the north is partly due to higher temperatures at the lower latitude (Sundal et al., 2009).

Following lake formation in spring or summer, depth, area and volume usually increases through the melt season, though maximum depth, area and volume do not necessarily occur on the same day (Box and Ski, 2007). Growth tends to be most marked early in the season and increases as the transition from snow to ice melting occurs (Georgiou et al., 2009). Increased melt as summer progresses is also associated with lake formation at higher elevations as the ablation zone expands towards the interior, McMillan et al. (2007) finding 95% of all lakes to be sited above 750m a.s.l. on July 7th and 95% above 880m a.s.l. on August 1st. Additionally, a positive albedo feedback mechanism with ablation beneath the lake enhances lake expansion. Luthje et al. (2006) modelled enhanced bottom-ablation to be up to 170% compared to bare ice and Tedesco et al. (2012) observed an enhancement of up to 135%. As the lake expands, the area of lower albedo increases, promoting more melt and so forth. While the effect appears to attenuate beyond a depth of 50cm (Luthje et al., 2006), Tedesco et al. (2012) measured a contribution of ~10% of total depth increase from the lower albedo, suggesting it is an important mechanism.

Lakes may expand such that they reach a maximum volume, as constrained by topography, and overflow (Luthje et al., 2006), in some cases cascading into another lake (Banwell et al., 2012). Banwell et al. (2012), in a study of the Paakitsoq region in west Greenland, found that Lake X drained into Lake Ponting

after reaching a maximum depth two days before Lake Y began overflowing into X and onto Ponting.

Alternatively, many lakes completely drain to the base. Drainage is thought to occur through hydrofracture and can rapidly deliver vast quantities of meltwater to the subglacial hydrological system. Das et al. (2008) observed the rapid drainage of a lake in under 2 hours through almost 1km of ice on the GrIS. Hydrofracture occurs from the propagation of a crack on the lake bottom, with van der Veen (2007) suggesting that the growth rate of a fracture is primarily determined by the amount of water flowing into it, as turbulent flow during rapid discharge through the fracture dissipates frictional heat, melting and expanding it and so increasing the drainage rate. This may play an important role in increasing the diameter of the flowpath, after initial drainage along long cracks (Krawczynski et al. (2009), creating moulins that remain open as the entry points to the subglacial system for the remainder of the melt season (Das et al., 2008). Krawczynski et al. (2009) suggest that only lakes ~250-800m across and 2-5m deep contain enough water to propagate a fracture to the base of 1km-thick ice, but ~98% of all ponded water in their study resided in such lakes. Following formation and expansion, drainage events migrate to higher elevations as lakes progressively reach the necessary volume to fracture and drain to the base (McMillan et al., 2007; Das et al., 2008). Some lakes, however, do not reach a high enough volume to drain before melt cessation and temperatures decrease sufficiently for them to freeze over (Johansson et al., 2013).

1.6 Ice dynamics

1.6.1 Hydrological forcing of dynamics

Meltwater at the glacier base has been shown to increase ice velocity, through basal lubrication and hydraulic jacking by increased subglacial water pressure. This has been shown to be important in Alpine glaciers (e.g. Iken and Bindshandler, 1986), the GrIS (e.g. Zwally et al., 2002) and GrIS outlet glaciers

(e.g. Bartholomew et al., 2010). Meltwater lubrication was previously thought to be of little significance on the cold, thick GrIS but Zwally et al. (2002) observed a strong correlation between changes in ice velocity and melt intensity and timing of melt in all years. Bartholomew et al. (2010) found no connection between meltwater production and ice velocity early in the melt season, but after a hydrological connection between the subglacial and supraglacial systems was formed, a 70-200% increase in velocity was measured. However, observations suggest that the capacity for variations in meltwater to influence ice dynamics is limited by the subglacial drainage system's tendency to adapt to high meltwater input by channelizing, thus reversing the relationship between discharge and hydraulic pressure (Rothlisberger, 1972). Van de Wal et al. (2008) observed a strong relationship between ice velocity and meltwater input on a weekly timescale but found no correlation between annual mass balance and annually averaged time scales. Velocities were measured at 50-100% higher than winter levels early in the season, when a distributed subglacial drainage system is thought to have existed, but de-coupling of velocity with meltwater occurred with channelization. Sundal et al. (2011) even suggested that warming and increased meltwater production could lead to lower overall ice velocities. Although they observed higher peak speed-ups in warm years, at 123±8% compared to 104±15% in colder years, the speed-up lasted only ~30 days in warm years compared to ~90 days in cold years. This suggests that increased meltwater supply causes channelization of the subglacial drainage system to occur earlier in the season, therefore decreasing subglacial pressures, increasing the effective pressures of the glacier and reducing velocity. Indeed, Sundal et al. (2011) measured a late-summer speed-up of just 39±14% in warm years compared to 102±8% in cooler years. This suggests a negative feedback cycle between meltwater and subglacial drainage may stabilise or even reduce velocities under high melt conditions, in contrast to the positive feedback cycle described by Zwally et al. (2002) and Parizek and Alley (2004).

However, the pressurization of channelized systems with the perturbation of steady-state conditions by rapid melt pulses, described by Schoof (2010), limits the conclusions that can be drawn from Sundal et al. (2011). Bartholomew et al.

(2010; 2012) observed short-term velocity spikes in late-summer alongside short-term meltwater spikes, suggesting a temporary re-coupling of ice-velocity and meltwater input, in a channelized drainage system. Bartholomew et al. (2012) attempt to reconcile the conflicting observations between papers such as Zwally et al. (2002) or Shepherd et al. (2009) and van de Wal et al. (2008) or Sundal et al. (2011). They suggest that seasonal ice motion is primarily an aggregation of many short-term speed-up events, such as those observed by Shepherd et al. (2009) and Bartholomew et al. (2010), caused by rapid meltwater delivery to the base perturbing the steady-state and increasing basal pressure. This supports observations (van de Wal et al., 2008; Bartholomew et al., 2011a) that it is the rate rather than the volume of meltwater supply that governs velocity. This further highlights the importance of supraglacial lakes in providing a hydrological connection and rapid meltwater delivery to the base.

1.6.2 Complexities of marine-terminating glacier dynamics

Marine-terminating glaciers have exhibited speed-ups over an order of magnitude higher than those observed in land-terminating glaciers (Joughin et al., 2004; Howat et al., 2005; Luckman and Murray, 2006; Rignot and Kanagaratnam, 2006).

The influence of changes in ice-front position is thought to be the source of the large changes in marine-terminating glacier dynamics, as retreat of the terminus leads to ice flow acceleration and causes increased longitudinal stretching (Joughin et al., 2004). This may be enhanced by a positive feedback mechanism of calving and retreat, as stretching enhances crevassing, potentially increasing calving rates (Vieli and Nick, 2011). Loss of ice at the terminus, most commonly through the calving of icebergs or on some glaciers the disintegration of a floating ice-tongue, removes a buttressing force, allowing the glacier to accelerate forward (Joughin et al., 2004; Luckman and Murray, 2005; Thomas et al., 2003). Loss of buttressing appears to have caused observed thinning of 1-15ma^{-1}, extending tens of kilometres inland through longitudinal coupling, steepening the slope and therefore increasing driving stress and ice velocity

(Krabill et al., 2004; Thomas et al., 2003). Ice-front processes seems to dominate the dynamics in many marine-terminating glaciers, with acceleration in spring and summer observed in phase with increased calving, rather than increased meltwater supply (Joughin et al., 2008). Removal of grounded ice at the front may be especially significant. Helheim Glacier was observed to accelerate to produce additional longitudinal and lateral stress gradients to compensate for the loss and restore force balance, propagating inland causing surface draw-down and thinning (Howat et al., 2005; Thomas, 2004). Additionally, thinning at the front may cause ice to move towards flotation as basal pressure reaches the hydrostatic pressure of the overlying ice (Vieli and Nick, 2011; Pfeffer, 2007; Vieli et al. 2000). Furthermore, this reduces friction at the base, increasing motion and drawing more ice downglacier where temperatures are higher at the lower altitude and the ice may be exposed to warm ocean waters. This increases thinning and potentially creating a positive feedback mechanism (Vieli and Nick, 2011), where deeper water may enhance retreat as ice flux increases with water depth (Schoof, 2007; Katz and Worster, 2010).

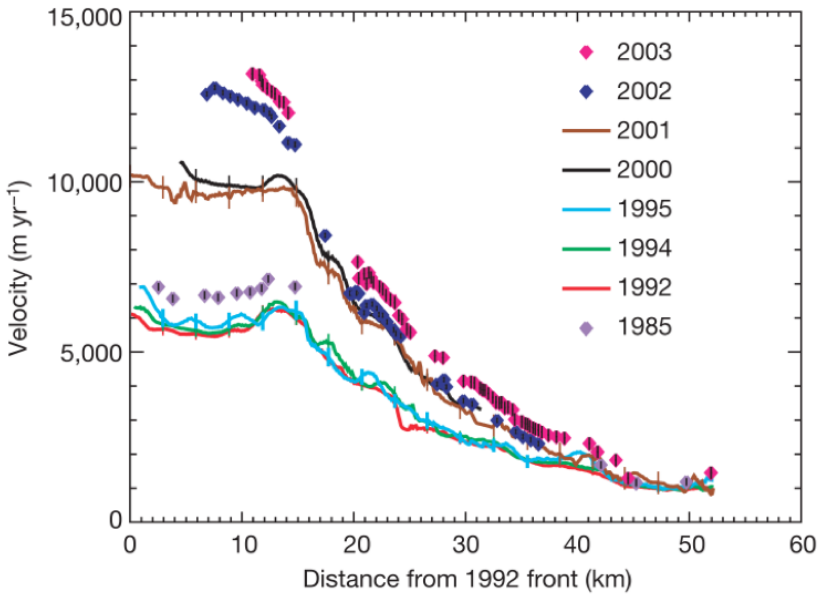

Figure 1.2: *Velocities of features on Jakobshavn Isbreae from Landsat feature-tracked speed measurements. The high velocities at the terminus indicate the importance of the calving front (Joughin et al., 2004)*

Although ice-tongue disintegration or calving may reduce backstress, Moon et al. (2012) found the majority of glaciers with floating ice-tongues to be slower than those with only a calving-front. It appears that the removal of thin, narrow tongues may have little effect upglacier, as the tongue may be too thin to provide significant resistive stress and too narrow to provide lateral resistance, therefore its removal does not significantly alter the buttressing force. Such behaviour was observed on Petermann glacier, with the glacier displaying no significant dynamic response to the catastrophic ice-tongue collapse event in 2010 (Nick et al., 2012).

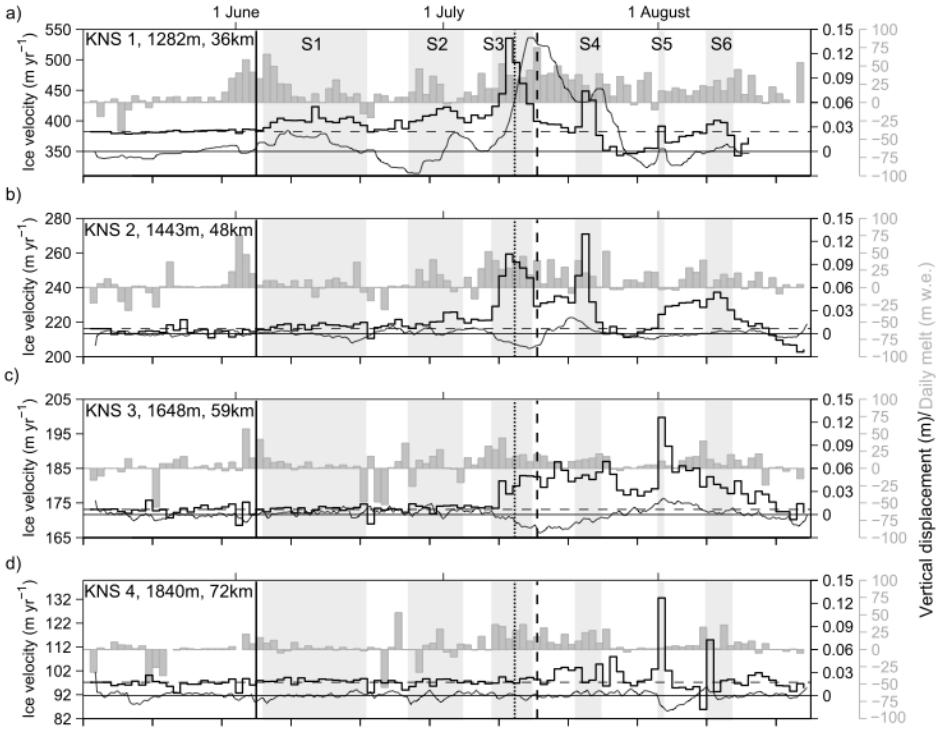

Figure 1.3: *(a-d) Daily horizontal speed (stepped line), 6-hourly vertical displacement (smooth line) and daily water equivalent ice melt (grey bars) at different elevation sites in Sole et al. (2011)'s study of Kangiata Nunata Sermia. Displays synchronous speed-ups at different elevations accompanied by increased melting.*

While the apparent great influence of changes at the ice-front of marine-terminating glaciers may seem to negate the significance of subglacial hydrology, Sole et al. (2011) argue that increased subglacial water pressures caused by meltwater input in fact play a large role, as on land-terminating glaciers. They contest that when measuring upglacier (36 and 72km from the calving-front), maximum horizontal speeds were observed alongside the maximum rate of

uplift, indicative of increased basal water pressure (Iken, 1981; Iken et al., 1983) (fig. 1.3). Additionally, the magnitude of the acceleration did not attenuate upglacier as would be expected if forced from the ice-front and the migration of maximum acceleration upglacier is indicative of the expansion of the ablation zone and hydrological connectivity between the surface and base (Sole et al., 2011). This evidence, and other observations (e.g. Joughin et al., 1996; Anderson et al., 2010; Howat et al., 2010) suggest that marine-terminating glaciers may in fact be predominantly governed by the subglacial drainage system as on land-terminating sections of the GrIS (e.g. Zwally et al., 2002; Bartholomew et al., 2010). However, it seems that the deep and narrow geometry that tends to be characteristic of fast-flowing marine-terminating glaciers limits their seasonal variability compared to land-terminating glaciers, with speed-up events smaller (40% compared to 220% [Sole et al., 2011; Bartholomew et al., 2010]) and slow-downs greater. The geometry reduces the importance of basal friction relative to lateral shear stress, and basal shear heating may produce relatively high basal pressure year-round, reducing the impact of variations in basal pressure and friction (Joughin et al., 2008). There is also evidence that subglacial meltwater can affect changes at the ice-front by forming channels in floating ice, promoting their fracture (Motyka et al., 2003).

1.7 A review of glaciological hydrological modelling

This section will review the most pertinent literature relating to the components of the model used in the study. As well as the subglacial model, the necessary preceding modelling will be reviewed: modelling of melt, surface-routing and drainage.

1.7.1. Surface melting

In the absence of measured ablation data, modelling of the glacial hydrological system requires the modelling of melt. Temperature-index models offer a simple option based on an assumed empirical relationship between air temperature and melt rate. Since their efficacy was demonstrated (Finderwalder and Schunk,

1887), they have been implemented successfully for many glaciers, yielding correlations as high as 0.96 between annual ice ablation and positive air temperature sums (Braithwaite and Olesen, 1989). The ratio of melt to temperature is usually based on a degree-day factor (DDF), calculated by dividing the mean ablation measured in a day by the mean temperature of all recorded above 0°C (Braithwaite, 1995). DDFs may vary spatially and temporally, particularly with elevation (Singh and Kumar, 1996) due to variations in the relative importance of energy components (Ambach, 1988a; 1988b). However, in the absence of measured melt data or sufficient information for an energy balance model, temperature-index models have proven sufficiently accurate for generating melt (e.g. Zwally et al., 2002; Bartholomew et al., 2010).

Alternatively, an energy-balance model may be used. They utilise more input factors than temperature-index models and therefore potentially more accurately constrain melt. They are, therefore, often preferred when the required meteorological data is accessible (e.g. Arnold et al., 2006; Banwell et al., 2012). The availability of data from reanalysis methods, such as ERA-40 (Simmons and Gibson, 2000), has made their implementation more feasible and has been shown to be sufficiently accurate in studies (e.g. Rye et al., 2010). However, their data requirements and the computational implications of their complexity mean that they are not necessarily the preferred option for meltwater studies.

Observations (Tedesco et al., 2012) and modelling (Luthje, 2006) also suggest that supraglacial lake presence necessitates special modelling for high accuracy to account for the significant effect of the lake's albedo on melt.

1.7.2 Surface routing

Modelling of the route that meltwater takes is necessary to determine where lakes and moulins form and to develop input hydrographs for the subglacial drainage system. This can be done using a flow direction matrix to determine

the route that meltwater takes. Arnold et al. (1998) did this, using a digital elevation model (DEM) of the glacier surface to determine the catchment area for each individual moulin. Arnold (2010) subsequently developed an algorithm to improve the use of DEMs in such models. Arnold et al. (1998) assumed single cells or contiguous areas forming closed depressions to be error and smoothed them to avoid trapping of water in small ponds. However, Arnold (2010) developed an algorithm to identify true representations of depressions, improving the potential to model realistic ponding. This was subsequently implemented into Banwell et al's (2012) 'supraglacial routing and lake-filling' (SRLF) model. This identifies depressions in the glacier surface where ponding is expected to occur, and the route meltwater will take across the glacier. This allows the catchment and thus input of each pond to be calculated and with flow-velocity also calculated, is able to generate input hydrographs for each depression. Though improved, the model was still limited by DEM error and discrepancies with observations were also likely due to the model's inability to replicate lake overflow channels (Banwell et al., 2012).

Leeseon et al. (2012) presented a two-dimensional model of lake development based on Darcy's law for flow through a porous medium (Chow, 1988) and Manning's equation for open channel flow (Manning, 1891). The model routed water to neighbouring cells of lower elevations, with the lowest cell classified as a sink. A sink surrounded by low cells was incorporated into a lake. Comparisons with observations revealed the model was moderately successful, identifying 66% of lakes over 0.125km^2 in area. The failures of this and other models can be largely attributed to the limitations of DEMs (Leeson et al., 2012). Low-resolution measurements, erroneous measurements and the smoothing processes that are deemed necessary to counter errors and reduce computational stress continue to hinder the accuracy and resolution of DEMs and limit accurate supraglacial routing and correct lake identification. While Arnold (2010)'s algorithm has improved this, higher accuracy and resolution is necessary in measurement.

1.7.3 Subglacial drainage

Subglacial hydrological models have developed since the seminal numerical models of Shreve (1974) and Rothlisberger (1974). Arnold et al. (1998) developed a model of a subglacial drainage system by adapting the EXTRAN block of the US Environmental Protection Agency Storm Water Management model, with moulins represented by drains and subglacial conduits represented by pipes. Each length of subglacial conduit could have its shape, size, length and roughness specified and the system would simulate pressure and discharge in response to input hydrographs at the moulins. The model had trouble successfully depicting a distributed drainage system, which was represented by bundles of small, circular, rough conduits or one shallow, wide, rectangular, rough conduit. The latter configuration produced fairly successful results but only early in the melt season, prior to channelization, while the former option was considered unsuccessful. However, the model did produce good results for a channelized drainage system, as represented by a single larger conduit. The model showed little sensitivity to conduit roughness, meaning roughness values derived from the linear relationship with conduit area or from the literature seemed to prove adequate. A notable weakness of the model is its lack of a mechanism to represent the transition between a distributed and channelized drainage system, particularly as this is of crucial significance in the behaviour of subglacial drainage. However, Arnold et al.'s (1998) study inferred channelization from the retreat of the snowline, designating the area downglacier of a moulin as channelized when the snowline passed it. Observations suggest that this is a reasonable assumption (Nienow, 1993) but it is nevertheless a imperfect way of constraining drainage system transition.

Alternatively, Flowers and Clarke (2002a) represented the subglacial drainage system as a two-dimension, vertically-integrated porous sheet that exchanges water with its adjoining layers, based on Clarke's (1996) lumped element model and observations at Trapridge Glacier, Canada (e.g. Blake, 1992; Stone and Clarke, 1993; Fischer and Clarke, 1994). The subglacial drainage system comprises sediment and water, is porous, distributed and is linked to a subsurface aquifer layer. Increased discharge causes it to accommodate by

expanding vertically. Importantly, the model is also able to calculate hydraulic conductivity, which may vary spatially as well as temporally, varying with ice thickness. This allows the representation of more nuanced variations, such as diurnally reversing hydraulic gradients as observed by Hubbard et al. (1995). Testing of the model by Flowers and Clarke (2002b) yields positive results, particularly noting successful modelling of the rapid transition from a hydraulically unconnected to connected state, coupling between the supraglacial and subglacial system and deterioration of the basal drainage network in the late melt season. The model seems a good alternative to that of Arnold et al. (1998) if, for example, the aim is to simulate interaction with the bed or the characteristics of a distributed system, rather than accurately model conduit evolution.

A one-dimensional, depth-integrated model by Colgan et al. (2011) to determine hydraulic head was developed to be run annually rather than just for the melt season. The model challenged assumptions by producing mean glacier water residence time of ~2.2 years, suggesting that conduit storage does not completely shut down at the end of the melt season but remains open in parts.

1.7.4 Subglacial drainage linked with dynamics

Recognising that the drainage system's relationship with ice dynamics is not a one-way process, some recent models have sought to incorporate interaction between the subglacial drainage system and the dynamics.

Schoof (2010) included a critical discharge level, 'Q_{crit}', below which an inefficient cavity system exists, with the associated inverse pressure-discharge relationship, kept open primarily by ice flow over bed protrusions. When discharge exceeds Q_{crit}, the system channelizes. The discharge becomes concentrated into a few primary conduits, causing faster wall melting, which is offset by stronger creep closure that is driven by increased effective pressure and therefore lower hydraulic pressure. The ice-flow component responds appropriately, producing ice velocities largely positively coupled with discharge

below Q_{crit} and de-coupled following the surpassing of Q_{crit}. For the system to return to its distributed form, discharge must be lower than a lower critical value, Q_m. Importantly, the model accounts for non-steady state conditions, with the system able to temporally re-couple with discharge when in channelized form, upon the delivery of rapid discharge spikes (Schoof, 2010), as inferred by Bartholomew et al. (2010).

Pimentel and Flowers (2010) treated the transition between distributed and channelized states in the subglacial drainage system as a morphological transition, developing upon Pimentel et al's (2010) higher order flowband model of subglacial drainage and ice dynamics. Additionally, the model incorporates uplift of the glacier, as is believed to occur in response to high subglacial pressures (Iken et al., 1983) but is hitherto neglected in subglacial models. Though limited by the model's two-dimensional nature, testing of the model suggests good performance on a seasonal scale and though the strength of diurnal cyclicity appears too week, this is likely due to ill-constrained meltwater input rather than a defective subglacial component.

Chapter 2: Study Site and Data

2.1 Study site

This study will focus on Petermann Glacier, a marine-terminating glacier in north-west Greenland (fig. 2.1). The glacier is situated around 81°N and 61°W and flows from south-east to north-west. The main trunk of the outlet glacier is approximately 100km long and 20km wide, and it drains an area of 73927km^2 (Rignot and Kanagaratnam, 2006) of the ice sheet into the Petermann Fjord. The glacier is marine-terminating, terminating in a large floating ice tongue. A substantial amount of the glacier trunk is therefore floating, and has no subglacial drainage system, with the grounding line ~39km along the main ice trunk. The tongue helps the glacier support a thick terminus, with ice at the grounding line ~600m thick (fig. 2.3). This study will incorporate all parts of the ice-sheet thought to be part of Petermann Glacier's drainage catchment and this part will also be referred to as 'Petermann Glacier' (fig. 2.2). The potential catchment area is thought to be larger, but this study incorporates all of the supraglacial catchment area that could supply surface melt, as verified by melt modelling. This area extends 72km inland from the trunk, to an elevation of 1475m. In total, an area of 6784.7km^2 is covered. The study site was determined from Landsat analysis and supraglacial melt and routing models, with all areas containing evidence of supraglacial lakes included.

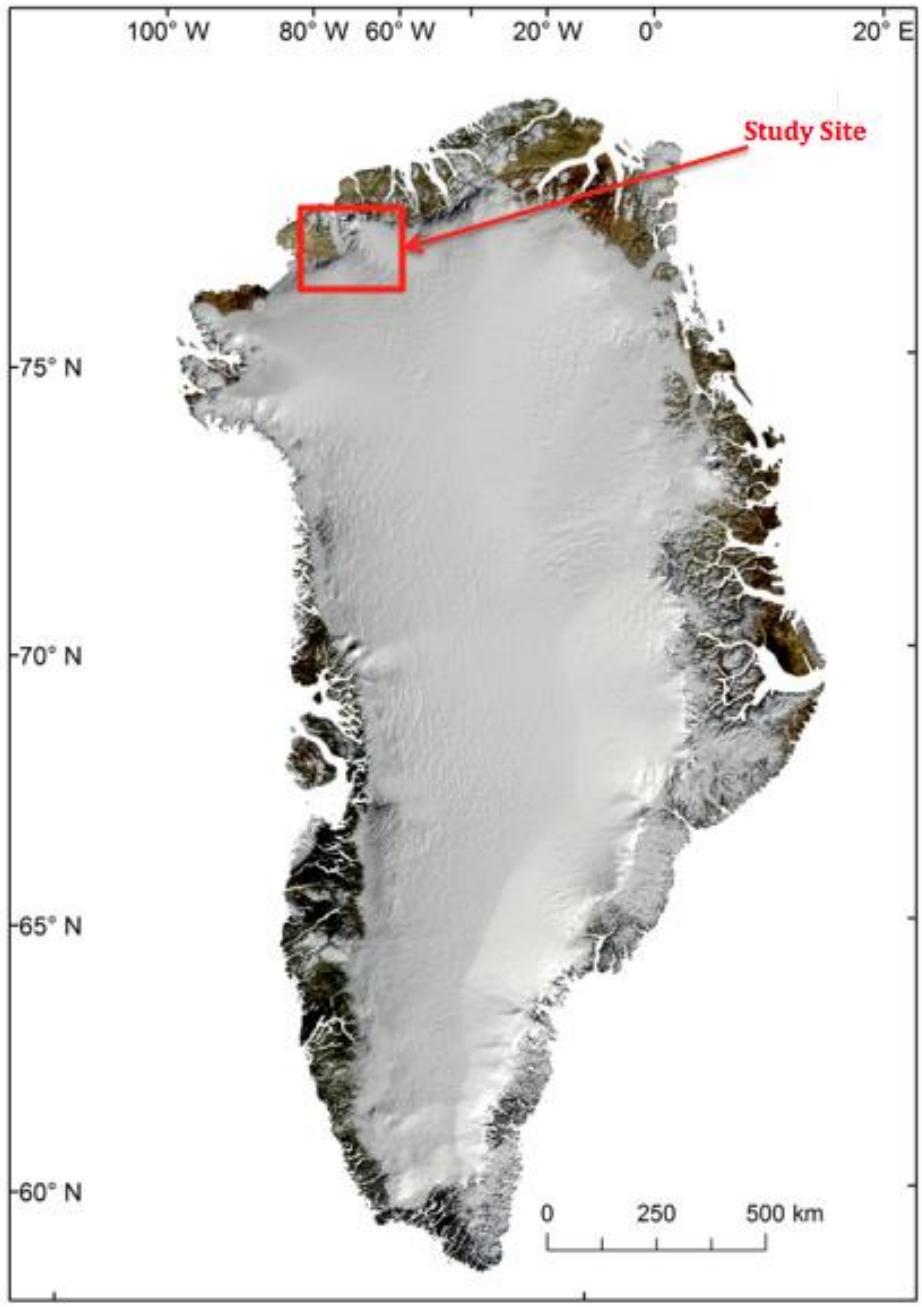

Figure 2.1: *The Petermann Glacier study site in the context of the GrIS (Polar Stereographic Projection)*

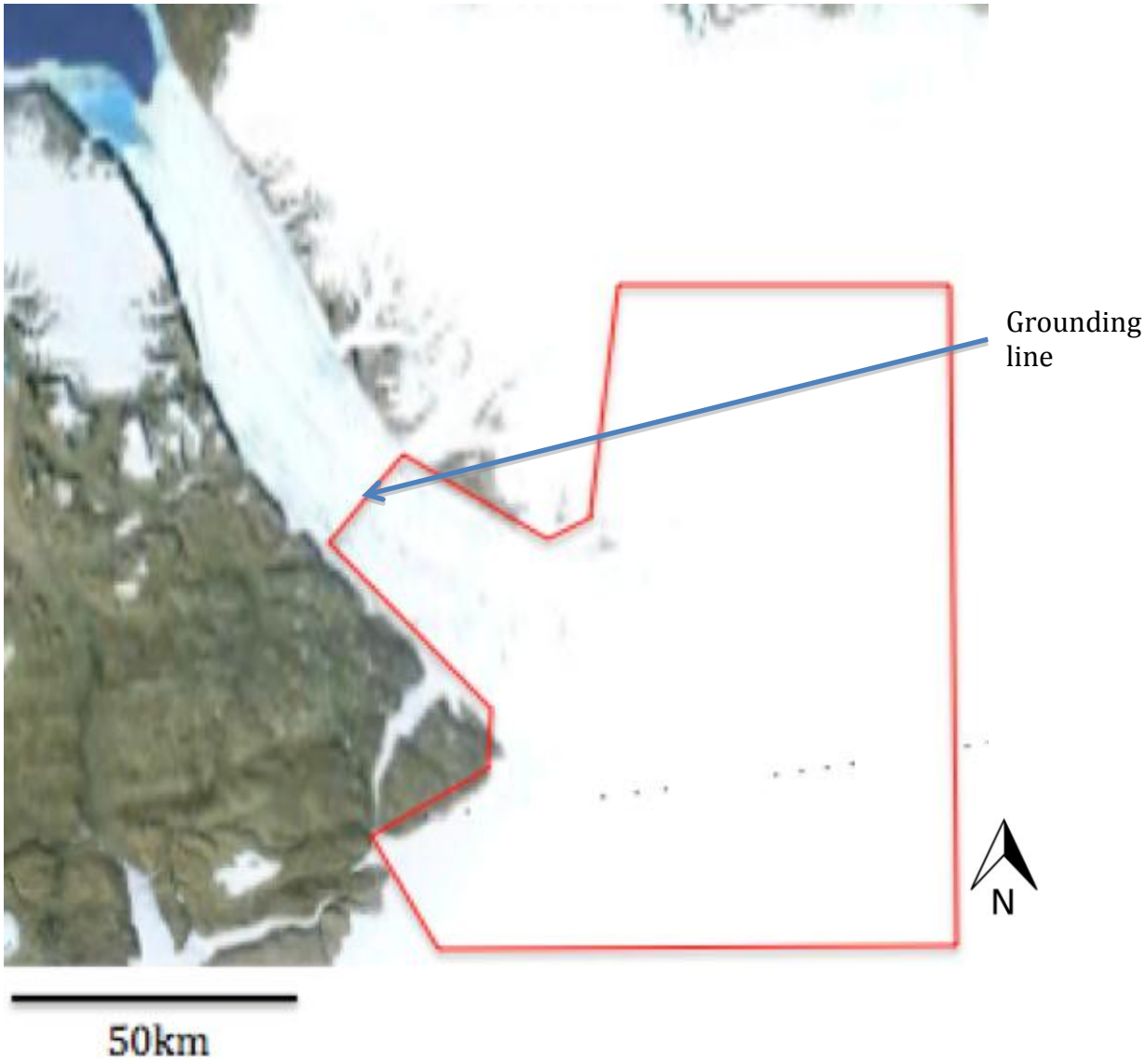

Figure 2.2: *Peterman Glacier study site (enclosed in red) (Google Earth). The grounding line, as determined by Rignot and Steffen (2008) is indicated. The area of the trunk north of the grounding line is the floating tongue and sea ice.*

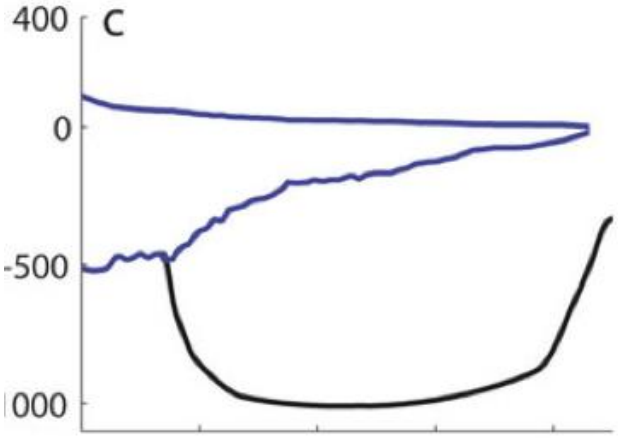

***Figure 2.3**: A thickness profile of the glacier (blue) and bedrock (black) at the grounding line (Nick et al., 2012)*

2.2. Previous research

Although Petermann Glacier was first recorded and examined in 1871 (Kollmeyer, 1980), there is not a wealth of literature on the glacier and none at all on the subglacial drainage system. There are a handful of existing studies that provide some context for the present study.

Petermann glacier transfers ~13km^2 of ice into the ocean annually (Rignot et al., 2001) but calving is rare, with 80% of mass loss from the tongue occurring through submarine melt. The tongue periodically experiences very large tabular calving events, which are likely part of a natural cycle (Johnson et al., 2011; Nick et al., 2012) but in recent years, these extreme events have been particularly common. Parts of the tongue have broken off in 2001, 2008, 2010 (Johnson et al., 2011) and 2012. In August 2010, 25% of the floating tongue was removed in one event, yielding a 25km-long iceberg (Falkner et al., 2011). This was followed by another event on July 16-17th (day 198-199) 2012, when ~120km^2 of ice was lost. The rapid acceleration of Jakobshavn Isbrae was attributed to the collapse of the ice-tongue, which caused the speed to increase by 121% in six years (Joughin et al., 2004; Luckman and Murray, 2005). This led to great interest in the potential response of Petermann Glacier to the tongue collapse, but observations and a modelling study by Nick et al. (2012) recorded minimal

dynamical response. Nick et al. (2012) proposed that this is because the glacier's tongue actually provides little buttressing force. They noted very low along-flow resistive stresses for the front part of the ice shelf, due to this part being thin (~100m) and wide (~15km) and not connected to the fjord walls. The driving stress and resistive forces along the shelf were recorded at below an order of magnitude smaller than those estimated for Jakobshavn Isbrae (van der Veen et al., 2011). Consequently, loss of the tongue seemingly does not result in a significant loss of buttressing. Their model, however, suggests that subsurface melting of the tongue could destabilise the geometry of the glacier and drive rapid grounding-line retreat (Nick et al., 2012). This could be exacerbated by tongue collapses, as the increased ice-free area in the fjord allows warmer sea surface temperature's to exist, which could affect fjord circulation and increased ocean-induced basal melting (Johnson et al., 2011).

In contrast to studies of other analogous glaciers suggesting that basal sliding due to meltwater lubrication and enhanced pressures play little role in dynamics (Joughin et al., 2008;c; Nick et al., 2009; Murray et al., 2010), Nick et al.'s (2012) study suggests that seasonal speed-up is in fact mainly driven by meltwater at the base, along with some variations in buttressing by sea ice. Despite meltwater being less abundant at such a high latitude, observed summer speed-up was short and corresponded to the period of surface melt, lasting around three months. Seasonal variation is around ~25% and has shown an increasing interannual trend since 2006. Attribution of enhanced velocities to meltwater-induced sliding are supported by model runs which produce velocity changes in line with observations when applying a seasonal variation in basal lubrication (Nick et al., 2012). They argue that changes at the ice-front have little impact on the grounding line, but variability in the grounded section manifests along the entire shelf and glacier. These findings suggest that the subglacial drainage system plays a critical role in the dynamics of Petermann Glacier, and highlights the need to better understand it.

2.2.2 Why study Petermann Glacier?

This section has demonstrated that Petermann Glacier is an excellent candidate for study. A large glacier, draining 6% of the GrIS (Johnson et al., 2011), it is clearly of pronounced significance. It is one of only four major outlet glaciers, grounded well below sea-level, and one of two with a large floating ice-tongue. The recent large calving events of the tongue have garnered much attention in both the scientific community and popular media, due to concerns over its implications for the glacier's stability following the acceleration of Jakobshavn Isbrae and the lack of understanding of marine-terminating glacier dynamics (e.g. Joughin et al., 2004; Sole et al., 2011). With evidence showing marine-terminating glaciers are changing more than land-terminating glaciers (Moon et al., 2012), the dearth of literature on the subglacial drainage systems of marine-terminating and high-latitude glaciers makes Petermann of particular interest. The findings of Nick et al. (2012) show that the subglacial drainage system plays a critical role in the dynamics of Petermann Glacier, and understanding it is therefore imperative for understanding the glacier and any potential response to climate change and further calving events. The knowledge obtained will also be of use in improving understanding of marine-terminating glaciers in general.

2.3 Input data

The models in this study are driven by publicly available temperature, DEM and satellite data. Due to time and financial constraints, discharge and pressure data could not be obtained to validate model results. Therefore the aim of the present paper is to analyse the behaviour of the system suggested by the models and input data, rather than to accurately produce an observable output.

2.3.1 Surface air temperature

Surface air temperature was collected hourly by the Greenland Climate Network's (GC-Net) 'Petermann' automatic weather station (Steffen et al., 1996). The station is situated at 80°41'01'N and 60°17'35"W, at an altitude of 37m and has been in operation since May 2002. Data was only consistently available for the summers of 2003, 2004 and 2005.

2.3.2 Precipitation data

Precipitation data was taken from Hakuba et al. (2012). Their study modelled precipitation based on a contemporary Greenland, producing an annual total precipitation (16-year mean) that compared well with the thirteen observational studies chosen for comparison. As well as seemingly providing a reliable precipitation estimate for the GrIS, this study was chosen to estimate Petermann Glacier's precipitation because it breaks down precipitation into 5 regions of the GrIS and into monthly means. This is important as summer precipitation is around double in the south compared to the north, due to regional climatic differences and orographic controls (Hakuba et al., 2012). Precipitation for this study was based on their precipitation values for the 'north' and hourly precipitation was interpolated between the monthly mean value for the beginning of each month.

2.3.3 Snow depth

Initial snow depth was sourced from the same weather as surface air temperature.

2.3.4 Surface Digital Elevation Model

The surface DEM was downloaded as a tile from the Byrd Polar Research Centre's Greenland Mapping Project (GIMP) DEM. The DEM was constructed from a combination of ASTER and SPOT-5 DEM's for the ice sheet periphery and margin i.e. areas below the equilibrium line altitude (ELA). Areas above the ELA were constructed from AVHRR photoclinometry (Scambos and Haran, 2002). The DEM has a nominal date of 2007 but it is registered to average ICESat elevation for 2003-2009. The data was downloaded in 30m resolution and smoothed using a 7 x 7 median filter and 10 x 10 Gaussian filter. It was then resampled to 250m using bilinear interpolation to better match the grid size with the available bed DEM data. It is projected in Polar Stereographic form.

2.3.5 Bed DEM

The DEM of the basal topography was provided by Stephen Palmer from the new dataset described by Bamber et al. (2013). It was posted at 1km resolution and resampled to 250m using bilinear interpolation to better match the grid size of the surface DEM. Resampling was limited to 250m rather than 30m, as available for the surface DEM, as interpolation to such a level was thought to compromise the quality of the dataset. It is also projected in Polar Stereographic form.

2.3.6 Satellite imagery

To analyse surface lakes, Enhanced Thematic Mapper Plus (ETM+) images from Landsat 7 were downloaded from the USGS Global Visualisation Viewer (GloVis) [https://lpdaac.usgs.gov/get_data/glovis]. The data has a ground pixel resolution of 30m and was downloaded for the summer of 2004 and 2012. There were a lack of quality images due to cloud in 2004 for the period of interest, including a 26 day gap between day 169 and day 195, a period of particular interest (fig. 4.1). This meant 2004 data was only available for general visual analysis. Relatively plentiful images were available for 2012 between day 164 and day 240, which were downloaded for lake depth analysis. Images from different tracks covering any of the area were utilised.

Chapter 3: Methods

This chapter will discuss the methods involved at the different stages of modelling. First the analysis of lakes from Landsat imagery will be considered, then the use of a temperature-index model to simulate melt. Then the routing model used to route water across the surface and bed, and fill and drain lakes will be discussed, before describing the subglacial drainage system model used in the study.

3.1 Lake depth analysis

Supraglacial lake evolution for the summer of 2012 was monitored using Landsat 7 ETM+ images and a depth-analysis algorithm. Images were analysed manually and used or discarded based on cloud cover, which is an inherent constraint on availability when using imagery from the visible and near-infrared spectrum, particularly during the melt season when cloud cover can be up to 70% (Cawkwell and Bamber, 2002). When running the depth algorithm on specific lakes, images with scan lines through the relevant lakes were avoided. These factors constrained depth analysis to a few images for each area and meant direct comparisons between areas are limited as analysis is often on different days. However, images with inconveniently-placed scan lines or cloud cover could still be used for manual validation, for example, to check a lake had not drained and reformed in between algorithm-runs. Overall, Landsat data was preferred to other options such as MODIS for its superior spatial resolution, an essential attribute when investigating such scales. An 'Area Upper' and Area 'Lower' were defined and used for lake analysis (fig. 3.1).

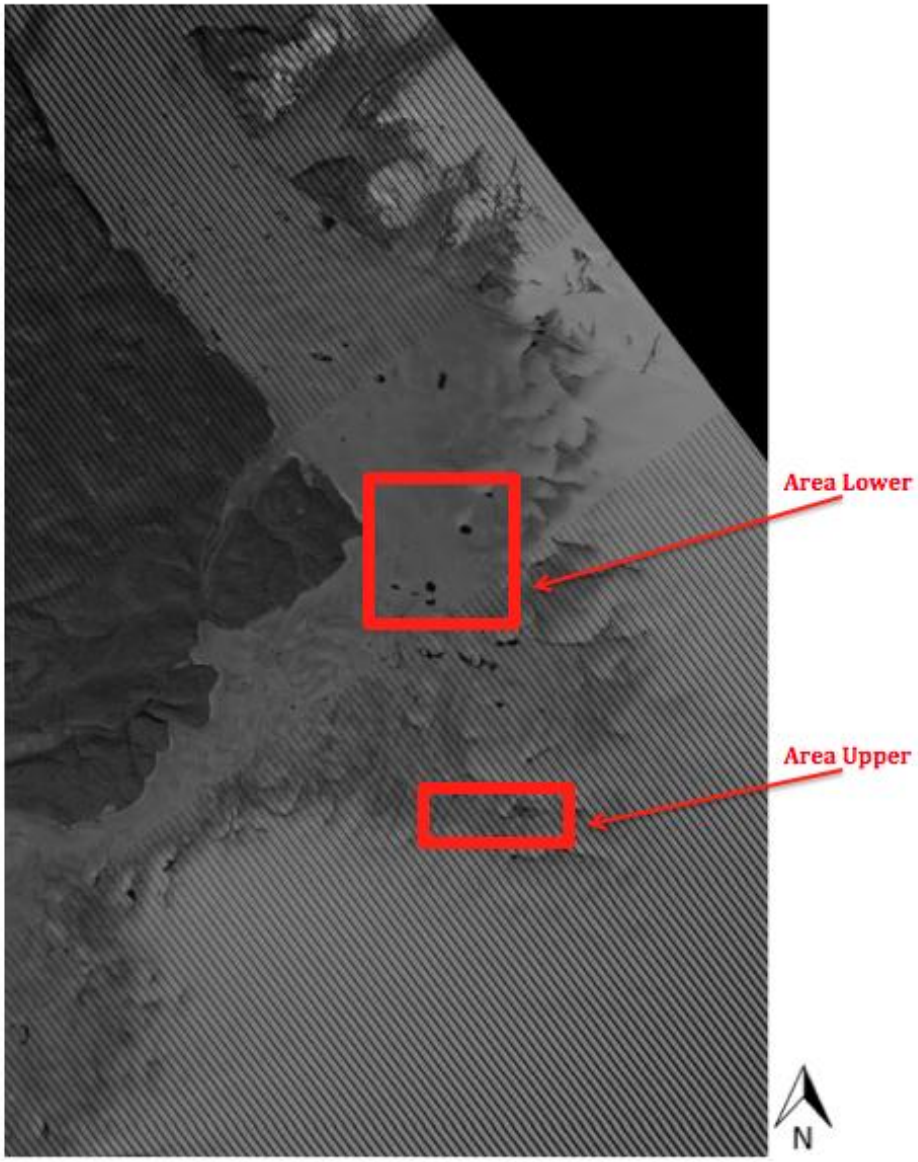

Figure 3.1*: The defined areas for lake depth analysis are shown in the context of a Landsat 7 ETM+ image from day 182, 2012.*

The lake depth algorithm was based on one developed by Sneed and Hamilton (2007). This method is fundamentally based on Bouguer-Lambert Beer law:

$$L(z, \lambda) = L(0, \lambda)e^{-(K_\lambda)(z)}$$

(Equation 3.1)

where L(z, λ) is the water-leaving spectral radiance at some depth, L(0, λ) is the spectral radiance at zero depth, Kλ is the spectral attenuation, and z is depth

(Sneed and Hamilton, 2007), which allows depth to be calculated from measured reflectance using bands 1-4 (0.45-0.90um).

The model relies on several assumptions: (i) the substrate of the melt pond is homogenous, (ii) suspended or dissolved organic or inorganic particulate is of a negligible quantity, (iii) there is no inelastic scattering, (iv) there is no effect from wind, (v) R ∞, reflectance over optically deep water, where bottom reflectance has no influence and must be measured at water deeper than ~40m, was assumed based on a value provided by Arnold (*personal communication*), due to the lack of such water within the images (Sneed and Hamilton, 2007). Further study verifies the efficacy of the algorithm despite these assumptions, which are of limited significance (Sneed and Hamilton, 2011). Wind and suspended particles may have a very small effect, and the assumption of substrate homogeneity may marginally distort results. The effect of cryoconite absorbance is less clear (Sneed and Hamilton, 2011), but all such small potential errors are not judged to significantly compromise the goal of the present study to assess trends and the behavior of the drainage system, rather than produce accurate absolute values.

Computational restrictions and the scope of the study restricted use of the depth algorithm to the two areas thought to provide the most useful comparison. Data was converted from radiance to reflectance before the algorithm was run as per Sneed and Hamilton (2007), with the implementation of a reflectance threshold based on the blue to red ratio as per Box and Ski (2007). This produce water depth values for each pixel, allowing the area and volume to be calculated based on the number of pixels producing a depth value above zero.

3.2 Temperature-Index modelling

3.2.1 The model

The first stage of the modelling is the production of meltwater at the surface, which provides a source for the moulin hydrographs that are the input for the subglacial drainage model.

A simple distributed glacier surface degree-day model (e.g. Reeh, 1989; Hock et al., 2003; Clason et al., 2012) was used to simulate melt across Petermann glacier. The model was developed by Cameron Rye (unpublished) and adapted by Mayaud (2012). Daily-averaged temperature was input into the model and the total melt volume for each surface grid cell was calculated following Arendt et al. (2009)

$$M = -T(z)\delta\,[T(z)]\mathrm{DDF}_{\mathrm{snow/ice}}\,\Delta t + P(z)\delta[-T(z)]$$

(Equation 3.2)

$$T(z) = T_{aws} + (z - z_{aws})\Gamma_T$$

(Equation 3.3)

$$P\,(z) = P_{aws}k + (z - z_{aws})\Gamma_P\,P_{aws}$$

(Equation 3.4)

Where M is the melt water depth (mm) produced during the time interval, T is the daily average air temperature (°C), P is the daily total precipitation (rain and snow (mm w.e.), $\mathrm{DDF}_{\mathrm{snow/ice}}$ is the degree-day factor for snow/ice ($\mathrm{mm°C^{-1}d^{-1}}$), z is the elevation (m), Δt is the time interval 1 hour, and the subscript 'aws' references the measurements made at the GC-net Petermann automatic weather station. The input of a constant temperature (Γ_T ($\circ\mathrm{Cm^{-1}}$)) and precipitation (Γ_P ($\%\mathrm{m^{-1}}$)) lapse rate causes the model to adjust T_{AWS} and P_{AWS} with elevation. δ determines the threshold between positive temperatures for melting and negative temperatures for accumulation of solid precipitation:

$\delta[T] = 1, T > 0;$

$0, T \leq 0$

(Equation 3.5)

Local parameters were lacking but a DDF of 8.9 $mm°C^{-1}d^{-1}$ for ice and 3.6 $mm°C^{-1}d^{-1}$ for snow were chosen following Braithwaite and Olesen (1989), Braithwaite (1995; 1996) for the GrIS. Similarly, a winter lapse rate of 0.8°C $100m^{-1}$, summer lapse rate of 0.6°C $100m^{-1}$ and precipitation gradient of 14%$100m^{-1}$ were taken from the literature for the GrIS (Steffen and Box, 2001; Banwell, 2012)

Refreezing of surface melt was implemented as in Radic and Hock (2011), with annual refreezing *R* (cm) related to annual mean air T_a (°C) by:

$R = -0.69T_a + 0.0096$

(Equation 3.6)

The model produces a melt array corresponding to the input surface DEM, displaying a spatial pattern of melt across the study area. Melt is calculated cumulatively within the model for each day, with the DDF for snow utilised until melt exceeds the initial defined spring snowpack depth, with the addition of precipitation that falls as snow (Clason et al., 2012).

3.2.2 Using TI models

Although energy-balance models take more processes involved in the surface mass balance of a glacier into account, it is believed that a temperature-index model is sufficiently accurate for the purposes of the study. Temperature-index models are based on the relationship between melt and temperature and are unable to account for the potential spatial and temporal variability induced by

other variables (e.g. Bougamont et al., 2005). However, data limitations ruled out the possibility of using an energy-balance model and observations confirm the efficacy of utilising temperature-index models. Braithwaite and Olesen (1989), for example, found a correlation of 0.96 between annual ice ablation and positive air temperature sums. Moreover, this study is concerned with large-scale patterns of melt across the catchment rather than small-scale spatial variations. Indeed, comparison studies have found that often temperature-index models match energy-balance models (WMO, 1986; Hock, 2003). The high correlation of air temperature with other energy balance components, means that melt results based on air temperature do not deviate much from observations. Longwave radiation and sensible heat flux contribute around 75% of the energy for melt and predominantly driven by air temperature (Ohumara, 2001). Many studies (e.g. Braithewaite, 1995; Bartholomew et al., 2010) have demonstrated the utility of temperature-index models on the GrIS.

Refreezing in the snowpack is not thought to be of great importance at the GrIS margin where there is little snowpack, but it can be of substantial importance towards the interior (Lefebre et al., 2002). Wright et al. (2007) criticised models for not including refreezing, with refreezing having the potential to delay transport and therefore affect the timing of peak discharge events (van Pelt et al., 2012).

Of course, as a model, the temperature-index model is fundamentally limited and cannot completely accurately simulate reality. Though the lack of a local DDF is a limitation, the best available values are used, spatial variations in DDFs are limited (Braithwate et al., 1998) and significant seasonal variations have not been observed over ice on the GrIS (Braithewaite and Olesen, 1993). Similarly, the lack of local precipitation data is a limitation, but the values taken from the literature should prove sufficiently accurate given the limited significance of precipitation in the area on the overall melt production (Hakuba et al., 2012). A higher spatial resolution of measured temperature would increase confidence in the model, but the inclusion of lapse rates will largely account for this.

3.2 Meltwater routing modelling

Supraglacial routing models are necessary for determining the route that meltwater takes across the glacier and where it ponds and enters the subglacial system or flows off the margins. This study employs a model developed by Arnold (2010), using the surface DEM and a daily melt array produced by the temperature-index model as input. Most such models smooth small surface depressions, assuming them to be an artefact of DEM error, and rely on artificial filling of depressions (Arnold, 2010). This model, however, treats depressions in the DEM as real, following evidence that depressions need not be assumed to be artefacts of DEM error (e.g. Lane and Chandler, 2003; Lindsay and Creed, 2006) in the current generation of high-resolution DEMs. This is imperative in the present study, which relies on the identification of lakes and the time-dependent routing of water into moulins to produce input hydrographs for the subglacial model.

The model calculates the surface slope, and from this the direction of steepest descent for each cell, thus compiling the route meltwater takes from the cell of melt to its arrival in a surface depression. Any cell with no neighbouring cell is considered a sink and may develop into a lake. The model searches a flow direction matrix to find the set of DEM cells which ultimately flow into each sink cell thus identifying catchment areas supplying each sink cell. Each catchment boundary is then analysed for its lowest possible cell over which water would pour. The timing as well as route of the water is calculated, with flow delay calculated under different surface conditions. Under conditions of snow cover, Darcian flow is applied. Under conditions of bare ice cover, Manning flow is applied. The maximum area of any lake can be calculated, with cells that are lower than the level of the outflow cell flooding as the lake fills (Arnold, 2010).

Upon reaching a critical lake volume, lakes drain. The critical lake volume is determined by a set crevasse surface area (cvol=) and ice thickness. The critical volume is the surface area multiplied by the thickness, meaning as ice thickness increases, the necessary volume of water to promote fracture to the base

increases. Lakes are said to drain over five hours, with the maximum rate in the second hour (fig. 3.2) to most accurately represent the evolution of the drainage conduit (Banwell et al., 2012). After drainage, lakes are considered open moulins. Otherwise, lakes may spill and cascade into other lakes as observed by Banwell et al. (2012), using the model's identification of the links between catchments. Additionally, the algorithm eliminates catchments which form 'closed loops of flow' and calculated the drainage network topology such that continuity of flow is maintained (Arnold, 2010). The model's production of the route and timing of water into lakes, and the simulation of lake drainage creates moulin input hydrographs for the subglacial model.

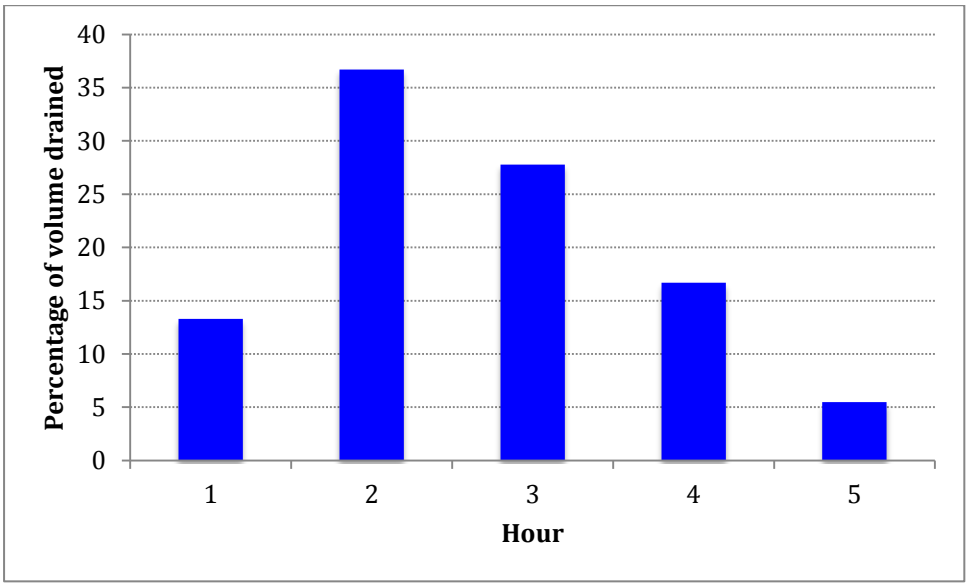

Figure 3.2: *The distribution of lake drainage discharge over five hours*

The model is also applied to establish the configuration of the subglacial drainage system. It is run using the surface DEM and bed DEM, over the hydraulic potential surface under different k values. Using the two DEMs and inferred ice thickness, Shreve's (1972) equation (equation 1) is used to calculate the hydraulic pressure potential field, before applying the flow routing model to create the subglacial hydrological network.

3.3 Subglacial drainage model

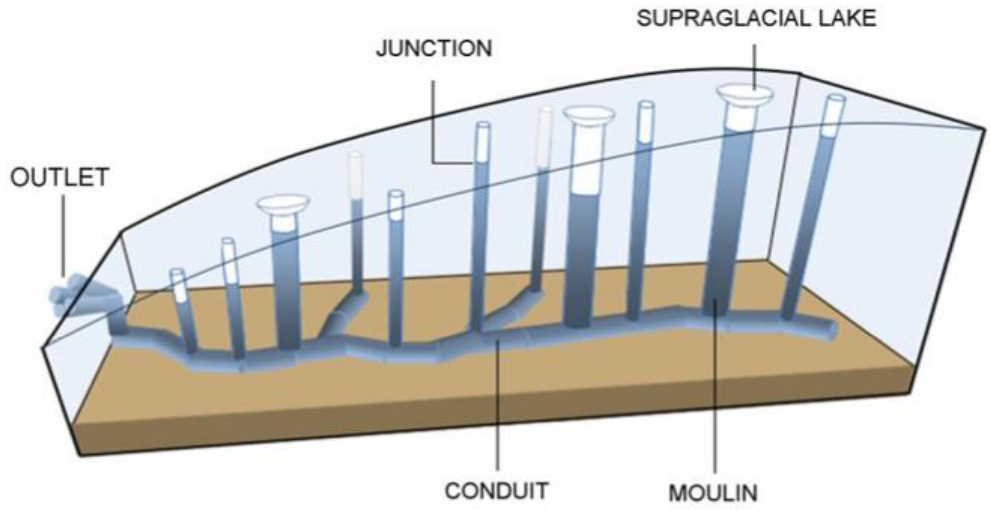

Figure 3.3: *A representation of the configuration of SWMM as applied to a glacier (Arnold et al., 1998; Banwell, 2012)*

The subglacial hydrology model is based on the subglacial component of the model developed by Arnold et al. (1998) for an Alpine glacier and adapted by Banwell (2012) for the (west) GrIS. The model is an adaptation of the EXTRAN block of the US Environmental Protection Agency Storm Water Management Model (SWMM). It was originally developed as a sewage pipe system, using a network of junctions, some of which are drains through which water can enter or leave the system, connected by pipes, to simulate the flow of rain water through the system, using the solution of Saint Venant equations (Roesner et al., 1988; Arnold et al., 1998). Each pipe can have an individually specified shape, size, length and roughness. Arnold et al. (1998) saw the potential for applying this system to a glacier, with the drains representing moulins and pipes representing subglacial conduits.

The model is pseudo two-dimensional, allowing conduits to branch and converge at junctions and only requiring conduit slope and length as spatial parameters. It is run at a time-step of 1 second, reduced from 1 hour in Arnold et al. (1998) after Banwell (2012) found this to enhance stability The conduit slope and length are defined based on the DEMs and subglacial routing model and it is attempted to limit length to approximately 1000m after Banwell (2012) showed this to increase model stability while avoiding the excessive processing time of

small conduits. The initial conduit diameter and Manning roughness must also be specified. At each connecting junction, the invert (bed) and ground (glacier surface) elevation must be specified, along with junction c (CSA). The slope of the conduits is calculated based on the invert elevation at each connecting node.

The hydrographs for each moulin produced by the surface routing model are used as input for the corresponding junction defined as a moulin. The primary dependent variable at each conduit is discharge and at each junction, hydraulic head, where water pressure is calculated based on the hydraulic head elevation in relation to the glacier surface elevation (Roesner et al., 1988).

At each link in the system, the model solves an equation that is a combination of the St. Venant momentum and continuity equations

$$\frac{\partial Q}{\partial t} + gA_f S_f - 2V\frac{\partial A_f}{\partial t} - V^2\frac{\partial A_f}{\partial x} + gA_f\frac{\partial H}{\partial x} = 0$$

(Equation 3.7)

where Q is discharge through conduit (m^3s^{-1}), V is water velocity in the conduit (ms^{-1}), A_t is the CSA of flow (m^2), H is the hydraulic head (m, here invert elevation plus water depth), S_t is the friction slope and g is acceleration due to gravity ($m\ s^{-2}$). Manning's equation gives the friction slope:

$$S_f = \frac{n^2}{AR^{4/3}}Q|V|$$

(Equation 3.8)

where n is Manning's roughness coefficient and R is the hydraulic radius of flow in the conduit. Equation 3.7 is converted into finite difference form for the numerical solution. This numerical solution employs the modified Euler method to calculate hydraulic head in each junction and discharge in each conduit for each time-step (t). The values of dependent variables Q and H after each time

step (Δt) are calculated by projecting the values from the pervious time step across a half-time step and then a full time-step according to the slope of the finite difference form of Equation 3.7. Water flow follows this process, and discharge through the ultimate downstream junction produces the modelled outflow from the system (Banwell, 2012).

Arnold et al. (1998) also adapted the model to assume conduits enlarge in response to release of frictional heat dissipation from water flow, and close in response to ice deformation. Equations developed by Spring and Hutter (1981) were implemented to represent this, with conduit wall melting (*M)*, expressed as the mass melted per unit length of conduit per unit time:

$$M = \left[(\pi A_c)^{1/2} \rho_w (f_r V^3 / 4) \right] / L$$

(Equation 3.9)

where Ac is the conduit CSA (m^2), p_w is the density of water (kg m^{-2}) f_r is a friction coefficient, *V* is the velocity of water in the conduit (m s^{-1}), and *L* is the latent heat of fusion of water (J kg^{-1}). Conduit closure through ice deformation *(C)*, expressed as the change in CSA per unit time is:

$$C = -(P_i - P_w) \left| P_i - P_w \right|^{n-1} 2(1/mB)^n A_c$$

(Equation 3.10)

where P_i is ice overburden pressure (Pa), P_w is conduit water pressure (Pa), *m* is the exponent in Glen's flow law and *B* is the Arrhenius parameter in Glen's flow law (N m^{-2} $s^{1/m}$). The friction coefficient and flow law exponent are given values of 0.25 and 3, respectively, as in Arnold et al. (1998). An initial 24 hour spin-up period where conduit adjustment is not permitted is incorporated to allow the model to begin without immediate conduit-closure. As sudden introduction of conduit adjustment was shown to destabilise the system, a subsequent 24-hour period gradually and linearly introduces conduit adjustment. For example,

conduit-closure and melt rates act at 0% after 24 hours, 25% after 30 hours and 50% after 36 hours and so on until they are fully incorporated at 48 hours (Banwell, 2012).

The system may experience pressurised flow and the reversal of the hydraulic gradient, with water spilling out of the system through moulins if the hydraulic head reaches the glacier surface. Therefore, the pressure values produced by the model are limited to Pw = 1.11Pi, representing junction water depth equal to ice thickness (Roesner et al., 1988; Banwell, 2012).

3.3.1 Parameters

Minimum conduit diameter is set at 0.5m to avoid complete closure of conduits. Banwell (2012) showed that setting the diameter too low restricted the capacity of the system to evacuate water when discharge increased, causing an exceptionally high loss of water through moulins to the surface. Setting it too high would not allow sufficiently realistic adjustment of conduits during times of low discharge. Arnold et al. (1998) found a diameter of 0.1m to function well for the thin ice of Haut Glacier d'Arolla, Switzerland but Banwell (2012) required a minimum diameter of 0.5m to keep conduits open for the higher deformation rates of the thicker ice of the GrIS, while suggesting a value any larger would compromise the realism.

Manning roughness is defined at 0.05. Setting roughness too high similarly results in excess backing-up of the system and loss of water at the surface. However, a degree of roughness is necessary to accurately represent the flow and capacity of the system (Banwell, 2012). Banwell (2012) found a Manning roughness of 0.05 to best suit the model while being realistic.

A background meltwater input of $2 m^3 s^{-1}$ is input into the model in models runs referred to as 'background melt' to simulate the likely drainage of basal melt from the thick interior. Under background melt, the model is run until reaching steady-state (stable pressure, discharge and CSA) before supraglacial meltwater

input is initiated. 'Zero melt' refers to runs which are only subject to measured supraglacial melt.

3.3.2 Limitations of SWMM

The primary limitation of SWMM is its inability to represent distributed drainage systems or the transition between drainage systems. As discussed, subglacial drainage systems are thought to typically begin the season as distributed and channelize after the onset of melt. Attempts to represent a distributed system with bundles of smaller, wider conduits before the snow-line passes upglacier of the relevant input (Arnold et al., 1998) or with bundles of first-order conduits have proven ineffective and unmanageable for long model runs with short time-steps (Banwell, 2012). Additionally, the model does not allow the driving out of water from conduits to adjacent areas during high pressure, hydraulic jacking or interaction between the subglacial system and dynamics. The setting of an arbitrary minimum conduit diameter is to some extent unrealistic, but studies have suggested that conduits are unlikely to completely shut-down during the summer (Colgan et al., 2011).

Conduit adjustment equations do not account for conduit wall expansion through mechanical ablation or the effect of water temperature, which is assumed to be equal to ice temperature. However, these factors are thought to be of relatively little significance (Spring and Hutter, 1981; Arnold et al., 1998; Banwell, 2012) and the equations are considered sufficiently representative for the purposes of the study.

However, the discussed limitations are not thought to critically detract from the usefulness of the model for the present study. While these limitations may compromise the production of observable, absolute values, they are not expected to compromise the ability of the model to produce useful information on the nature of, and temporal and spatial variations in, the subglacial drainage system of Petermann Glacier.

Chapter 4: Results

This section will present results from each stage of the modelling process. The results presented are those necessary to explain the choices made in the modelling process at each stage and to illustrate the themes discussed.

4.1 Modelling supraglacial melt

The melt seasons, considered to be day 121 to 273, of 2003 and 2004 were initially considered for analysis due to availability of temperature data for these years.

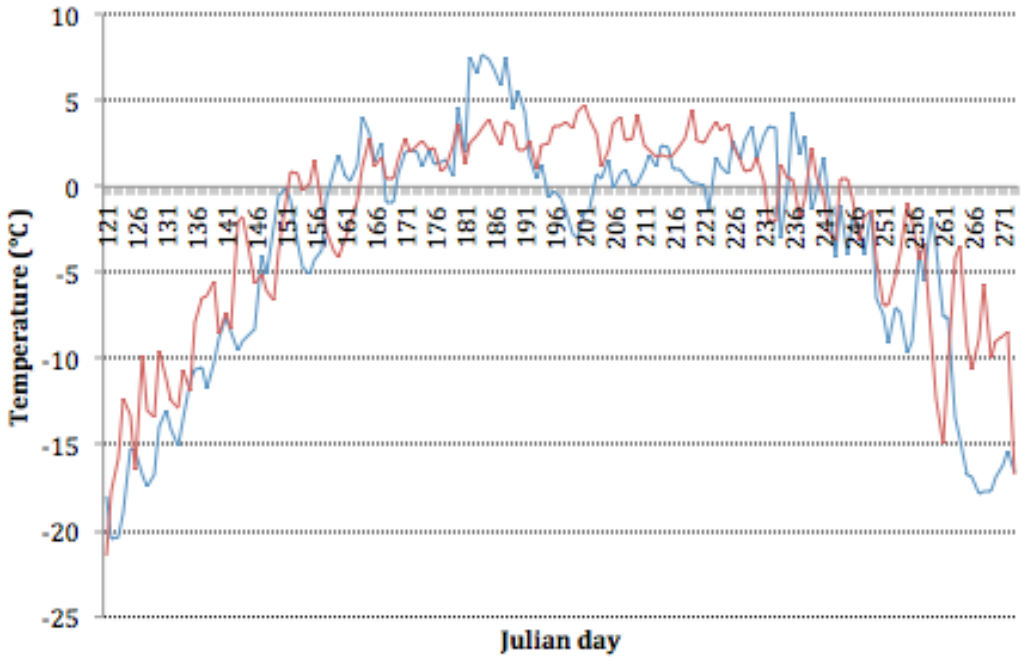

Figure 4.1: *Mean daily temperature plotted for 2003 (red) and 2004 (blue) from day 121 to 273.*

The melt season of 2004 was chosen for analysis after consideration of temperature across the season at Petermann Glacier. Although 2003 had a higher mean melt season temperature, at -2.1°C compared to -3.4°C, 2004 had a higher peak, of 7.7°C on day 184, compared to a peak of 4.7°C in 2003 (fig. 4.1). The melt season appears to be longer in 2003, with the first positive daily mean temperature occurring on day 152 and the last on day 245, a period of 94 days.

The first positive daily mean temperature in 2004 was on day 159 and the last on day 241, a period of 83 days. A total of 79 days were positive in 2003 compared to 68 in 2004. There was a continuous stretch of positive temperatures in 2003 from day 164 to 211, while in 2004 temperature dipped below freezing on three occasions over the same period, with a notable cold spell from day 195 to 202. This suggests that melt would have occurred over a longer period and on more days in 2003 compared to 2004. However, 2004 was also notably characterised by a distinct warm period of 10 days from day 182 to 191 and a second cooler, but distinct, warm period around days 221 to 239. During this period, temperatures averaged 6.4°C and ranged from 4.4°C to 7.7°C, with eight of these days above the peak temperature for 2003. As studies suggest that it is not the mean seasonal temperature, but periods of intense meltwater input that causes changes in the subglacial drainage system (van de Wal et al., 2009; Shepherd et al., 2009; Bartholomew et al., 2010; 2011a; 2012), the subglacial drainage system was deemed more likely to be of significance in 2004, and therefore the study proceeded with this year.

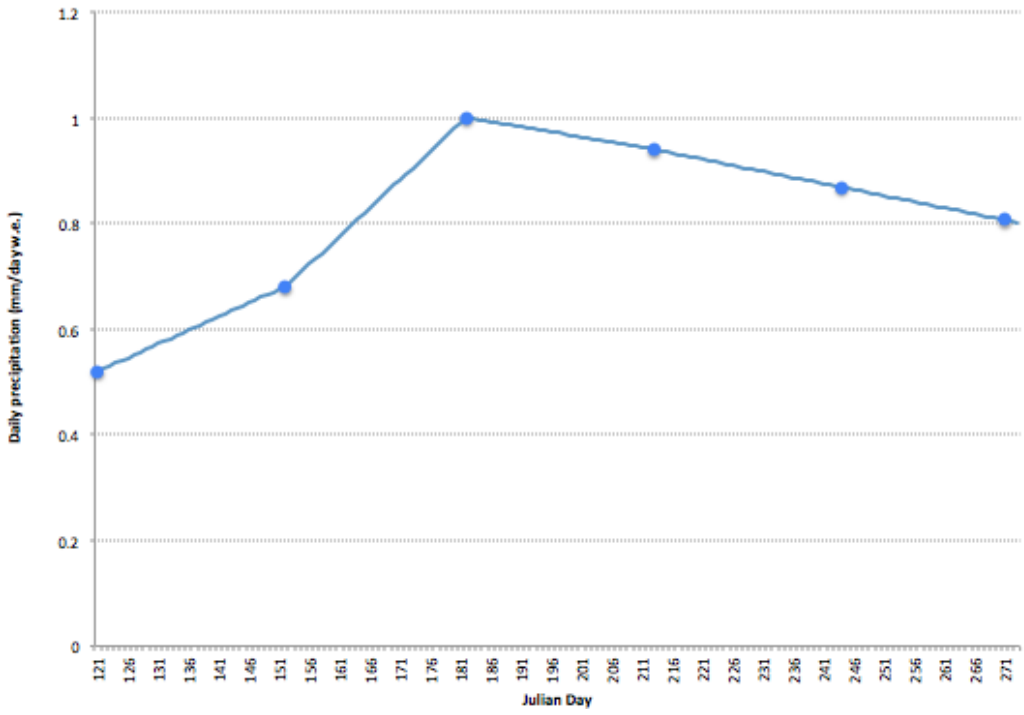

Figure 4.2: *Daily precipitation interpolated by bilinear interpolation between points for the beginning of each month (dots) taken from Hakuba et al. (2012).*

Estimated precipitation for the 2004 melt season is shown above (fig. 4.2) shows precipitation increasing until the beginning of July before falling towards the end of the season. Precipitation increases from 0.52 mmd^{-1} w.e. on day 121 to 1.00 on day 182, before steadily decreasing for the rest of the season.

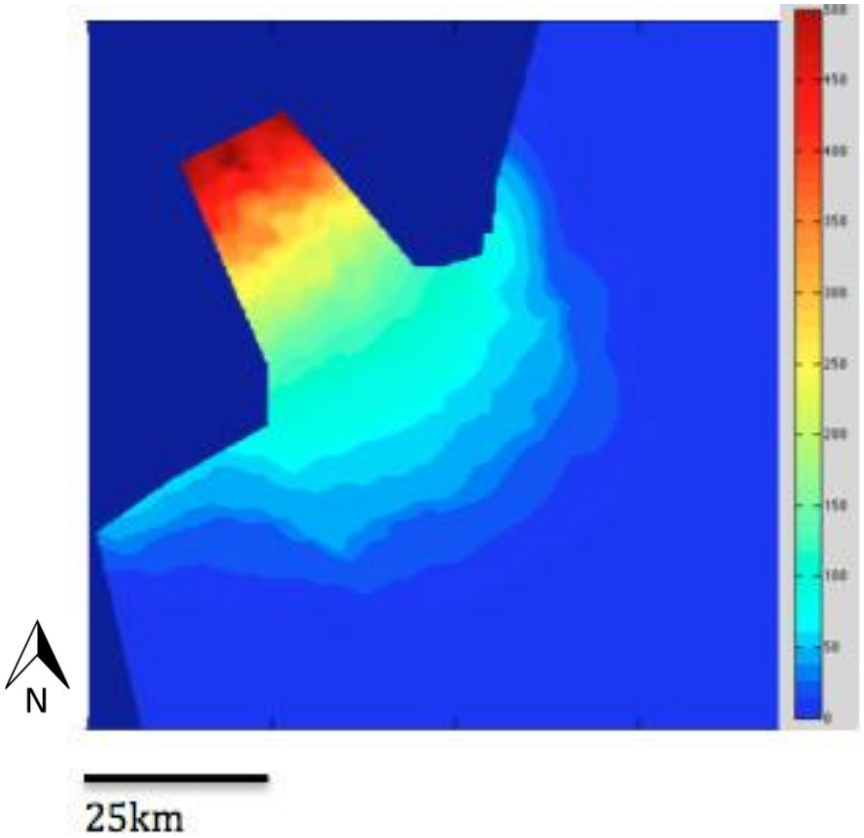

Figure 4.3: *Cumulative melt (mm w.e.) across the study area in the summer of 2004.*

Fig. 4.3 shows the distribution of melt across the study site for the whole melt season. The entire study site is thought to be part of the Petermann Glacier drainage zone, based on analysis of supraglacial water routing and subglacial routing under different k-value scenarios. The maximum ablation zone extent extends approximately 30km from the grounding line. As expected, melt generally increases towards the glacier trunk and grounding line as elevation decreases, with patches of higher melt in topographic highs.

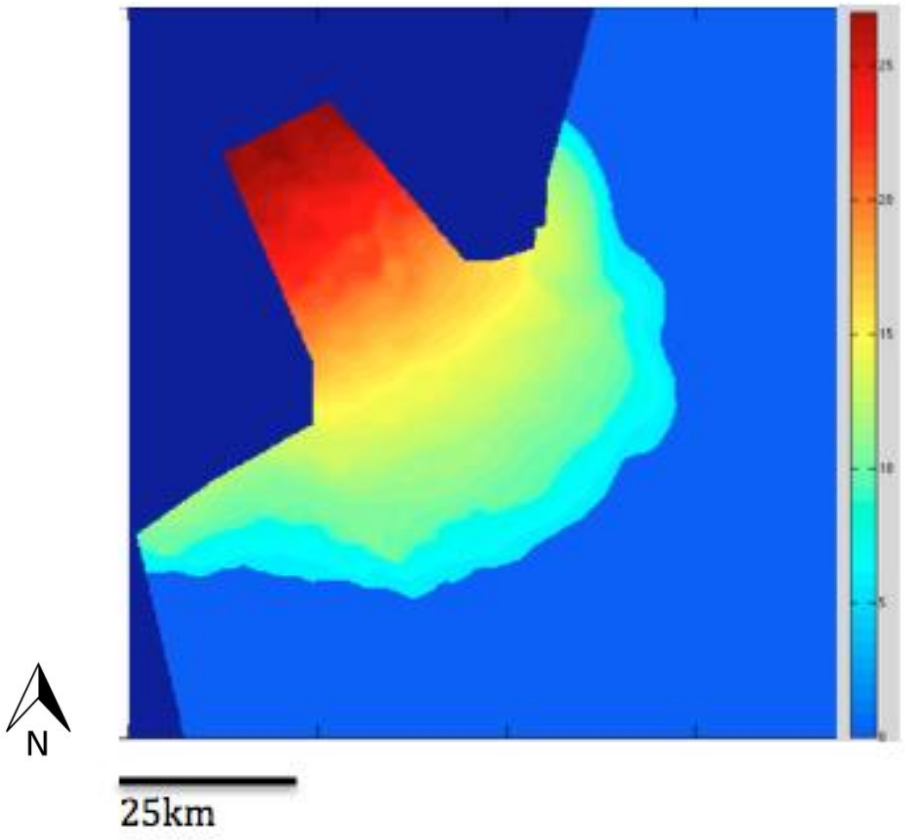

Figure 4.4: *Melt distribution on day 184 (mm w.e.)*

Fig. 4.4 shows the distribution of melt on day 184, the day of maximum melt when the mean daily temperature was 7.7°C. A total of 35345000m^3 occurred across the catchment on this day, with melt above 20mmd^{-1} across the main trunk of the glacier. Melt for the warm period between day 182 and 191 exhibited a daily mean of 9.97mmd^{-1} for all areas that experienced melt, compared to the daily mean of 7.76mmd^{-1} for days 159-241, when positive temperatures were recorded.

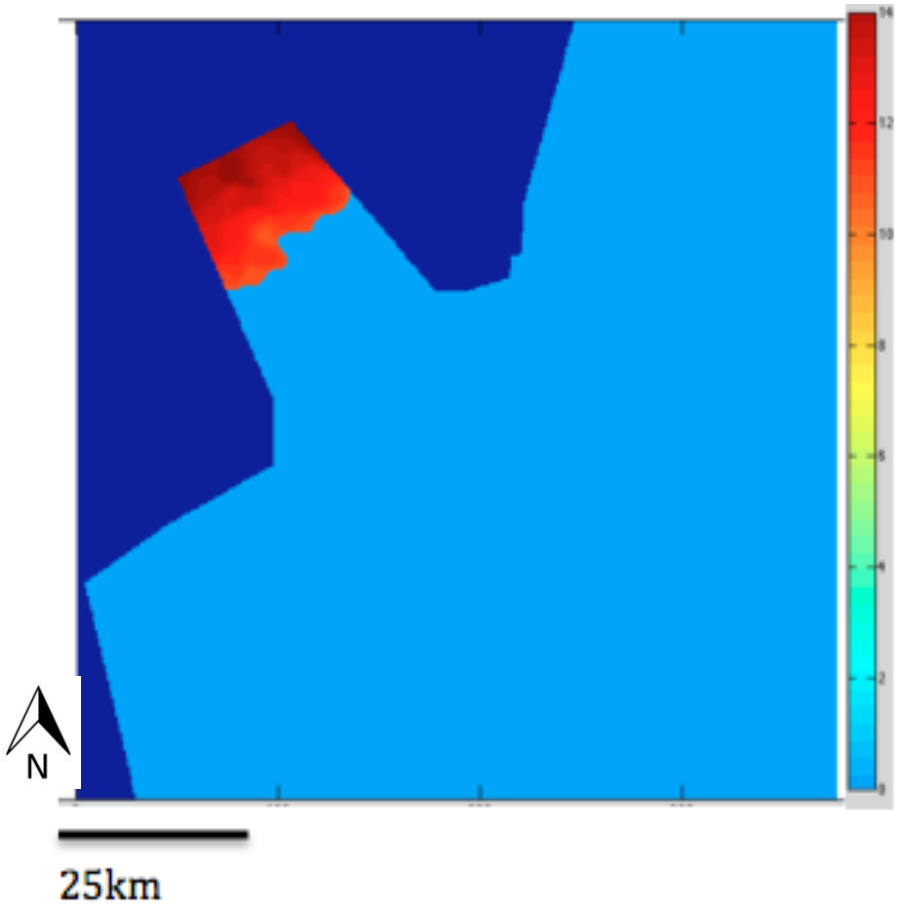

Figure 4.5**:** *Melt distribution on day 159 (mm w.e.)*

Fig. 4.5 shows the stark difference in melt distribution twenty days previous, on day 159, and is indicative of melt on days of low temperatures (0.86°C at the station). While no melt occurs across the majority of the catchment, ablation reaches 14mmd^{-1} at low elevations by the grounding line.

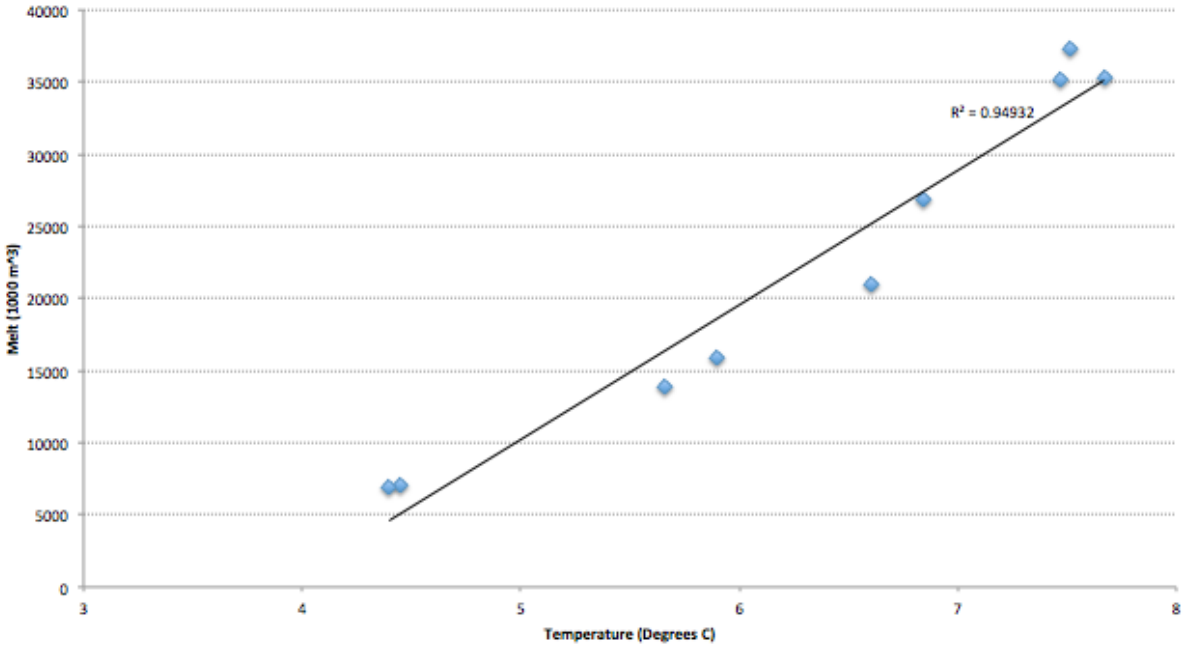

Figure 4.6: *Total melt for the catchment plotted against daily temperature for the warm period days 182-191*

A comparison of the daily mean melt value and daily mean temperature (fig 4.6) reveals a 0.95 correlation between the two. There is no way to validate the model results, but the high correlation between melt and temperature is promising as temperature data is the most reliable data for the site, due to the assumption of precipitation based on the literature. The high correlation is supported by many studies, such as Braithewaite and Oleson (1989), who found a correlation of 0.96 between positive air temperature sums and ice ablation.

4.2 Modelling supraglacial meltwater flow

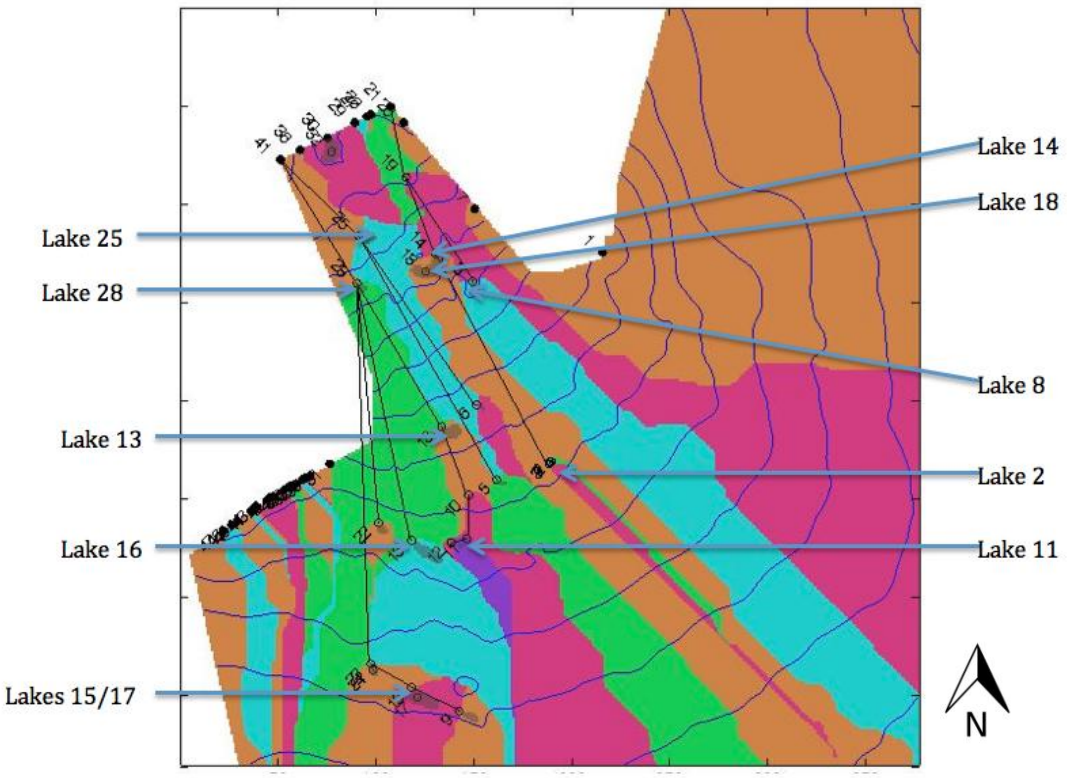

Figure 4.7: *A visual of the catchments (arbitrary colours) and connections between them (lines). Maximum lake extents are indicated by darkened areas and circles indicate the outlet point of a catchment. Dark circles indicate an outlet off the ice. Numbers are assigned to lakes and outlets. All draining lakes (cvol=500) are marked with blue arrows, as well as discussed lakes: lake 2 and lakes 15/17.*

Above, fig. 4.7 displays the supraglacial catchments, the connections between them and predicted maximum lake extents. Apart from nine small catchments to the south-west of the study area, and one outlet at the ice margin in the north-east, which appear to drain to the neighbouring ice margin, all meltwater appears to pond or drain onto the main glacier trunk. The model identifies sixteen ponding sites within the ablation zone, though lake 2 receives negligible meltwater supply. Some of these are single lakes, and some are the result of two lakes combining. Lakes 15 and 17, for example, could form a large double lake if supplied with sufficient meltwater. The model suggests that water on the main trunk and most of the area towards the interior drains to the ice-front in the absence of drainage to the base. It will then drain past the grounding line onto

the floating ice tongue where it may pond, penetrate the tongue through fractures or drain into the sea (Nick et al., 2012). This is with the exception of two eastern lateral outlets, around 3km and 15km from the grounding line.

On the main trunk of the glacier and the areas immediately upglacier towards the interior, catchments are elongated longitudinally and connected longitudinally, suggesting that overall meltwater runs linearly downglacier. In the southwest of the catchment, the neighbouring lakes 9, 15/17 and 22/23 in neighbouring catchments flow from east to west, suggesting that if the depressions maximum volume is exceeded before drainage is initiated, overspilling will results in a cascading flow between lakes and again onto 28 if 22/23 too overspills. Potential overspill from lake 22 and 16 would also flow into the catchment of lake 18, as would 13, which in turn is fed by the connected catchments of 10, 11 and 12. The catchments of lake 5 and 6 independently feed the catchment of lake 25 and the catchment of lake 2 feeds lake 14, which supplies lake 19.

4.3 Modelling lake filling and drainage

Three lake filling scenarios were considered. One in which lakes were considered to be open moulins for the whole season, i.e. cvol=0, with any meltwater routed to it immediately draining to the base. Next, two lake volume drainage thresholds were considered, cvol=500 and cvol=1500.

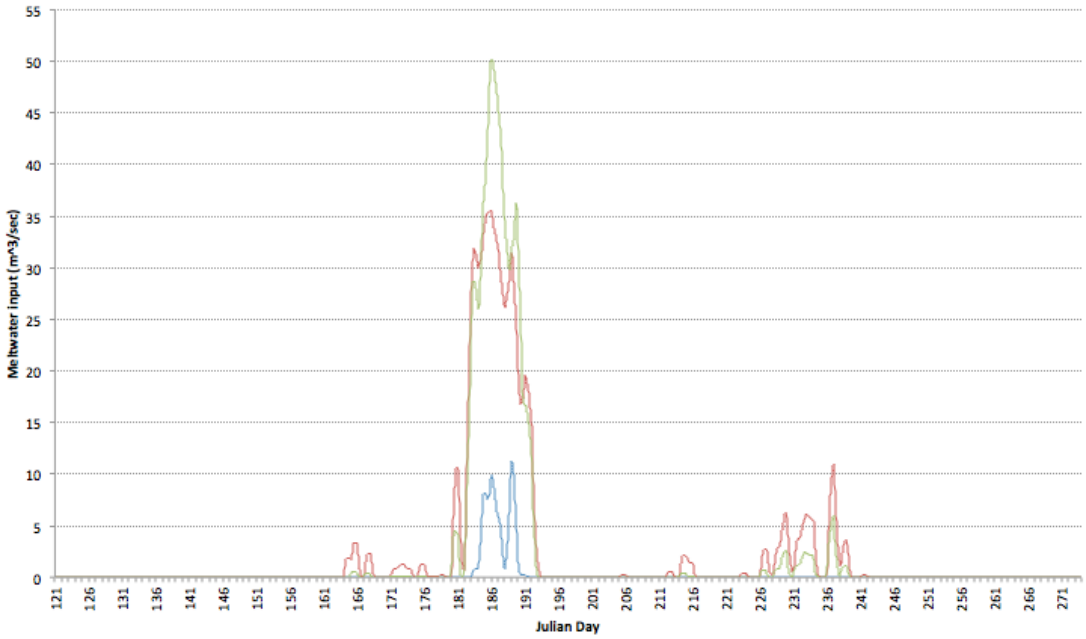

***Figure 4.8**: Hourly meltwater input into selected lakes in an open moulin scenario across the season, two downglacier lakes (lake 28 [green] and lake 25 [red]) and one upglacier lake (lake 16 [blue]).*

Meltwater flow into the depressions is low, below 4m^3s-1 at all sites during the early stages of melt, from day 163 (fig. 4.8). Evidently altitude largely determines melt input with lower lakes receiving water earlier and generally in large quantities. A large spike occurs accompanying high temperatures, and peaking at 50.4m^3s^{-1} at Lake 28 and remaining over 50.0m^3s^{-1} for five hours. This lake is at a relatively low elevation of 327m but is higher than other lakes, including nearby lake 25 at an altitude 98m lower, that peaks at 35.6m^3s^{-1}. This shows the importance of catchment area as well as temperature in determining melt input. Later in the season, melt input fluctuates at a low level and ceases at all lakes for 9 days from day 195. A second warm period causes another distinct input spike at lower elevations, peaking at 11.0m^3s^{-1} at Lake 25 on day 237.

4.3.1 Lake drainage

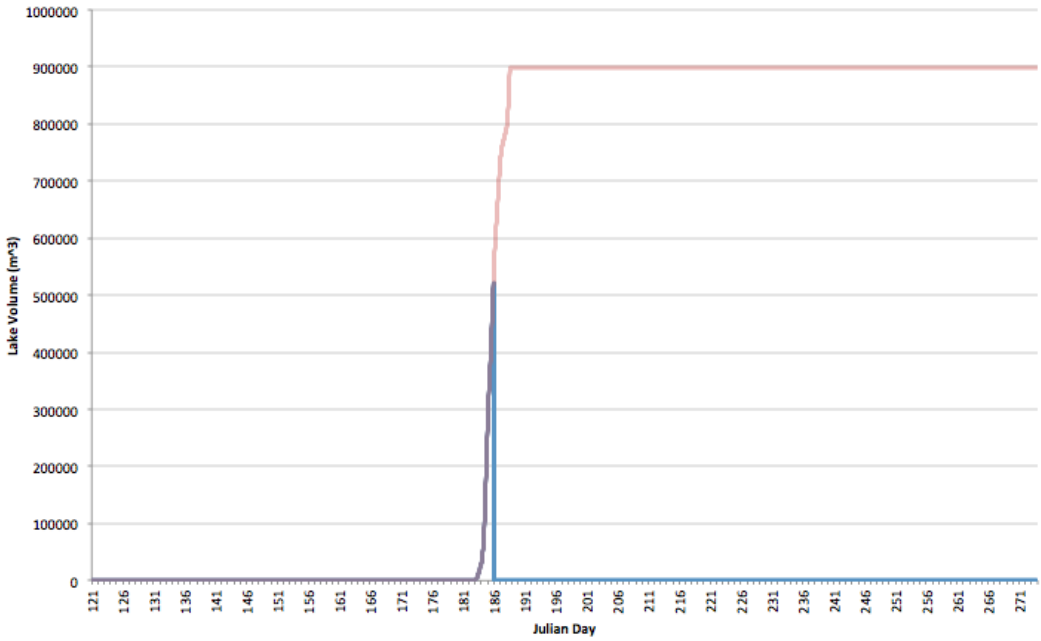

Figure 4.9: *Lake 11 volume through the season at cvol=500 (blue) and cvol=1500 (red) scenarios.*

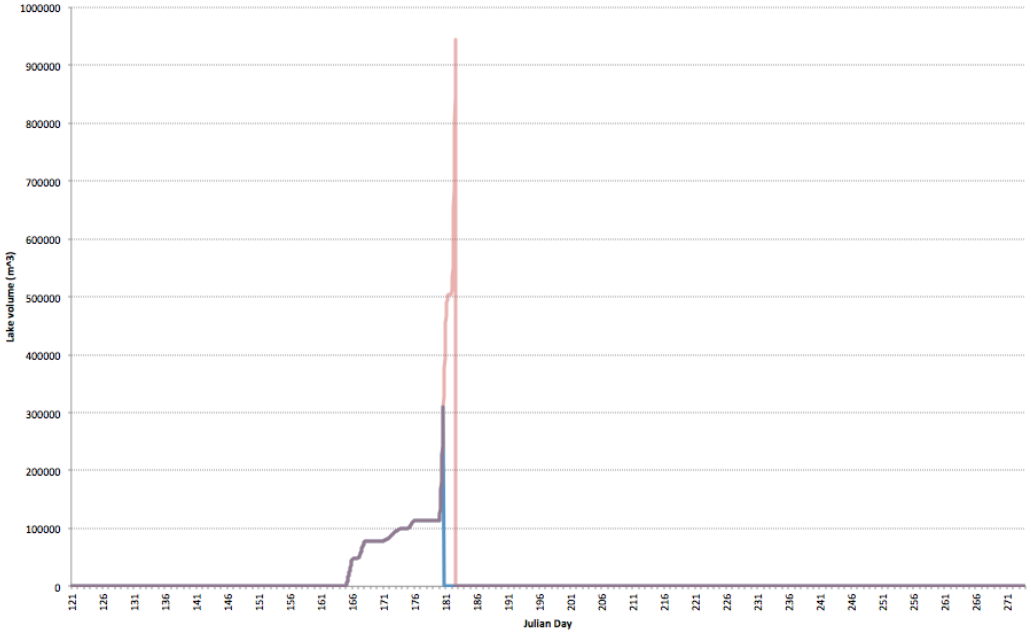

Figure 4.10*: Lake 28 volume through the season at cvol=500 (blue) and cvol=1500 (red) scenarios.*

Comparing fig. 4.9 and fig 4.10 shows the effect of varying the necessary volume of water needed to penetrate a crevasse to the base. Lakes drain at higher volumes with cvol at 1500, causing greater input event. However, two of the higher lakes, lakes 13 and 11 do not reach the sufficient volume to drain with cvol at 1500. Lakes 5, 6, 10 and 25 do not reach the necessary volume in either scenario. Lake 5 does not drain despite having a higher lake volume than lake 22 due to the relationship of cvol with ice thickness.

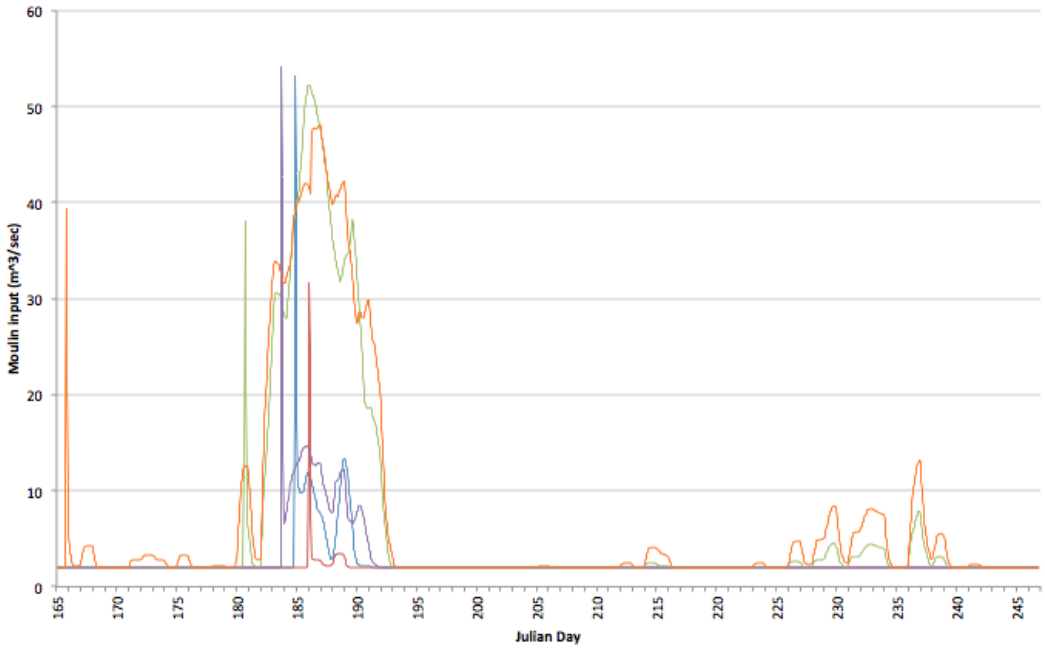

Figure 4.11: *Hourly moulin input hydrographs for the western channel (k=0.95, cvol=500) with background melt. Lake 16 (blue), lake 22 (red), lake 28 (green), lake 13 (purple) and lake 25 (orange) are shown, from day 165, the day of first drainage.*

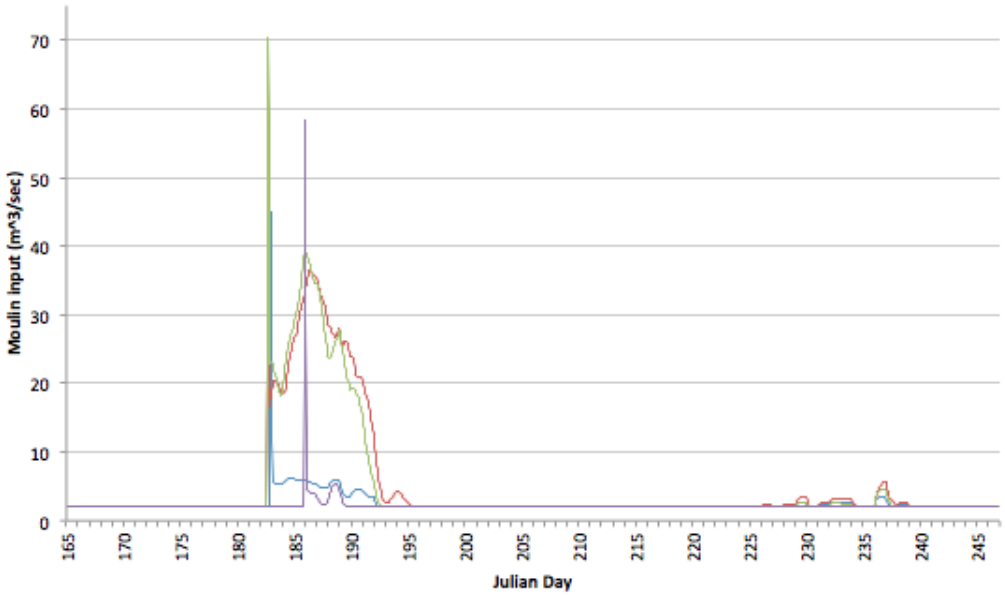

Figure 4.12: *Hourly moulin input hydrographs for the eastern channel (k=0.95, cvol=500) with background melt. Lake 18 (blue), lake 14 (red), lake 8 (green) and lake 11 (purple) are shown, from day 165, the day of first drainage.*

Hour	Lake 8	Lake 11	Lake 13	Lake 14	Lake 16	Lake 18	Lake 25	Lake 28
1	18.0	19.3	11.5	19.7	15.6	14.1	12.3	11.5
2	68.3	56.3	36.2	65.7	51.3	43.0	37.4	36.2
3	57.0	43.3	28.5	53.0	41.0	33.5	29.2	28.5
4	42.3	27.1	18.9	37.3	28.0	21.7	19.0	18.9
5	27.7	10.7	9.3	21.7	14.9	9.7	8.8	9.3

Table 4.1: *The lake drainage event (m^3s^{-1}) for each lake when cvol=500*

Figs. 4.11 and 4.12 show the variation in moulin input hydrographs between the western and eastern channel for the chosen cvol=500 drainage scenario. Most distinct is the greater temporal spread of drainage in the western channel both in the first warm period and with the early drainage of lake 25, and generally the greater magnitude of input into the western channel. However, the eastern channel experiences a greater peak drainage event, with lake 8 exceeding $70m^3s^{-1}$, while no lakes reach $60m^3s^{01}$ in the western channel. Table 4.1 shows how the drainage volume is distributed across the 5-hour drainage event

4.4 Analysis of lake evolution from Landsat data

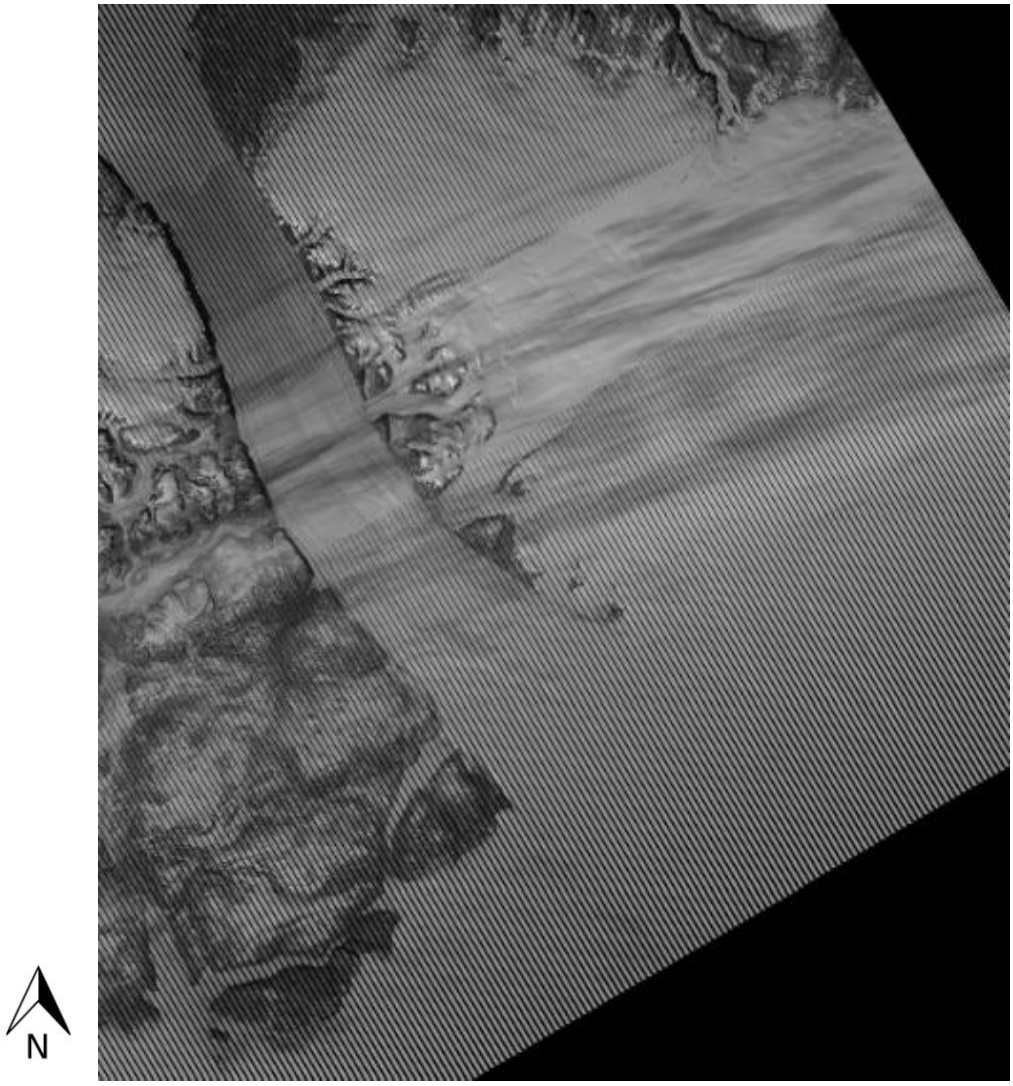

***Figure 4.13**: Landsat 7 ETM+ (band 4) for day 156, 2004, before ponding is evident.*

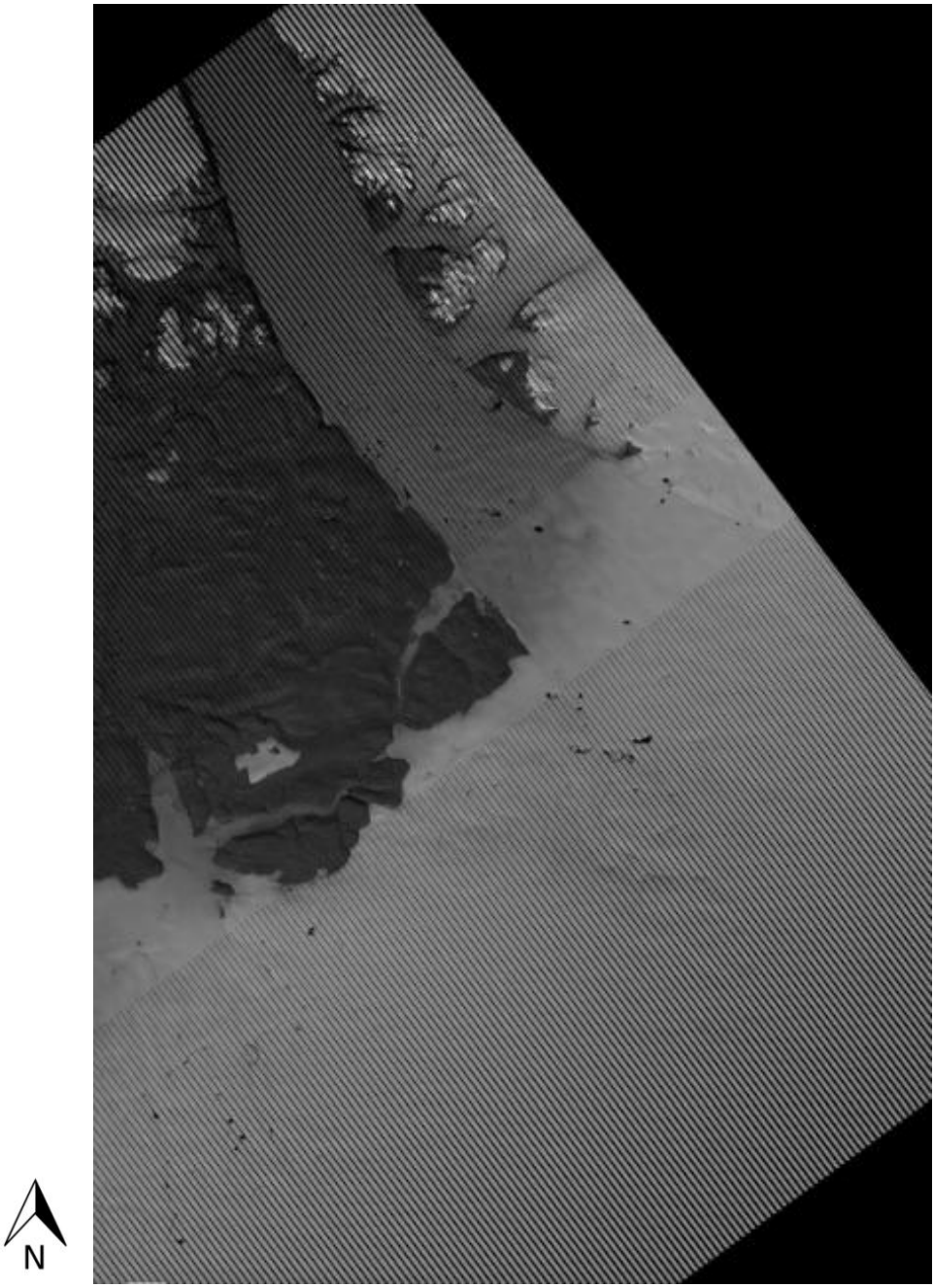

***Figure 4.14**: Landsat 7 ETM+ (band 4) for day 208, 2004, the maximum extent of ponding in the imagery.*

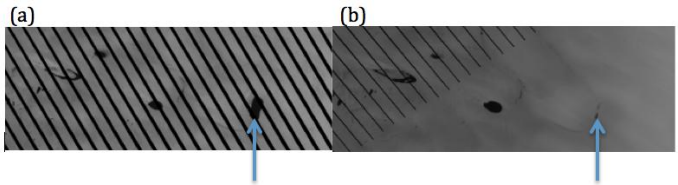

***Figure 4.15:** Landsat 7ETM+ (band 4) images for day 195 (a) and 201 (b). The blue arrows indicate the same site on the two dates. This site is at the approximate location of lake 11 in 2004.*

Analysis of satellite imagery of the study area from 2004 reveals an upglacier expansion of lakes. Images for day 156 show no ponding anywhere on the ice, this being shortly before initiation of melt. By day 163 there was prominent ponding in what appear to be fractures, north of the grounding line run in a longitudinal line marginally west of the centre and are orientated approximately 15° to ice flow and sized ~60m by 150m, with longer ponds by the western margin but fade upglacier with none being evident above the grounding line. By day 195, ponding is clearly visible across the glacier trunk, primarily towards the western margin, with a large patch of ponds approximately 1km from the western margin by the grounding line and west of the centre. By this point, ponding is also evident in the western part of the interior. The disappearance of a lake (fig.4.14) between day 195 and 201 suggests the occurrence of rapid drainage. Between day 201 and 208 lakes near Area Lower reduce in size, but ponding does not extend to Area Upper in 2012 images.

4.4.1 Modelling of 2012 volume

The evolution of lakes across the study area developed upglacier, with lakes forming and draining at lower elevations earlier in the season than at higher elevations. The different stages of evolution are highlighted by the fact the area of ponded water increased at the higher elevation Area Upper while it decreased at the lower elevation Area Lower.

4.4.2 Area Lower

(a)

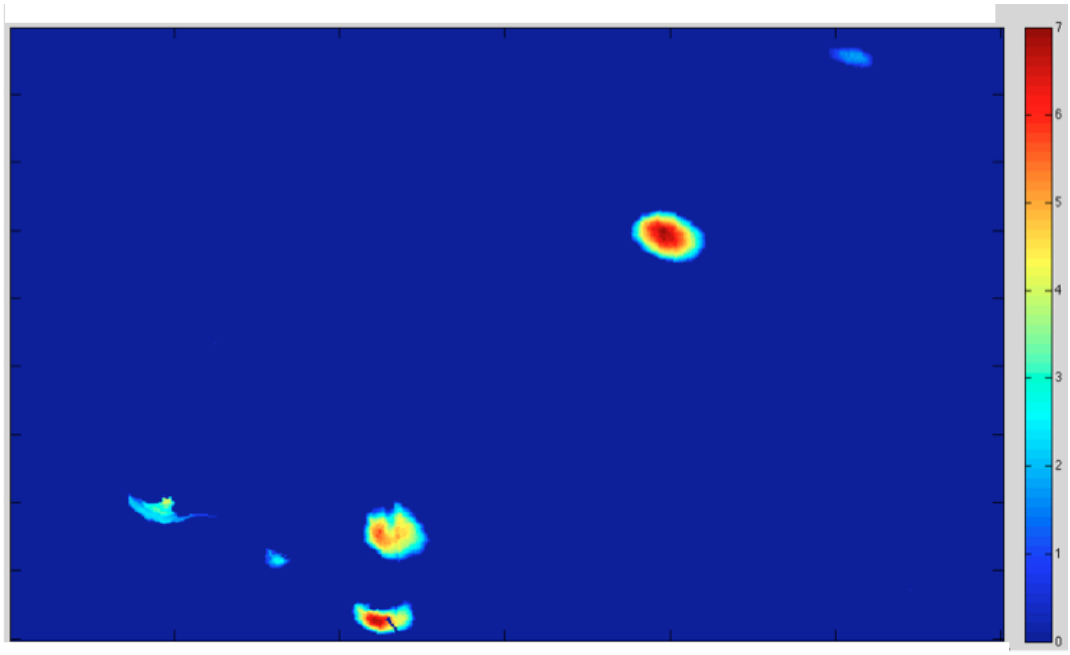

(b)

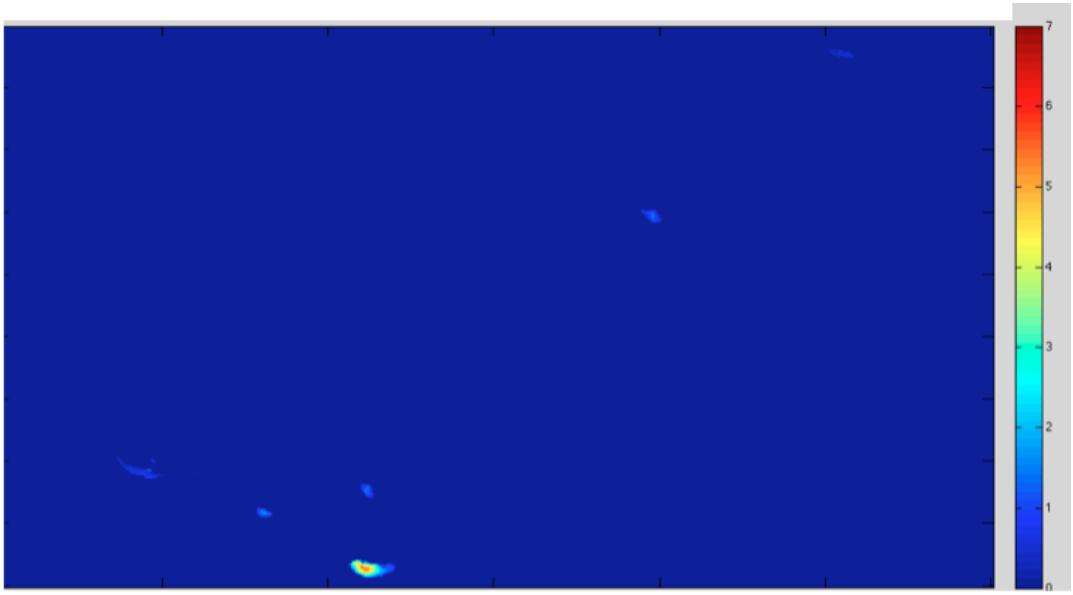

(c)

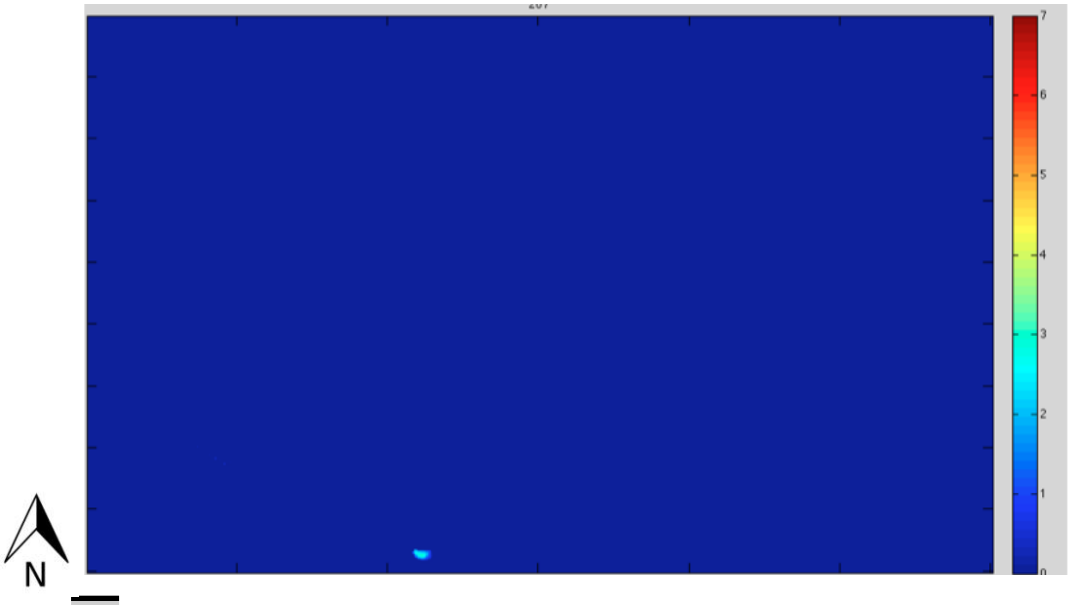

Figures 16(a, b, c): *Lake depth (m) of Area Lower on days 182 (a), 191 (b) and 207 (c).*

Within the period of study dictated by the availability of suitable imagery, Area Lower had already reached maximum melt extent by day 182 (fig. 16a). On this day, the mean depth was 3.07m and maximum depth 6.96m, with 3.66km^2 covered by ponded water, containing a volume of 11228832m^3. Ponding was concentrated into four lakes. By day 191 (fig. 16b), mean depth of the area had reduced by 56% to 1.35m and maximum depth by 21% to 5.53m. All six of the lakes had reduced in size and depth, with only the most southern lake still reaching a depth of over 3m. Over the following 16 days, by day 207 (fig. 16c), five of the six lakes ceased to contain any meltwater at all, with only the most southern still existing, with a mean depth of just 1.40m and maximum depth of 2.97m. By day 207, ponded meltwater occupied just 2.6% of the area it did on day 182.

(a)

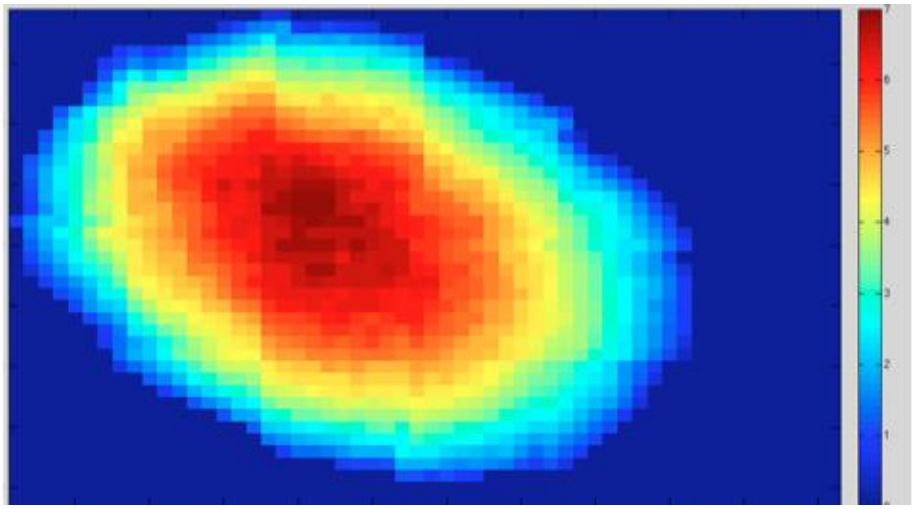

300m

(b)

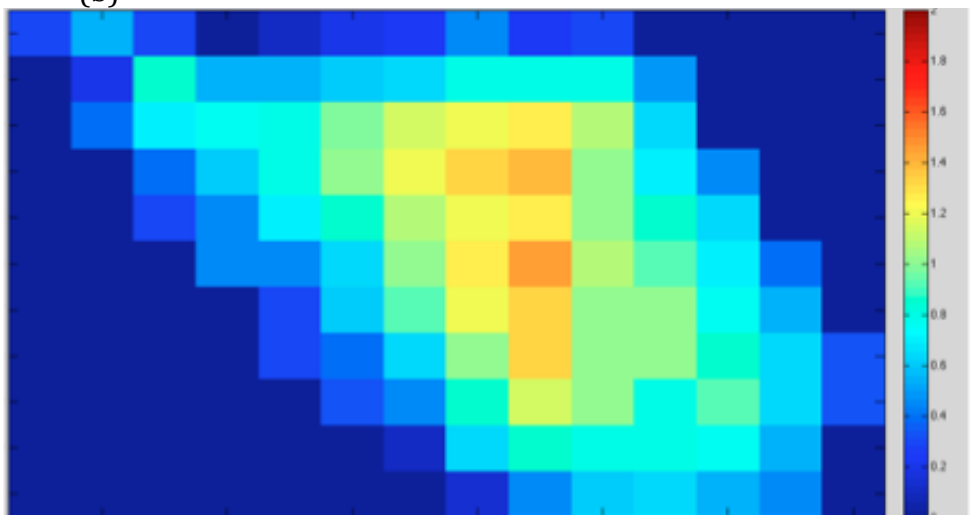

50m

Figures 4.17 (a, b): *Lake depth (m) for the largest lake in fig. 4.16a on days 182 and 191.*

A particular lake, corresponding to lake 13 in the surface routing model, is focused on in the above figures (figs 14a,b). The lake reduced in area by 92.3% between day 182 and day 191, reducing from a mean depth of 3.86m and maximum depth of 6.96m at its centre, to a mean depth of 0.73m and maximum depth of 1.44m. This represents drainage of 84% of its volume.

4.4.3 Area Upper

(a)

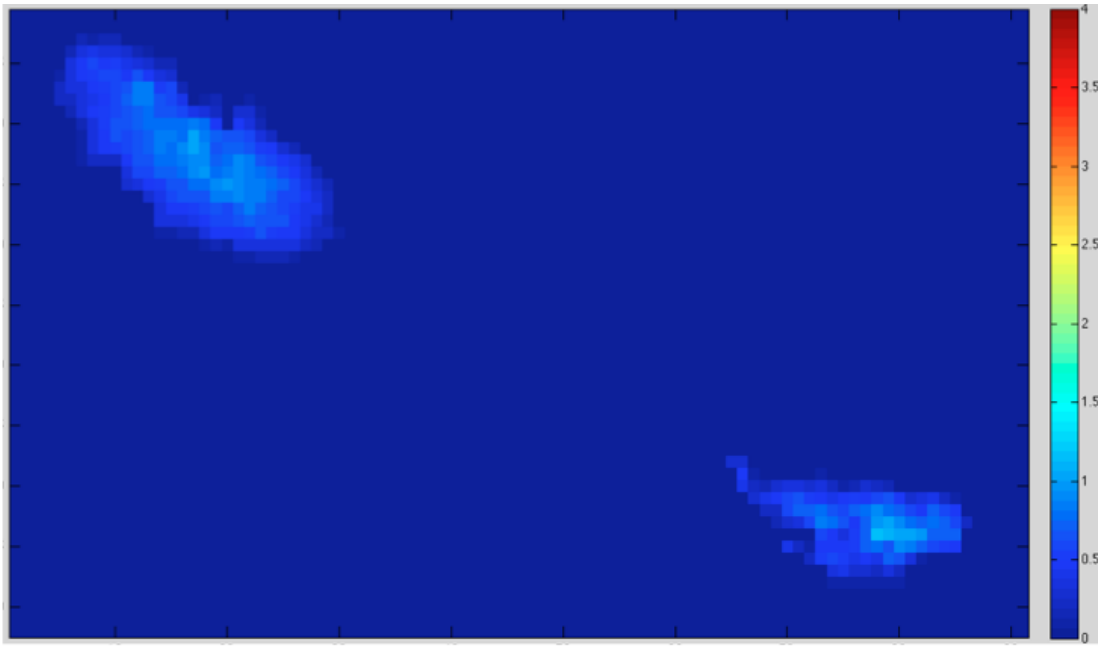

(b)

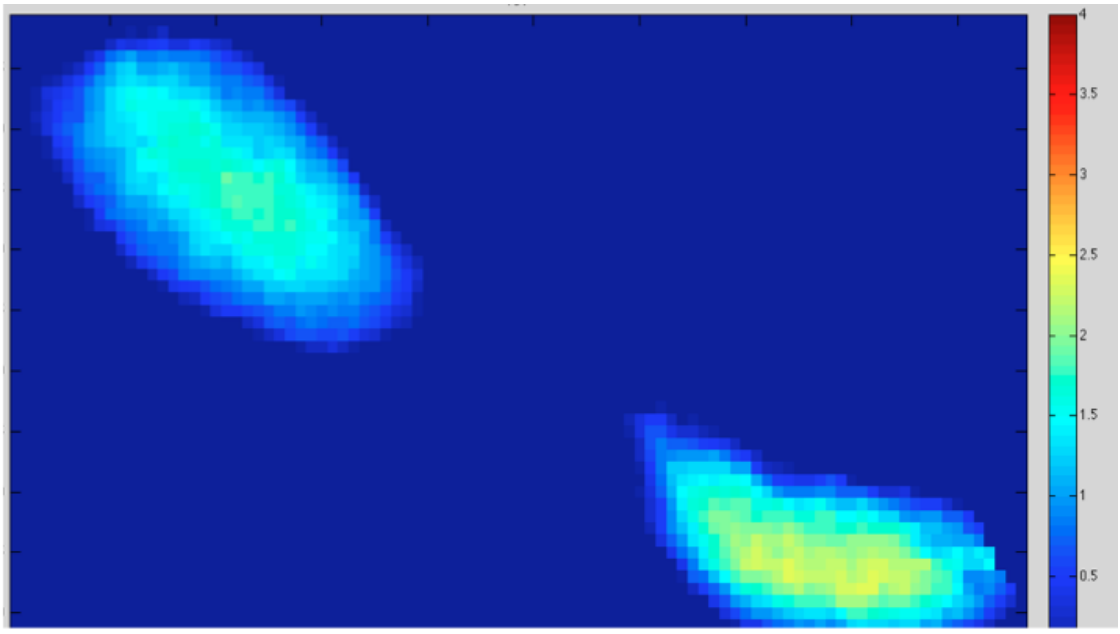

(c)

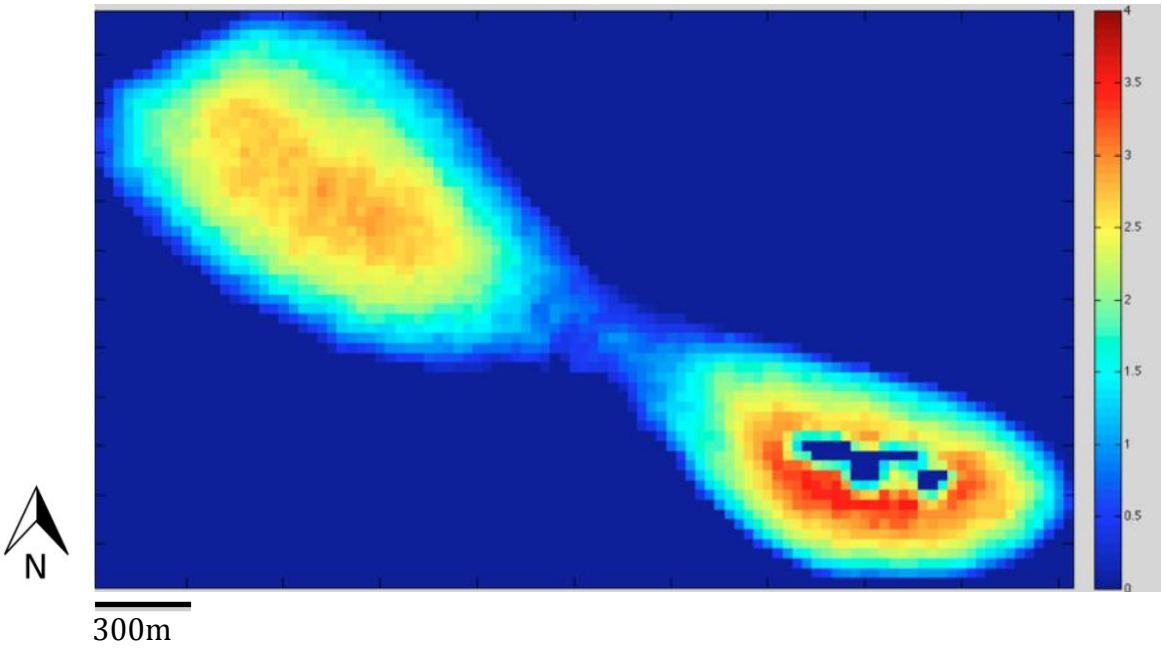

Figure 4.18 (a ,b, c): Area Lower lake depths on days 186 (a), 191 (b) and 209 (c). 'Lake X' is to the east and 'Lake Y' to the west.

Over the same period that lake 13 lost 92.3% of its area, at a higher elevation, Area Upper increased in area by 28% in just five days from day 186 to day 191. On day 186, meltwater was contained in two lakes, lake X with a mean depth of 0.45m and area of 0.027km^2 and lake Y also with a mean depth of 0.45m but area of 0.49km^2. By day 191, the mean depth of lake X had reached 1.25m and area of 0.42km^2 and lake Y had a lower mean depth of 0.99m but higher area of 0.57km^2. By day 209, both of the lakes in the area had expanded to the point of merging and forming one lake. This meant the lake occupied two depressions, with two separate areas of high depth connected by a thin, shallow area. For the combined lake, mean depth was 1.74m and it now contained a volume of 3258846m^3. However, the model produces an apparent depth of 0m at the centre of the eastern part of the lake.

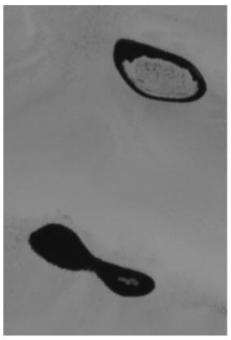

Figure 4.19: *Area Upper on day 209, showing the double lake merged from lake X and lake Y. A small ice-cover can be seen in the centre of Lake X. A neighbouring lake also displays ice-cover.*

However, inspection of the image (fig. 4.19) reveals that in fact an area of ice had begun to form on the surface of the lake, thus preventing the true depth being calculated and causing an underestimation of the volume of the new lake. The imagery also reveals ice similarly on the surface of a neighbouring lake.

4.5 Subglacial flow routing

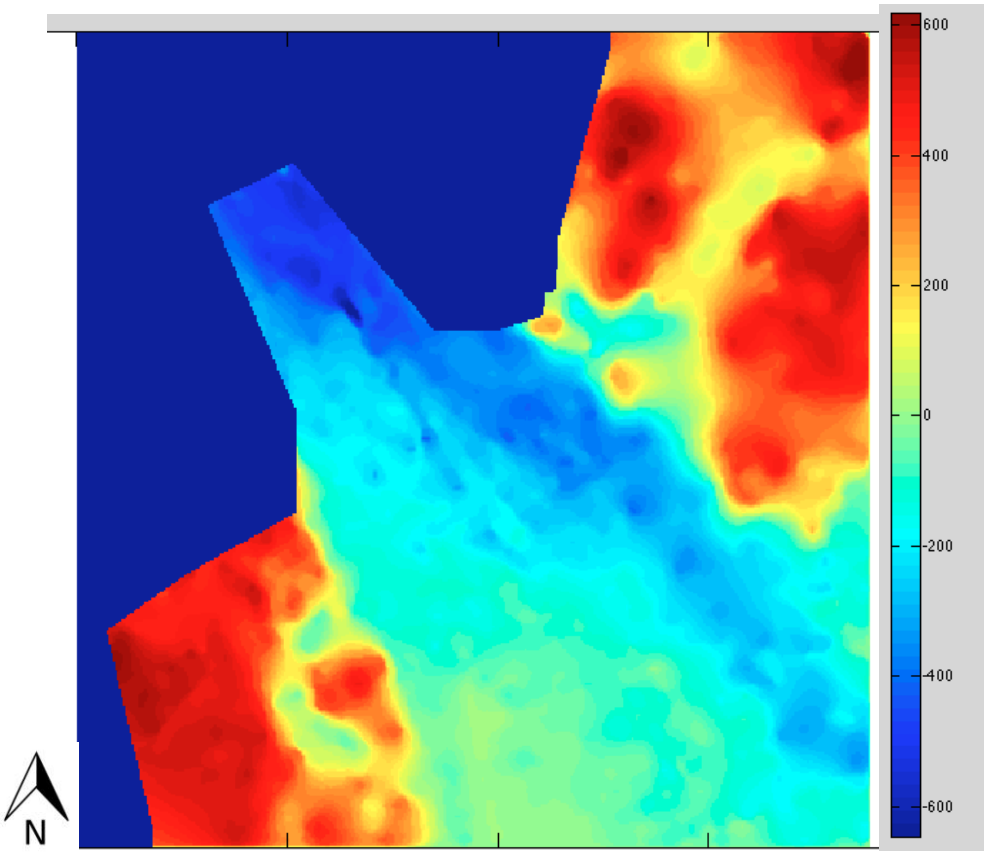

Figure 4.20: *Basal topography of the study site. The colourbar indicates elevation in relation sea-level.*

The main trough beneath the glacier extends to the south-east edge of the study area, shifting to the north/east as it extends towards the interior, developing into a distinct channel (fig. 4.20). The trough is up to 410m below sea-level, and parts of the bed remain below sea-level all the way along the trough. All areas immediately upglacier the from the trunk are below sea-level, with patches of low-elevation ice in the surrounding higher areas, most notably to the west.

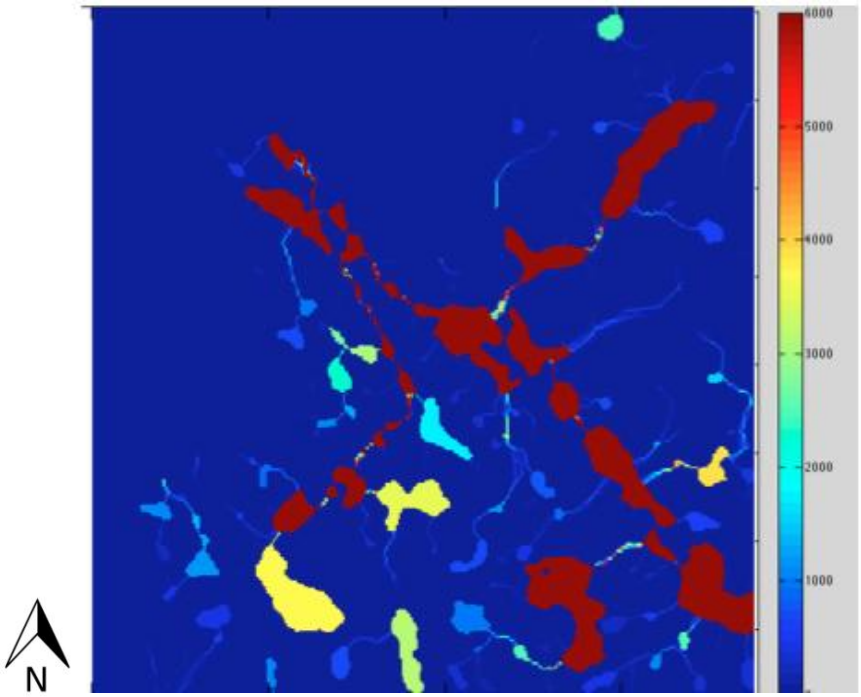

Figure 4.21: *Flow accumulation along the glacier bed when k=0. Colourbar indicates number of upstream cells. Large area indicate pooling.*

Forcing drainage in a basal scenario of k= 0 would mean drainage follows the basal topography, as demonstrated by fig (4.21). In such a case, many subglacial lakes form in depressions as water is not driven out under pressure. Lakes and drainage mainly form along the below-sea level trough on the eastern side of the glacier, identified in fig 4.20. A drainage path to the west connects a distinct area of low topography to the west, which also exhibits ponding in this scenario.

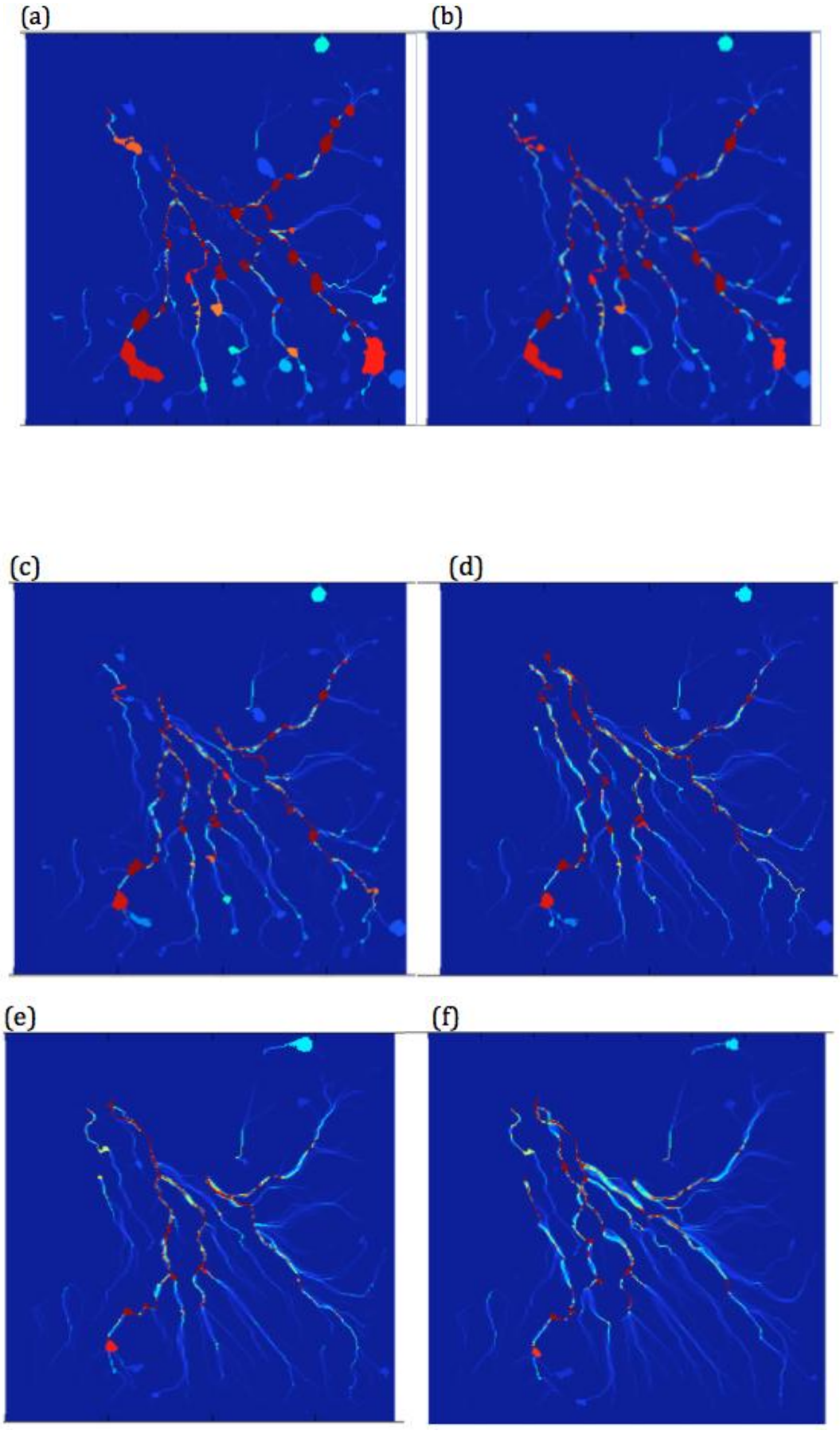
(a)
(b)
(c)
(d)
(e)
(f)

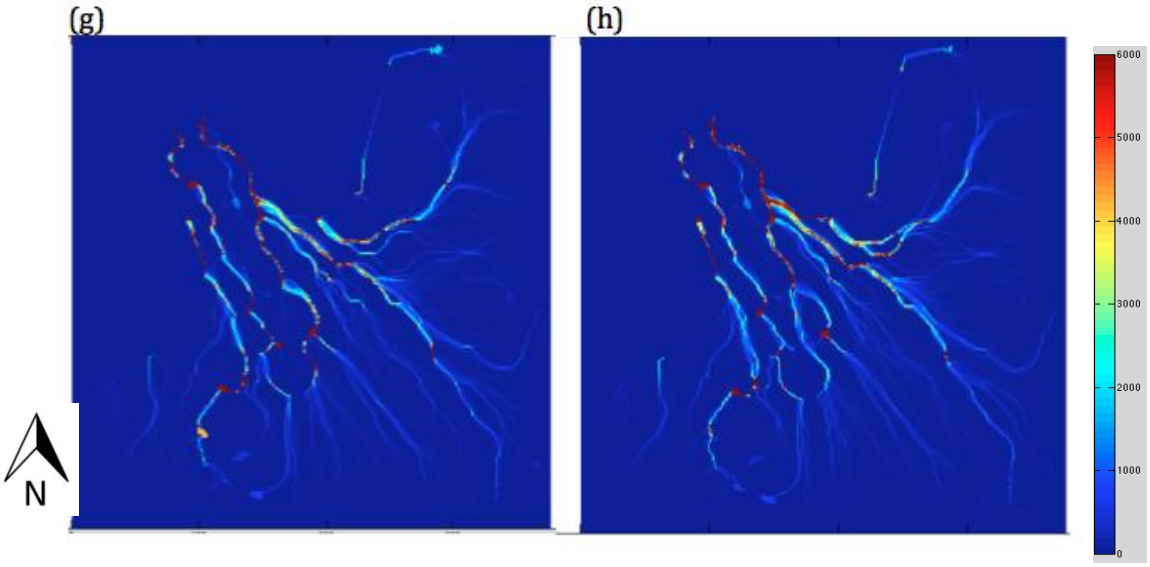

Figures 4.22 (a-h): *Flow accumulation along the glacier bed when k=0.5 (a), k=0.6 (b), k=0.7 (c), k=0.8 (d), k=0.9 (e), k=0.95 (f), k=0.975 (g), k=1 (h). Colourbar indicates number of upstream cells.*

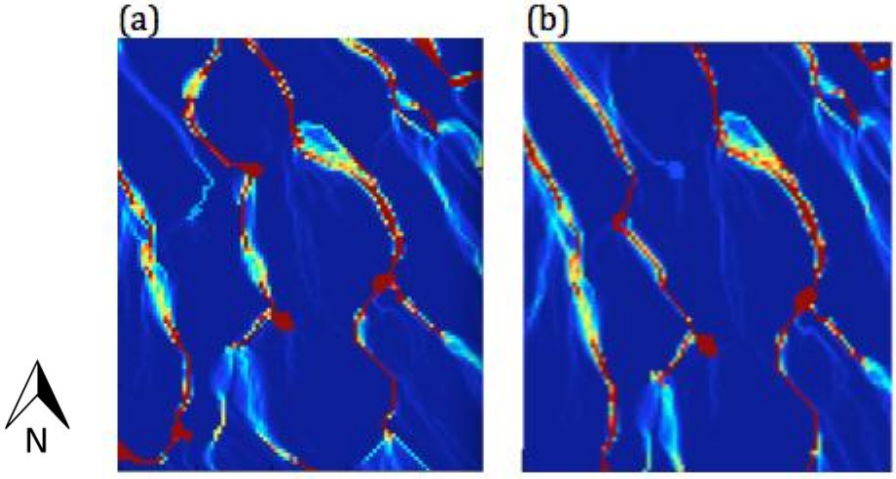

Figures 4.23 (a, b): *A close-up of the change in channel configuration between k=0.95 and k=0.975 systems that causes lake 11 to into the eastern channel (a) or western channel (b).*

As the k-values increase, figs. 4.22a-h show that the drainage path deviates from that dictated by the basal topography as in fig 4.21. Instead, drainage flows perpendicular to the equipotential lines as additionally forced by ice thickness. Notably, as pressure increases, the impact of overdeepenings is reduced as higher water pressures drive water. Two connected channels run down the west to form the 'western channel' and channels entwine along the east to form the 'eastern channel'. Drainage along the western channel increases with k-value. A distinct step-change in the configuration occurs between the k-values of 0.95 and 0.975 (figs 4.22e,f) with the pathway at a certain point (figs. 4.23a,b) switching

westward with a pressure increase. This small deviation leads to a whole channel, potentially fed by four lakes, diverting from the eastern channel to the western channel.

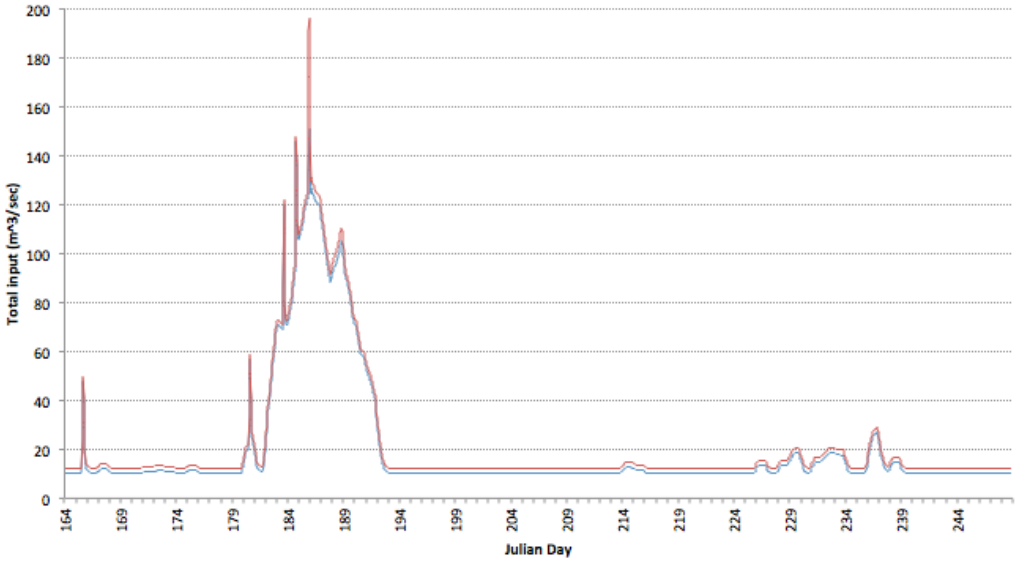

Figure 4.24: *Total hourly input into the eastern channel in a k=0.95 (blue) configuration and k=0.975 (red) configuration, with background melt.*

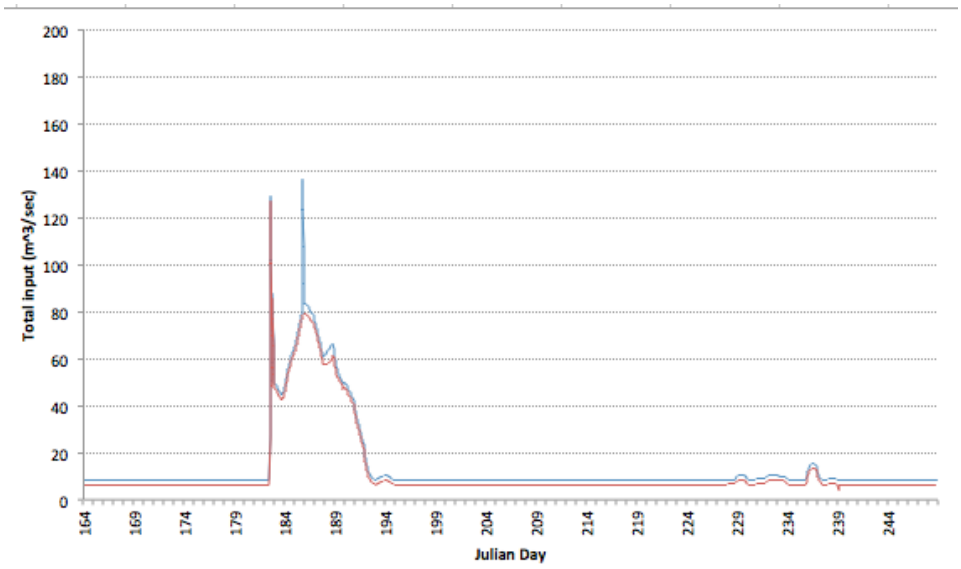

Figure 4.25: *Total input into the western channel in a k=0.95 (blue) configuration and k=0.975 (red) configuration.*

Figs. 4.24 and 4.25 show the differing bulk discharges for each channel depending whether a k=0.95 or a k=0.975 configuration is chosen. The difference is clearly more marked for the eastern channel, with lake 11 providing

peak drainage in the k=0,95 configuration. However, inclusion of lake 11 into the western channel appears to make little difference to the overall discharge pattern, with the drainage event just a spike on a the rising limb in bulk discharge amid three other drainage events, two of greater magnitude.

4.5. Subglacial drainage system configuration for model

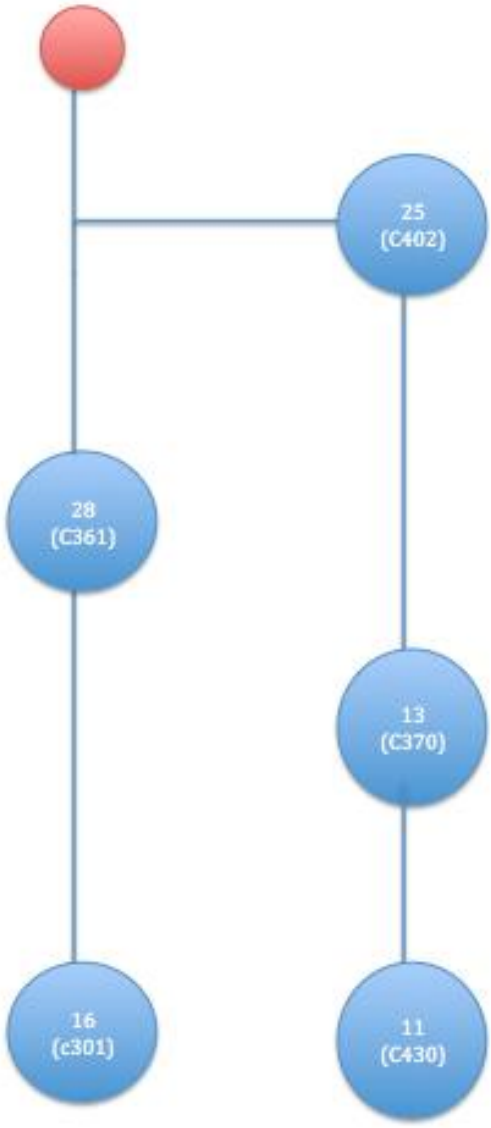

Figure 4.26a: *Simplified subglacial drainage model configuration for the western channel (k=0.975). Blue circles indicate moulins and lines are channels. The number indicates the corresponding lake number and the bracketed number the conduit leading from it. Red circle indicate the output point. The discussed conduit downstream of the confluence is C405.*

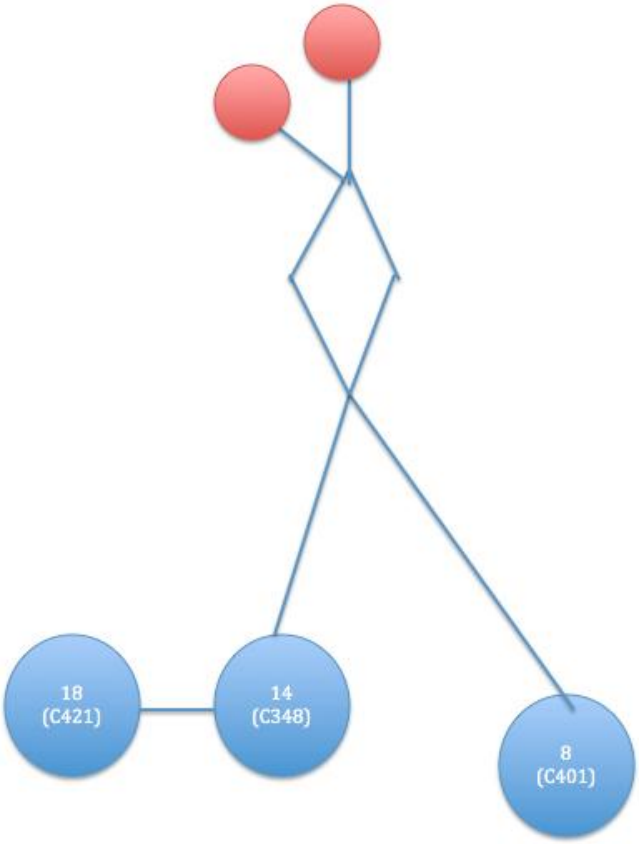

Figure 4.26b: *Simplified subglacial drainage model configuration for the eastern channel (k=0.975). Blue circles indicate moulins and lines are channels. The number indicates the corresponding lake number and the bracketed number the conduit leading from it. Red circle indicate the output point. C362 is to the left (west) of the first confluence.*

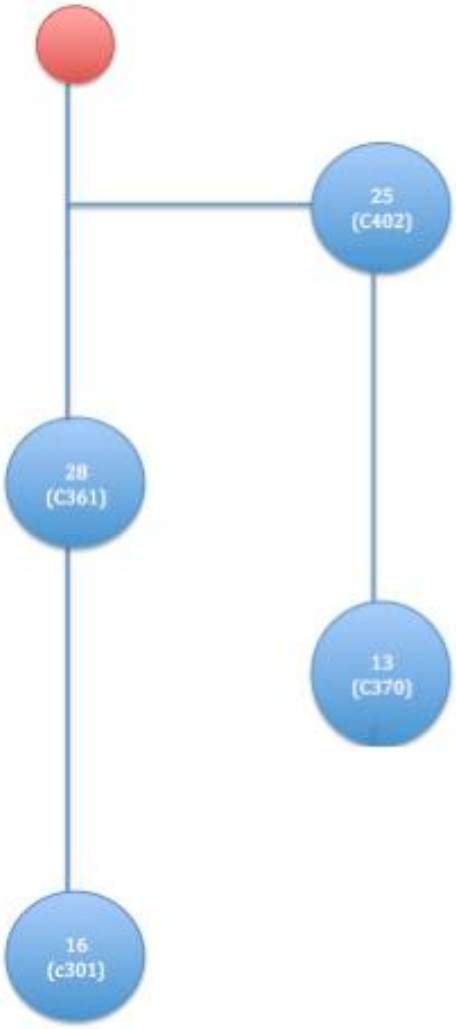

Figure 4.27a: *Simplified subglacial model configuration for the western channel (k=0.95). Blue circles indicate moulins and lines are channels. The number indicates the corresponding lake number and the bracketed number the conduit leading from it. Red circle indicate the output point. The discussed conduit C405 is downstream of the confluence.*

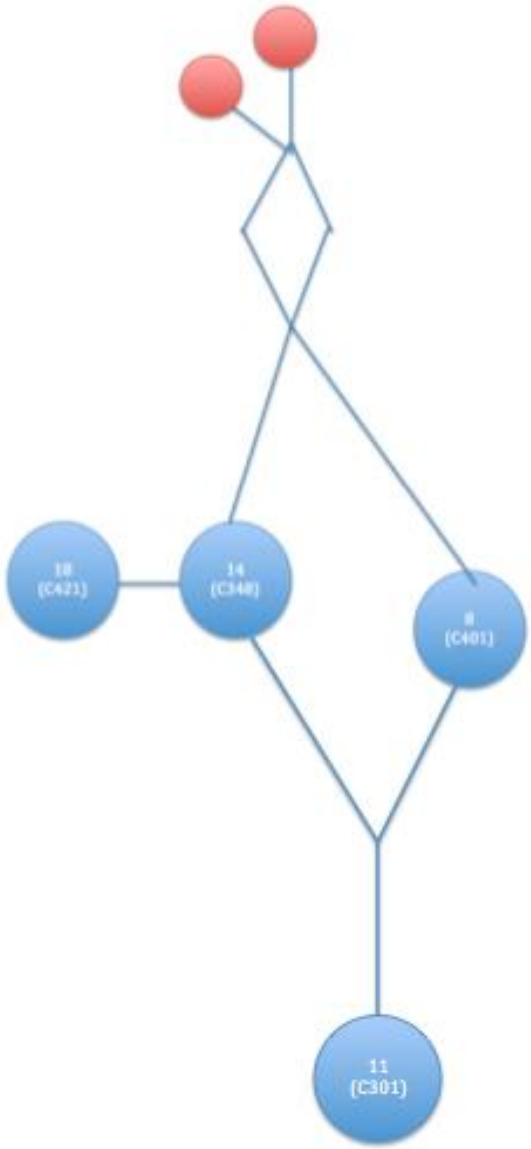

Figure 4.27b: *Simplified subglacial model configuration for the eastern channel (k=0.95). Blue circles indicate moulins and lines are channels. The number indicates the corresponding lake number and the bracketed number the conduit leading from it. Red circle indicate the output point. C362 is to the left (west) of the second confluence.*

Figures 4.27a-b and 4.28a-b show the construction of the subglacial drainage system model based on the flow route indicated by the subglacial flow routing model.

4.6 SWMM results

4.6.1 Comparing zero-melt and background-melt conditions

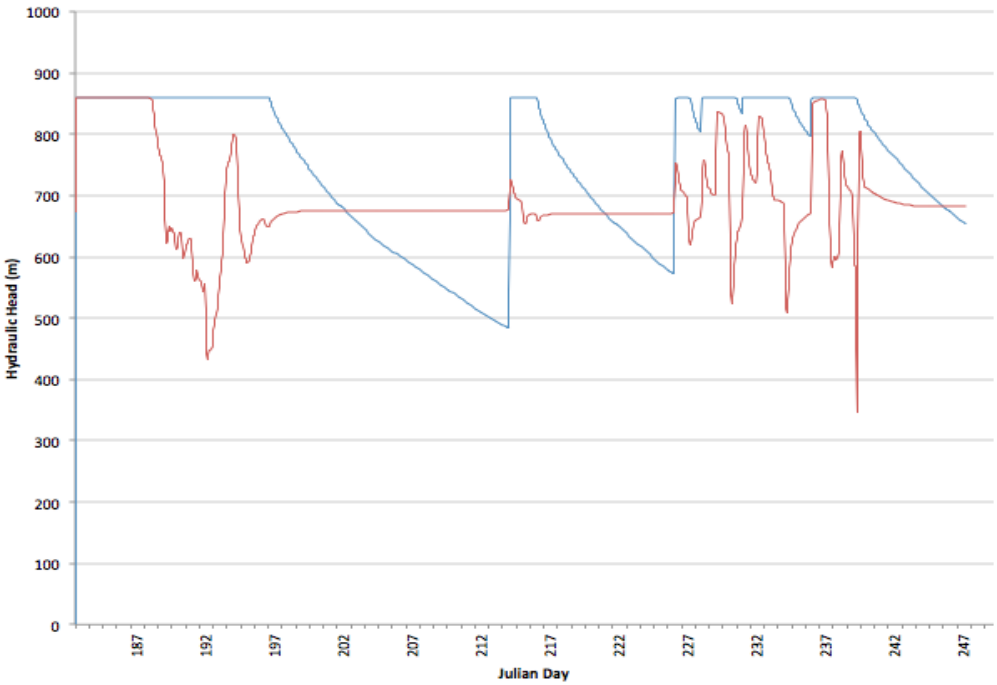

***Figure 4.28**: Hourly hydraulic head (m) at the conduit (C348) below Lake 14 from the point of lake drainage under background conditions of zero-melt (blue) and background melt of 2m^{3}s^{-1} (red)*

Fig. 4.28 shows the difference in the response of hydraulic head for the same junction, lake 14, under initial model conditions of zero-melt and of steady-state established by background melt. The hydraulic head initially reaches surface height, as meltwater input to the junction is initiated with the drainage of the lake. The system then remains unable to reduce the head with zero-melt for 746 hours compared to 131 hours with background melt. Head continued to fluctuate but does not reach surface height again under background melt. Under zero-melt, it reaches the surface again on the 33rd day, and remains at maximum for most of the period between 44 and 57 days after melt input.

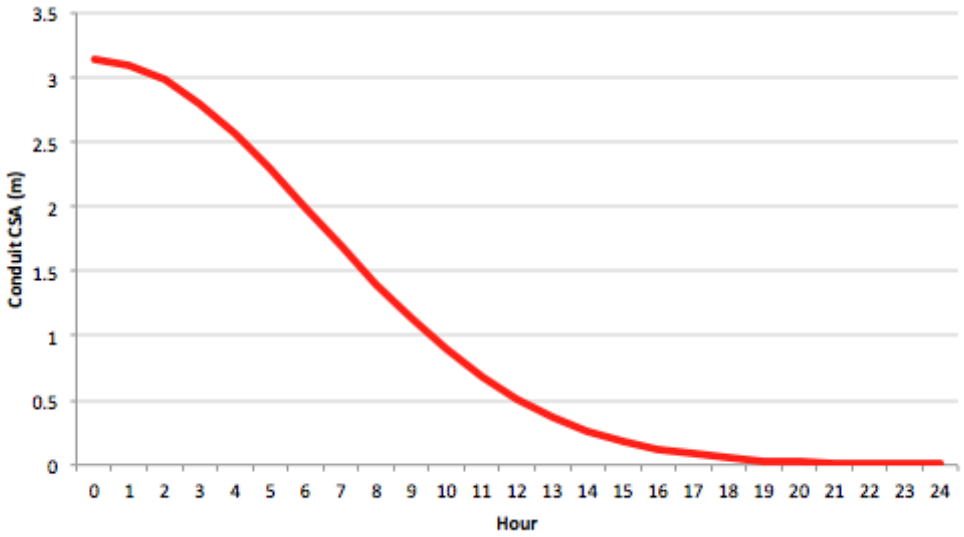

Figure 4.29: *The closure of conduit C348 below lake 14 under conditions of zero-melt from the point of spin-up period cessation, when conduits are allowed to close.*

Fig. 4.29 displays the rapid closure of the conduits under conditions of zero-melt. The conduit reached its minimum diameter by the 17th hour of conduit-closure incorporation in the model. This means that before meltwater arrives at the base, the conduits possess a CSA of just 0.008m.

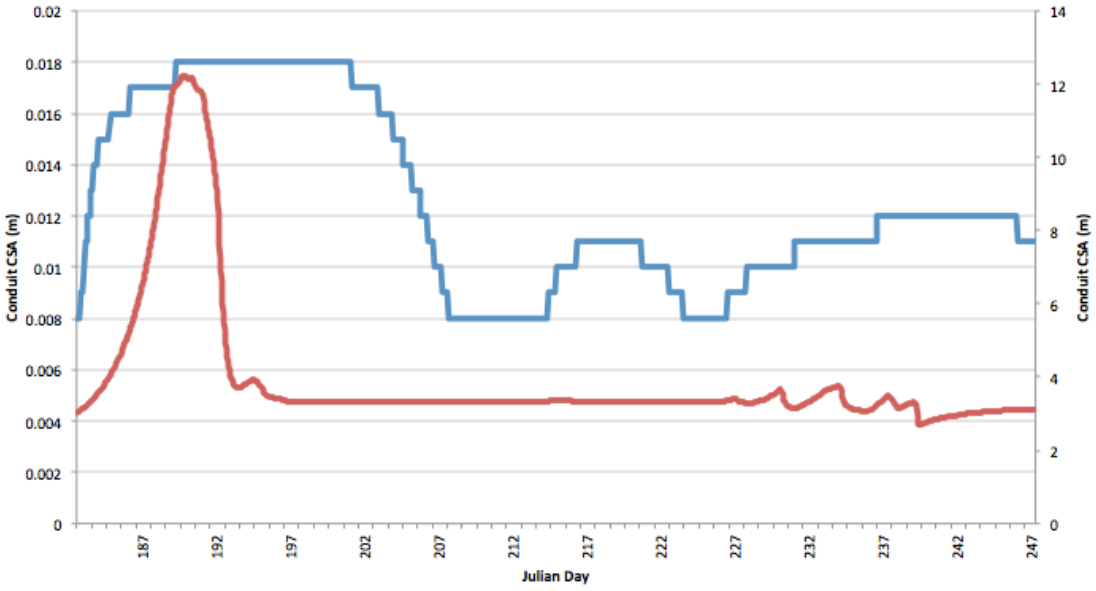

Figure 4.30: *The reaction of the same conduit (C348) below lake 14 to initial melt input under background conditions of zero-melt (blue, primary y axis) and background melt of 2m³s⁻¹ (red, secondary y axis)*

The above figure (fig. 4.30) displays the different behaviour of the conduits under the contrasting conditions upon the initiation of meltwater input and provides a context for the contrasting behaviour of hydraulic head. As shown, the conduits both adjust rapidly to the meltwater arrival, but from a base-level of just 0.008m, the zero-melt conduit increases to only 0.018m, while the background-melt conduit begins at a base-level of 3.07m and expands to 12.065m. It immediately falls from its peak as hydraulic head is reduced, while the smaller conduit retains its peak for 283 hours as it more slowly evacuates the hydraulic head (fig. 4.28).

4.6.2 Seasonal and spatial observations

(a)

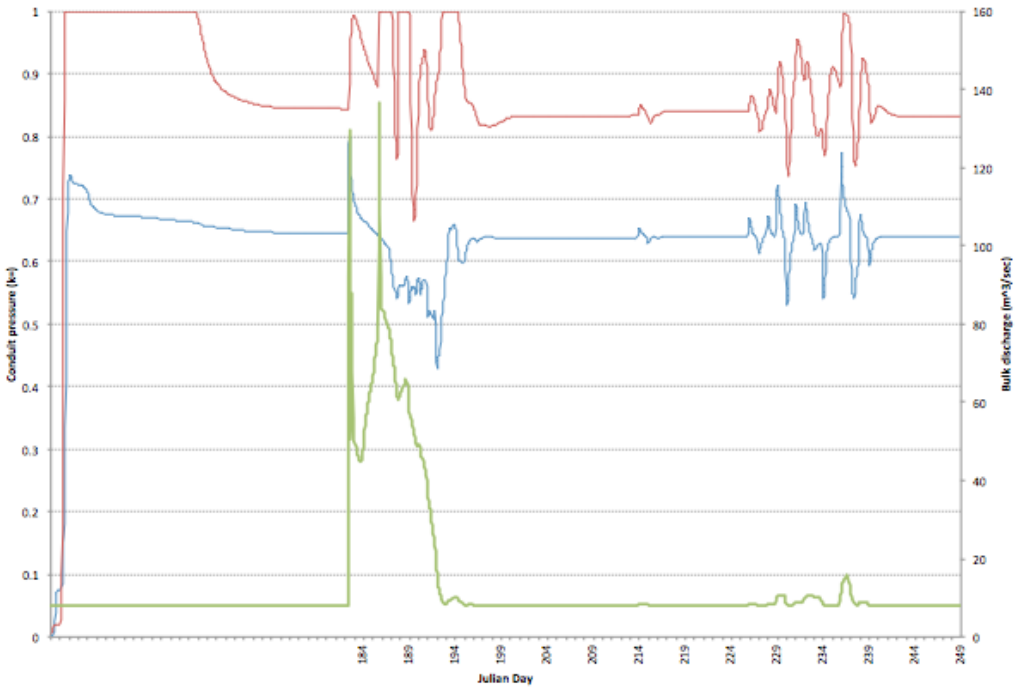

(b)

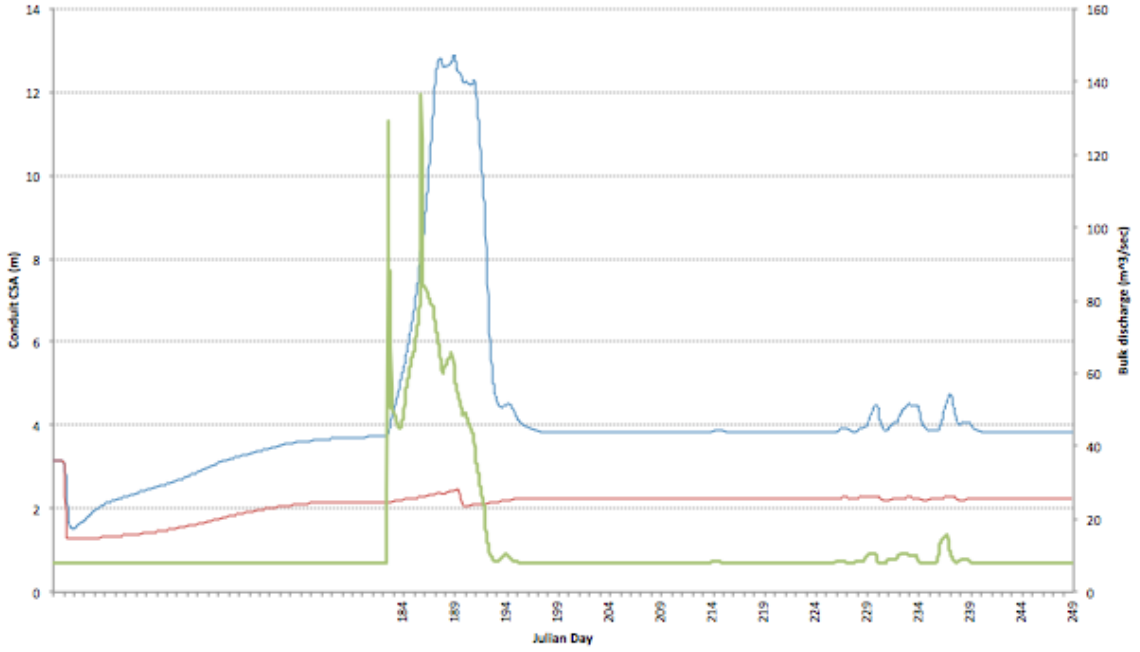

(c)

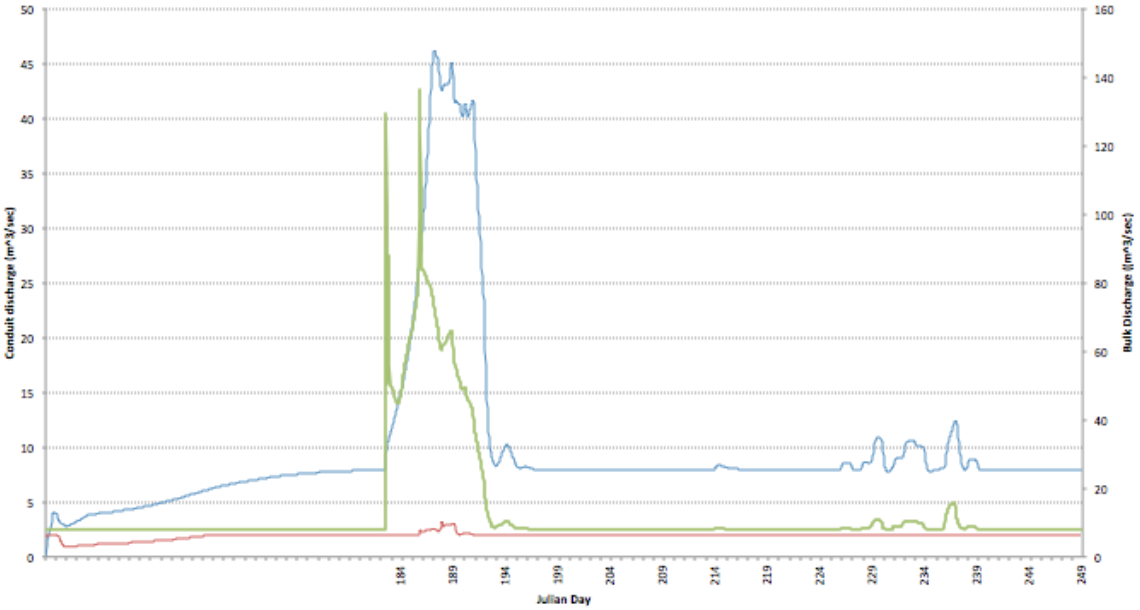

***Figure 4.31 (a-c)**: Conduit pressure (a), CSA (b) and discharge (c) for the downglacier conduit C423 (blue) and upglacier conduit C301 (red) below lake 11, plotted against bulk discharge (total input, green, secondary y axis) in the eastern channel (k=0.95). First modelled input is at day 182 with preceding melt only 'background melt'. Julian Day is not indicated for the initial period of background melt, so as to mark the change.*

The figures (4.31a-c) displaying the evolution of the drainage system across the season for the eastern channel (k=0.95) show a close relationship with melt for all the parameters and at both the upper and low conduits/junctions. At the upper junction below lake 11, pressure fluctuates rapidly from its steady-state level, repeatedly reaching overburden pressure when bulk discharge dramatically increases during the first warm period as a series of lakes drain. Pressure tends to remain at its steady-state of k=0.84 until it rapidly fluctuates again, above its steady-state, along with the second warm period. Pressures repeatedly reach close to ice overburden (up to 0.995) but never stabilise until returning to steady-state. Notably this is a period of increased melt but not lake drainages. The CSA and discharge in the conduits leading from this junction mirror each other in sync but vary on a much smaller scale than bulk discharge or pressure.

It is clear from the figures that the lower junctions/conduits express the reverse relationship between pressure and bulk discharge. Pressure responds on a similar timescale as the upglacier junction but instead of fluctuating above its steady-state conditions, it primarily drops below and never reaches overburden-pressure. Fluctuations and lowering of pressure is matched by synchronous increases in conduit discharge and CSA, which lag variations in bulk discharge by up to 5 days. The rate and magnitude of changes in discharge and CSA are much higher for the downglacier area, reaching a CSA of 12.91m from a steady-state of 2.38m compared to a peak of 2.44m from 2.16m

(a)

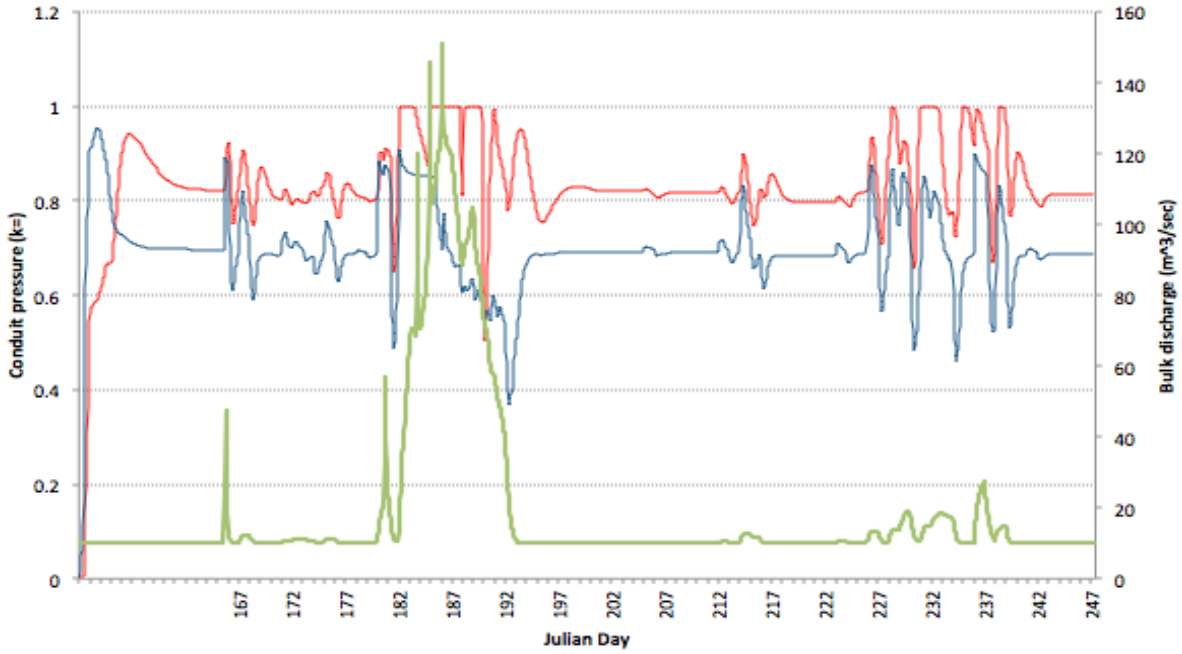
Conduit pressure (k=)
Bulk discharge (m^3/sec)
Julian Day
1.2
1
0.8
0.6
0.4
0.2
0
160
140
120
100
80
60
40
20
0
167
172
177
182
187
192
197
202
207
212
217
222
227
232
237
242
247

(b)

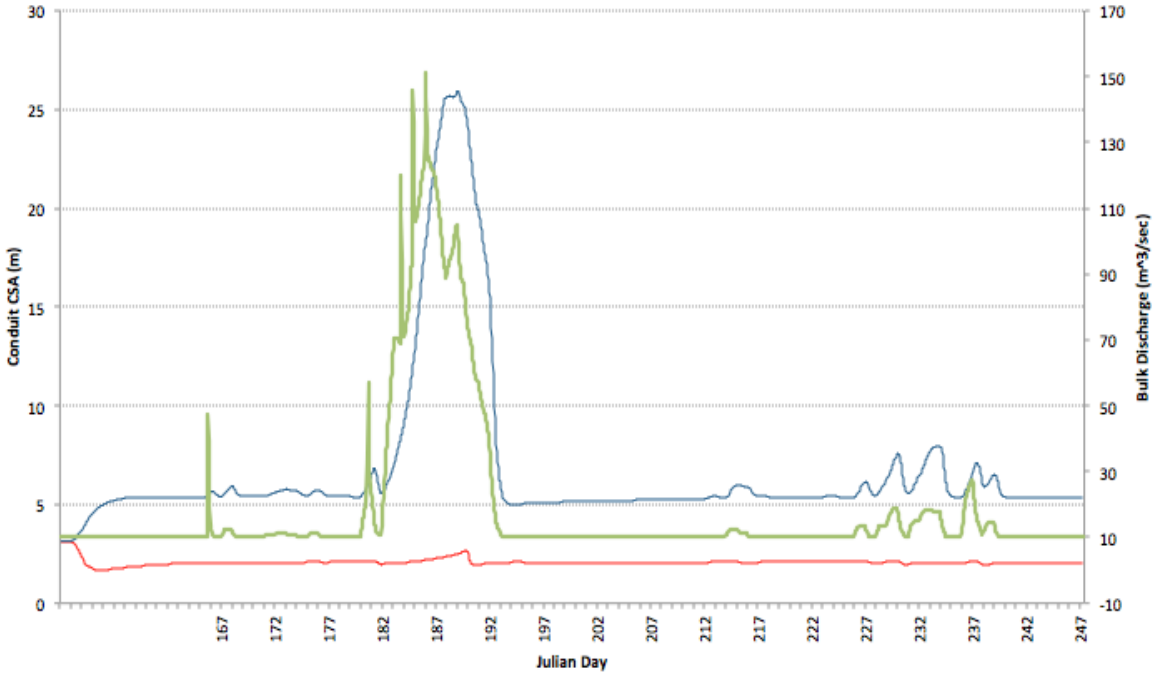
Conduit CSA (m)
Bulk Discharge (m^3/sec)
Julian Day
30
25
20
15
10
5
0
170
150
130
110
90
70
50
30
10
-10
167
172
177
182
187
192
197
202
207
212
217
222
227
232
237
242
247

(c)

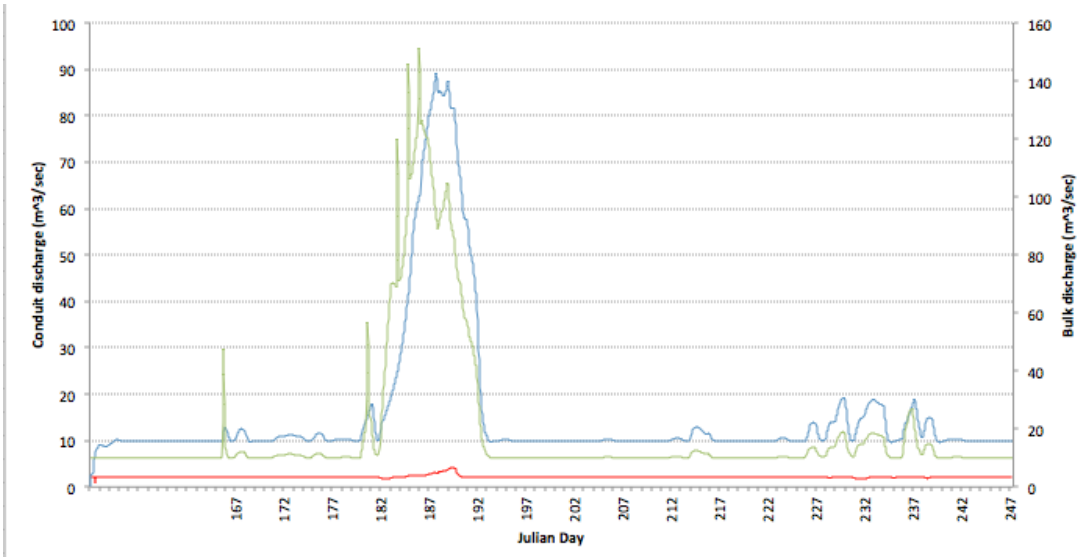

***Figure 4.32 (a-c)**: Hourly Conduit pressure (a), CSA (b) and discharge (c) for the downglacier conduit C405 (blue) and upglacier conduit C301 (red) below lake 16, plotted against bulk discharge (total input, green, secondary axis) in the western channel (k=0.95). First modelled input is at day 166 with preceding melt only 'background melt'. Julian Day is not indicated for the initial period of background melt, so as to mark the change. The period of background melt shown is shorter than in figure 4.29 because steady-state was achieved more quickly.*

The overall pattern of distinct periods of increase in pressure, discharge and CSA at the upglacier conduit, along with the two warm periods, the first of which similarly triggers a series of lake drainages, is the same as in the eastern channel (figs. 4.32a-c). The most noticeable difference is the earlier fluctuation in pressure due to a spike in discharge caused by the drainage of lake 28. This causes a fluctuation in pressure at both junctions though neither reach overburden. Notably pressure increases at C301 despite being upglacier of the drainage event. Pressure increases at both junctions in the initial warm period, C301 reaching overburden-pressure on several occasions in this period as lake 16 drains into it and discharge remains high in that and other moulins. C405 initially increases its pressure but then decreases as the discharge and CSA of its conduit rapidly increase. Pressure fluctuates rapidly about steady-state during the late warm period, more often above steady-state in the upglacier junction and below it at the downglacier junction. However, the downglacier junction

displays a less consistent negative relationship with bulk discharge than the analogous junction in the eastern channel.

4.6.2. Comparing the effect of alternate configurations on the subglacial drainage system

(a)

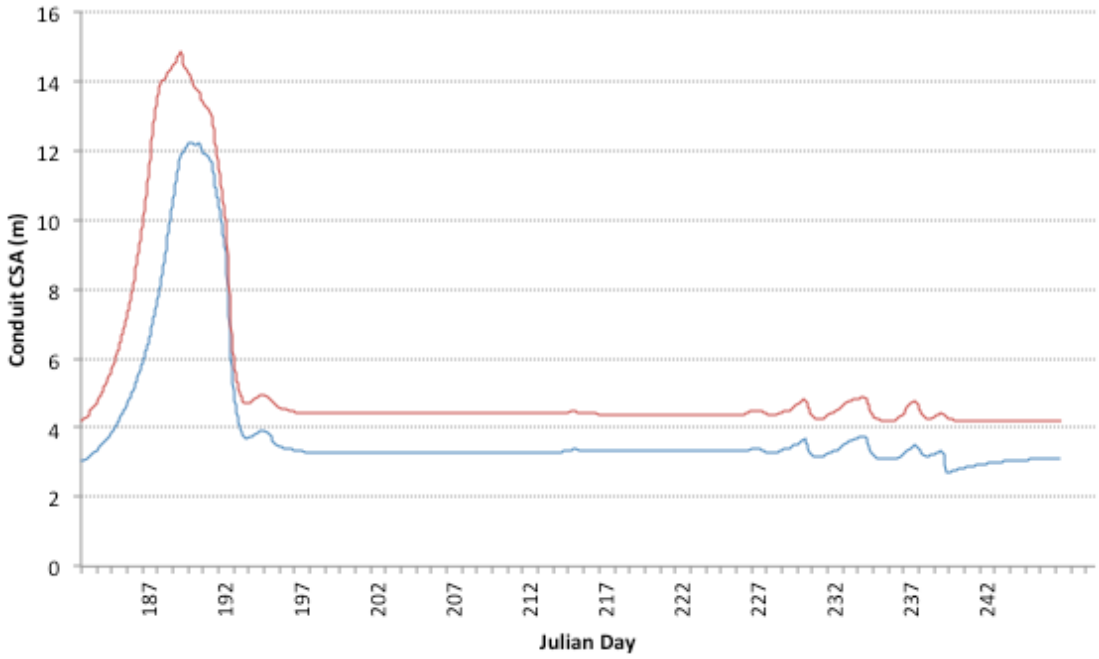

(b)

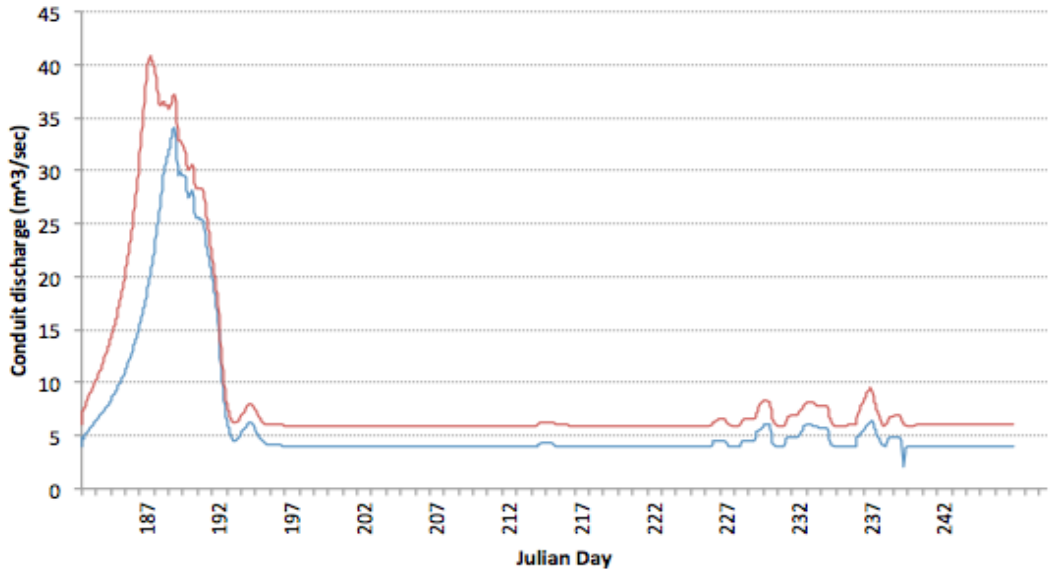

***Figure 4.33 (a,b)**: Hourly conduit CSA (a) and discharge (b) at conduit 348 (eastern channel) for the system configurations k=0.95 (red) and k=0.975 (blue).*

The above figures (fig. 4.33a-b) show how discharge and CSA contrast for a junction depending on whether it is part of the k=0.975 or k=0.95 configuration. The results display little difference in trend between the two, for both parameters. The evident difference is one of magnitude, with discharge and CSA being higher for the k=0.95 configuration. Both parameters remain lower for k=0.975 throughout the season apart from a convergence on the first falling limb. The CSA is steady at 3.31 compared to 4.41 for k=0.975 and k=0.95 respectively, and the peak at 14.81m compared to 12.17m. Conduit discharge is steady at $4m^3s^{-1}$ and $5.96m^3s^{-1}$ for k=0.975 and k=0.95 respectively and the peak $40.86m^3s^{-1}$ compared to $34.54m^3s^{-1}$.

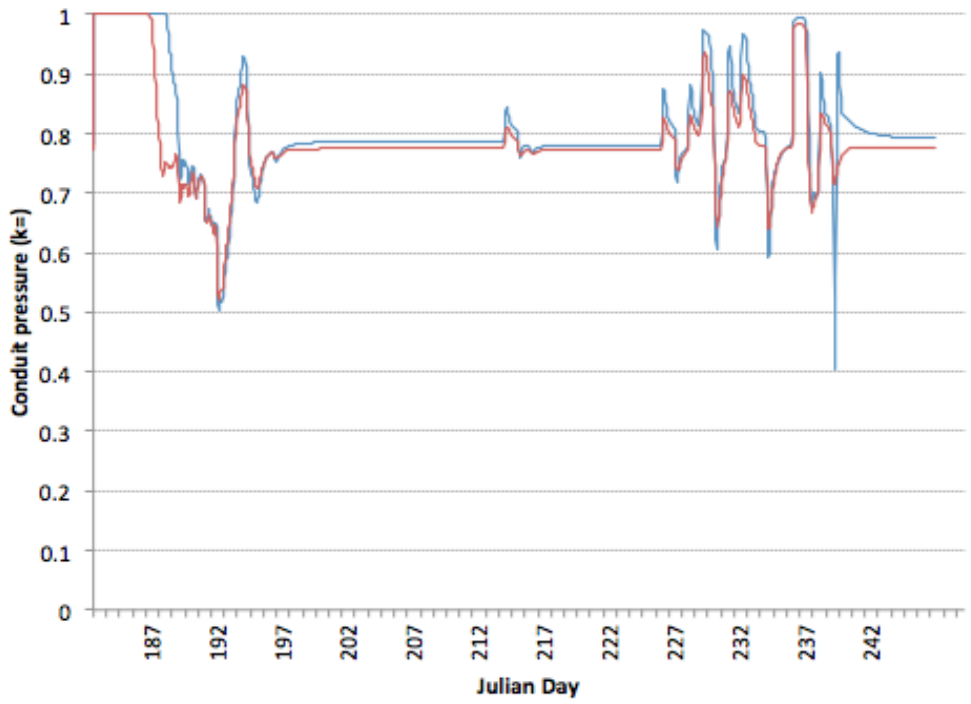

Figure 4.34: *Hourly conduit pressure at conduit 348 (eastern channel) for the system configurations k=0.95 (red) and k=0.975 (blue).*

Fig . 4.34 shows that the different configuration has a similarly limited effect on pressure. However, it can be observed that pressure fluctuates to a higher degree and maintains overburden-pressure for a longer period under the k=0.975 configuration. Figs. 4.24 and 4.25 show that these differences are associated with a higher input in the k0.975 configuration and additional lake

drainage due to the inclusion of lake 11 in its system. The lake drainage is evidently distinct from other lake drainages in the channel due to its timing and relatively high magnitude. The inclusion of lake 11 in the western configuration makes relatively little impact on the bulk discharge of the channel due to the timing and magnitude of other linked-drainages (figs. 4.11 and 4.12).

Chapter 5: Analysis and Discussion

This section will first discuss the results of observations and depth-analysis of lakes in 2004 Landsat images. Secondly, the lakes produced by the supraglacial routing model will be compared with the Landsat images and the sensitivity of the model to differing crevasse surface areas will be discussed. Thirdly the results of the subglacial routing model and its sensitivity to differing k-values will be discussed. Fourthly, the results of the subglacial drainage model will be discussed, and then the implications of the study's results for the dynamics of Petermann Glacier. This will be followed by some comparison between the present study and the application of the model to the Paakitsoq region of west Greenland by Banwell (2012). Finally there will be discussion of the limitations and scope for further study.

5.1 Lake evolution from Landsat imagery

The floating tongue area of the glacier is characterized by small water-filled fractures while upglacier of the grounding line, much of the main trunk of the glacier is characterised by ponding in larger depressions henceforth referred to as lakes. Ponding in Area Lower is concentrated in seven lakes. This, and the interannual recurrence of lakes, as revealed by comparing between 2004 and 2012 images, suggests the strong influence of topography on ponding in this area, with the lakes presumably occupying topographic depressions (Echelmeyer et al., 1991). The evident dominance of topography in lake formation also justifies the use of a supraglacial routing based on topography for determining the locations and character of supraglacial lakes in the modelling study.

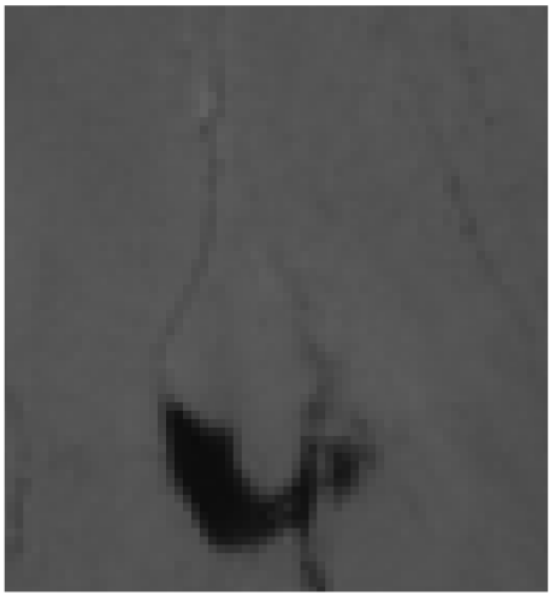

Figure 5.1: *Evidence of lake overfilling through a supraglacial channel in Area Lower*

The 82% reduction in ponded area in nine days between day 182 and 191 suggests that Area Lower could have drained dramatically over the study period, as has been observed in numerous studies (e.g. Das et al., 2008; Shepherd et al., 2009). Indeed, observation of lake disappearance between day 195 and 201 in 2004 (fig 4.15) at a similar elevation suggests that rapid drainage is likely at this elevation. However, the drainage of a further 15.4% of the original area over the subsequent sixteen-day period suggests that drainage did not occur in one catastrophic event through hydrofracture. Partial drainage could be due to drainage into a fracture that propagates but does not reach the base (Das et al., 2008). However, examination of the imagery (fig. 5.1) for the latter two dates reveals what appear to be incised channels on the surface leading from the lakes, suggesting lake drainage by overspill. Such cases are relatively likely on Petermann Glacier due to its high ice thickness (800-1000m in this area), making the volume of water necessary to propagate a fracture to the base greater than for analogous areas of other glaciers, such as Paakitsoq (Banwell et al., 2012). Such drainage has been observed elsewhere on the GrIS (e.g. Das et al., 2008; Johansson et al., 2013). Das et al. (2008) observed drainage occurring over weeks as overflow melted and deepened a spillover channel leading to a moulin.

This suggests that the drainage system is less likely to become pressurised, particularly if channelized, in this area as overspill likely will allow the water to enter the system downglacier through open moulins or drain onto the tongue, and deny the possibility of the large pulses of water possibly required to perturb the system (Bartholomew et al., 2010; 2011a;; 2012; Schoof, 2010). Alternatively, the overspill may flow into another lake and promote rapid drainage to the base there (Banwell et al., 2012).

Overspill could also flow beyond the grounding line, which would remove any potential direct influence on the subglacial drainage system. However, water pooling on the ice tongue could have implications for ice tongue stability. Increased ponding on the tongue could lead to fracture and break-up of the tongue with potential implications for the whole glacier's stability (Nick et al., 2012). This mechanism is thought to have contributed to the collapse of the Larsen B ice-shelf in Antarctica, promoting the connection of surface crevasses with underlying sea water by hydrofracture (Scambos et al., 2000) and has the potential to act similarly at Petermann Glacier.

Although minimum extent, volume and the lowest maximum depth occurred on day 207, the lowest mean depth occurred on day 191, supporting Box and Ski's (2007) suggest that area, depth and volume are often, but not necessarily, correlated.

The evolution of two lakes further upglacier at Area Upper, exhibit distinct behaviour from lower lakes. While lakes in Area Lower were draining, the lakes in Area Upper were expanding, with the area covered by ponding increasing 47% in just five days from day 186 to 191. The mean depth of the two lakes increased from 0.45m each to 1.25m and 0.99m in the period, which coincides with the warmest period in 2004, suggesting that this approximate period of time tends to when temperature increases and melting expands upglacier. Increased meltwater runoff is thought to account for the majority of the expansion of the lakes in this period, but the positive feedback between lowering albedo and increasing melt likely plays a significant role, contributing around

17cm of the depth to the lakes, based on Tedesco et al.'s (2012) proposed relationship. The lakes appear to have formed in surface undulations, with the water expanding to a point that it overspills between the two main depressions across a narrow, shallow depression that allowed the two lakes to join. This gave the lake two depth-centres connected by a 0.55m 'bridge'. Such combining of lakes has been observed previously (Box and Ski, 2007) and may play an important role in facilitating the creation of lakes large enough to propagate fractures to the base and rapidly drain. This could be particularly important in the low-melt, high ice thickness environment of Petermann Glacier.

However, it seems that some lakes do not drain either through overspill or fracture propagation. Lakes that appear as 'rings' of deep water in the depth algorithm output indicate the formation of ice on the surface of the lakes, as previously observed by Johansson et al. (2013). In Area Upper, the ice expands and the detectable-depth decreases through the season. This indicates that summer temperatures and melt supply begin to drop before the lake reaches the critical volume sufficient to initiate hydrofracture of large supraglacial channels and the lake freezes over. This has important implications for the relationship between lakes and the subglacial drainage system in the area. Instead of providing a means for connecting the supraglacial and hydrological drainage systems and supplying meltwater pulses, these perennial lakes appear to take meltwater out of the system, seemingly storing it until the surface melts the following summer (Johansson et al., 2013). Conversely, they could also increase the likelihood of drainage in subsequent years, especially if the lake remains insulated and does not freeze below the ice-cover. It could supply a lake already close to the critical drainage volume when the following melt season begins, thus requiring less meltwater input to drain.

Comparison of the 2012 images with 2004 images suggests that temperatures were not great enough in 2004 to melt the perennial lakes surface or deliver new ponding, with visual analysis of the 2004 images revealing features resembling the lakes evident in 2004 but no ponding being detectable. The neighbouring lake in Area Upper (fig 4.19) seems to provide an example of a perennial lake at a

different stage, before the surface has completely melted or later in the development of freeze-over. Images suggest that this lake never completely loses its ice-cover. The images from both years suggest that all lakes around ~1200m elevation are perennial and therefore the occurrence of melt here is irrelevant to the base of this part of the glacier. This suggests that a developed subglacial drainage system bed by surface melt is unlikely at such elevations.

5.2 Comparing observed and modelled lakes and sensitivity to crevasse surface area

Comparing the lakes predicted by the supraglacial routing model and those observed in Landsat imagery (fig. 4.7 and 4.14) suggests that the model broadly predicts the pattern of ponding. This supports studies suggesting that basal (Lampkin and Vanderberg, 2011) and the associated surface topography (Echelmeyer et al., 1991) are the main factors determining lake location. Both suggest ponding on the main trunk and a spread of ponding to the south-west and towards the interior. Three main patches of lakes are visible, two of which are represented well by the model. The best represented area is the area of discussed perennial lakes around Area Upper. The frequency of small lakes not produced by the model is immeasurably greater in the imagery, a consequence of necessary smoothing. Specific lakes are not well produced, although some, such as lake 13 are directly visible in the imagery. However, it is believed that the pattern and distribution of lakes is sufficiently well produced to allow the scope of the subglacial drainage system and the distribution of meltwater input to be well represented.

Variations in the defined crevasse area caused significant variations in the volume of lake drainage events, though did not affect timing to a great extent due to the concentration of melt and drainage in one main period. Two lakes, 13 and 11, drained at a cvol of 500 but not 1500. Cvol 500, therefore, was chosen for implementation due to observation of high melt and drainage in these areas of the glacier.

5.3 Subglacial routing

Analysis of subglacial flow routes under different k-value scenarios reveals significant variations (fig. 4.22a-h). Flow under k=0 follows basal topography and forms numerous subglacial ponds (fig. 4.21). The flow accumulation suggests that under increasing k-values the basal topography becomes progressively less significant and ponding less likely, with flow following the direction perpendicular to equipotential lines and high water pressure driving water out of depressions (Shreve, 1974).

Choosing any K-value for Petermann is problematic both because of the lack of knowledge of the subglacial drainage system in the region and because evidence suggests that subglacial pressures may vary substantially temporally and spatially (Hubbard et al., 1995; Bartholomew et al., 2011a). However, evidence from other studies (e.g. Thomsen and Olesen, 1991; Mottram et al., 2009; Banwell, 2012) suggests that a K-factor upwards of 0.90 is a good approximation for regions near the margins of the GrIS. Additionally, the high ice thickness suggests that when meltwater input reaches the base it will promote high subglacial water pressures (Rothlisberger, 1972). This is supported by the subglacial model results. Thus, k-factors of 0.95 and 0.975 were chosen. These values were chosen because they are believed to be realistic and because they represent a step-change in the drainage configuration, with four of the supraglacial lakes switching their input's destination between the western and eastern channels (though only one that drains [lake 11]) as the K-value increases from 0.95 to 0.975. Therefore, implementing these two configurations is thought to account for a relative breadth of possible subglacial configurations.

5.4 Subglacial drainage

5.4.1. Initial observations

The results in chapter 4 suggest that the supraglacial and subglacial drainage systems of Petermann Glacier are closely related. The raising of pressure in

response to meltwater input indicates that the input is too rapid for the drainage system to accommodate, and supports observations and modelling studies that suggest that discharge and pressure are only negatively related in a steady-state (e.g. Schoof, 2010; Bartholomew et al., 2011a; 2012). The initial high pressures, and the evident lag between input and conduit discharge (fig. 4.31, 4.32) and expansion suggest that it takes time for the drainage system to adjust and achieve stability when input varies. This occurs when lakes drain, but daily variations in temperature also play an important role, as demonstrated by variations induced by the second warm period. The greater stability and increased capacity for downglacier conduits to cope with melt input highlights this (fig 4.32). It is thought that the conduit C362 responds to increased input by reducing pressure because it already receives double the discharge of the upglacier conduit C301 due to its downstream location at a confluence. The greater initial discharge means its cross-sectional area is higher allowing it to more easily cope with increased input and more quickly increase its capacity. Additionally, its location, more remote from the input and downstream of narrower conduits means that it receives the input more slowly than upglacier, especially directly below the moulin. Additionally, the lower ice-thickness downglacier allows quicker conduit expansion. In both cases, the lower junctions never reach ice-overburden pressure, suggesting significant spatial variations in subglacial response to input across the glacier. These observations support claims that it is the rate rather than magnitude of meltwater input that determines the subglacial response (Shepherd et al., 2009; Bartholomew et al., 2011a; 2012).

The model suggests that the alternative system configurations associated with k=0.95 and k=0.975 do not cause the system to differ greatly, though the effect is more pronounced on the eastern channel due to the inclusion of a peak drainage event when k=0.95 (fig. 4.33). Though not affecting downstream conduits greatly, expansion of the eastern channel does increase pressures in the east of the glacier as the high pressured conduits shown to be associated with lake drainage (from lake 11) flow to the eastern channel. The western channel experiences lake drainages at such elevations anyway, suggesting that k=0.95

spreads high pressures across more of the glacier. Increased temperatures would be expected to increase the significance of configuration variation, as the destination of drainage from lakes 5, 6 and 10 would also be contingent on the configuration. Regardless of the configuration it appears that the eastern channel experiences lower pressures, due to its lower input and fewer rapid drainage events.

5.4.2. Under conditions of 'zero melt'

Analysis of meltwater input into a system containing no meltwater prior to lake drainage suggests that the system immediately reaches ice overburden pressure, with the hydraulic head reaching the surface at all input locations upon lake drainage. This appears to be the consequence of a combination of high meltwater input and low conduit CSA due to rapid closure under thick ice. Within 17 hours of the end of the initial spin-up period, the conduits reach minimum diameter (fig. 4.29). This is due to the high overburden pressure from the thick ice causing high deformation of the subglacial conduits, which is not countered by any wall-melting due to the absence of discharge and thus heat dissipation (Rothlisberger, 1972; Spring and Hutter, 1981; Arnold et al., 1998). When meltwater reaches the base, the conduits are too small to allow evacuation of the water to maintain pace with input, resulting in conduit discharges of as low as $0.012 m^3 s^{-1}$ despite an input of $65.69 m^3 s^{-1}$. As conduit CSA can only increase as discharge increases, and it is impossible for discharge to increase rapidly under such a small cross-sectional area, the hydraulic head remains at the ice surface for as long as 746 (31 days) hours. With the system at full capacity, excess water spills onto the surface of the glacier, so there is little relationship between input and basal parameters under these conditions, beyond the initial pressurisation. Conduit CSA increases for a period while pressure drops as the conduits eventually expand sufficiently to evacuate a significant amount of the hydraulic head (fig 4.28, 4.30). As water is evacuated and conduit discharge decreases, conduits quickly shut down again under the high deformation rates.

Observations (e.g. Cowton et al., 2012) support the possibility of the hydraulic head reaching the ice surface. However, it could also be concluded that the results suggest that a conduit drainage system is not likely at Petermann Glacier. Although studies (Colgan et al., 2011; Banwell, 2012) suggest that channelized drainage systems remain open through the summer for parts of the GrIS, and possibly even during winter, such studies were carried out in areas of much lower ice thickness. The rapid shutdown of conduits under zero-melt conditions during short summer cold periods across the Petermann site suggests that a channelized system may be unrealistic, with ice thickness as high as ~600m at the grounding line and reaching over 1200m at upglacier elevations where melt occurs. While this model, and observations (e.g. Zwally et al., 2002; Das et al., 2008) suggest that meltwater can reach the base at such great ice thickness, this model, by demonstrating the difficulty of conduit sustainability, suggests that this is likely into a distributed system. Though the model is inherently channelized, it is contested that to some extent the results accurately represent input into a distributed system. The high pressures induced by meltwater input into narrow conduits are similar to what would be expected in a distributed system, with both unable to efficiently evacuate melt, and therefore raising hydraulic head for a period as a result (Rothlisberger, 1972). Observations (e.g. Das et al., 2008; Bartholomew et al., 2012; Cowton et al., 2013) suggest the existence of such behaviour on the GrIS.

5.4.3 Under conditions of background melt

The large area of the ice-sheet drained by Petermann Glacier (Rignot and Kanargatnam, 2006) and evidence of a large subglacial channel in the bedrock topography (fig. 4.5) suggest that the subglacial drainage system of Petermann Glacier may be channelized from basal melt produced upstream under the thicker ice of the interior, as is thought to be produced under thick ice in Antarctica (Bougamont and Christoffersen, 2012). This is supported by Bartholomew et al.'s (2011a) observation of proglacial discharge before melt initiation in west Greenland. Therefore, an alternative model run, with background melt of $2 m^3 s^{-1}$ provides an opportunity to discus potential

conditions where a conduit system does exist. While under zero-melt, conduits rapidly shut down, $2m^3s^{-1}$ of background melt allows a steady-state conduit system to develop, with pressures stable and relatively high, with a stable K-value of 0.80. Under this condition lake drainage similarly leads to full pressurisation, but conduits are able much more efficiently evacuate input, the same drainage event leading to full pressurization for 131 hours at conduit 48 (lake 14) rather than 746 hours under background conditions of zero-melt. The higher cross-sectional area of conduits at the time of lake drainage means that they can accommodate higher discharges, which allows a positive-feedback response with increasing discharge, increasing-wall melting, thus allowing increased discharge. The system is then less vulnerable to input spikes at the conduits do not shut down again, due to the background melt, as observed elsewhere by Colgan et al. (2011). This pattern of high hydraulic head at times of high input followed by evacuation and CSA expansion may be indicative of an intermediate stage between a distributed system and full channelization, as proposed by Cowton et al. (2013) based on similar observations. Such a period, characterised by a continually readjusting channel, seems especially likely to exist and last-longer under the high ice thickness of Petermann. The high discharge of lake drainage could channelize the system, but the inconsistent level of input and high conduit closure rate would make maintaining stability difficult.

Importantly, the establishment of steady-state under background melt conditions demonstrates the importance of rate of change of meltwater input, rather than the absolute value, in determining conditions, as suggested by observations (e.g. Bartholomew et al., 2012). While an input of $2m^3s^{-1}$ into an empty system causes it to reach maximum hydraulic head, maintaining input at the same level causes it stabilise at a K=0.80, though it is still perturbed by input spikes. It is clear, therefore, that it is the ability of the system to adjust to a variation that is key.

5.5 Implications for dynamics

Though the extent to which forcing at the base drives dynamics will be limited by the deep geometry of the glacier, suggesting high lateral drag (Joughin et al., 2008), the suggestion by Nick et al. (2012) that meltwater-induced basal forcing is the main driver of motion on Petermann Glacier, suggests that the high pressures observed will have important implications for dynamics. The high vulnerability of the system's pressure to lake drainage suggests that lakes and the subglacial drainage system likely play a role in the ice dynamics of Petermann Glacier. Observations and modelling by Nick et al. (2012) suggest that, due to a lack of buttressing force from the ice tongue, the glacier is responsive to variations in meltwater lubrication at the base, in contrast to other marine-terminating glaciers (e.g. Joughin et al., 2004). The rapid and long-lasting pressurizations suggest that the enhanced velocities will be pronounced and sustained, with hydraulic-jacking and thus reduced friction being maintained for up to 131 hours. Studies that propose it is rate of perturbations in pressure that cause the most significant velocity enhancements (e.g. Bartholomew et al., 2011b; Bartholomew et al., 2012) suggest significant velocity enhancements on Petermann accompanying lake drainage and enhanced input during the second warm spell. The model supports observations of a velocity response to melt input, assuming velocity increases with pressure (e.g. Zwally et al., 2002; Bartholomew et al., 2010) but suggests that the nature of the relationship is characterised by velocity spikes responding to meltwater spikes, rather than of a general correlation between input and velocity (van de Wal et al., 2008; Shepherd et al., 2009; Schoof, 2010; Bartholomew et al., 2011b).

The rapid closure of conduits in the absence of meltwater suggests that the postulation by Sundal et al. (2011) that the velocity of Greenland's outlet glaciers will decreased with warming does not apply to Petermann Glacier and other high ice thickness, high-latitude areas. Under such high ice-thickness, the Q_{crit} proposed by Schoof (2010) to initiate channelization is much higher at Petermann Glacier, while meltwater production is lower than at lower-latitude sites (Banwell, 2012). Instead of causing earlier channelization and thus earlier

disruption of the positive relationship between meltwater and basal pressure, warming would cause increased melt to enter a distributed or poorly-formed channel (Cowton et al., 2013) system throughout, or late into, the melt season and continue to enhance velocity. However, if temperatures increase to such an extent that meltwater increases sufficiently to surpass Schoof's (2010) Q_{crit} and remain above the lower Q_m for dechannelization, the assessment of Sundal et al. (2011) could apply.

If a channelized system already exists as proposed in model runs with background melt, the model suggests that meltwater would nevertheless play an important role in dynamics due to the ability of spikes in meltwater by lake drainage and warm period to pressurize the system. This too contests the suggestion by Sundal et al. (2011) that warming will reduce overall velocities. Warming would be expected to cause more pressurizing melt spikes, as postulated to be the main driver of velocity (Bartholomew et al., 2012), and lead to the expansion of lake formation and drainage at higher elevations (Liang et al., 2012). This would also expand hydrological connectivity and increase melt delivery and velocity across new areas of the glacier (Bartholomew et al., 2011b). Sufficient warming would allow the observed perennial lakes at high elevations to expand for a longer period, facilitating drainage before freeze-over.

Both modelling and observations suggest that lakes play a critical role in the dynamics of Petermann Glacier, by storing meltwater, supplying moulins through overspill, creating a hydrological connection between the surface and base and delivering large quantities of meltwater to the bed. However, observations of freeze-over at high elevations suggest their influence is limited towards the interior and they may in fact counter the meltwater forcing at the base in some cases by storing surface runoff, preventing it from reaching the base. Subglacial discharge could also have implications for dynamics through the influence of meltwater plumes on terminus stability (e.g. Motyka et al., 2003).

5.6 Comparing with Paakitsoq, west Greenland

The subglacial model used in this study was adapted for the GrIS by Banwell (2012), and implemented in the Paakitsoq region in west central Greenland at around 69.6°N.

Most notably, both the lower ice thickness and higher meltwater supply in Paakitsoq are conducive to a channelized drainage system, with thicknesses ranging ~50m to 600m . Conduits are maintained throughout the season and close at a slower rate allowing the system to accommodate the delay between model initiation and meltwater input and for the system to survive troughs in meltwater supply. Comparing the two systems suggests that ice thickness is the main reason for the differing behaviour. Increased meltwater would account for greater ice thicknesses, but the almost instantaneous closure of conduits at Petermann when there is no melt supply suggests that a channelized system is more difficult to sustain at Petermann and therefore the model is not suited to its drainage system. The model could be adapted to keep conduits open on Petermann, but testing by Banwell (2012) suggests that increasing minimum conduit diameter above 0.5m would not be realistic.

The present paper supports modelling results at Paakitsoq that suggest that lake drainages play an important role in establishing a hydrological connection between the surface and base. It also supports the suggestion that meltwater runoff into already-opened moulins is able to pressurize the base, with high pressures shown alongside input increases distinct from lake drainages (figs. 4.31, 4.32). However, application at Petermann Glacier does not support results from Paakitsoq suggesting that lake drainage only accounts for short <24 hour pressurization spikes, with hydraulic head remaining at ice-surface level for up to 131 hours (5 days) (under background melt conditions).

5.7 Limitations and further study

Aside from limitations discussed in the methods and data sections, there are some key limitations apparent in the results. Firstly, the smoothing and reduction in resolution of the DEMs likely accounts for the limited ability of the routing model to accurately predict lake locations when compared with Landsat images. The model has been shown to produce good results (Banwell et al., 2012) but is limited by the coarseness of the DEM as required by processing limitations. However, for the purposes of the study it is thought to be sufficiently accurate in producing the general pattern of lake formation and drainage, with the accurate prediction of drainage of specific lakes on specific days not necessary for the study's aims.

The inherently channelized nature of the model could be a problem in such a high-thickness, low-melt environment. It is likely that drainage is distributed at least at the beginning of the season, and the rapid conduit closure suggests that it may sustain a distributed system throughout the season. However, based on the evident basal channel feature and pond formations, the present study suggests a channelized system likely exists. Nevertheless, at least developing accurate representation of a distributed system before channelization would improve the ability of the model to accurately represent the drainage system. Incorporation of critical discharge values for channelization and dechannelization based on conduit characteristics, as in Schoof (2010) would improve application. Additionally, addressing the model's isolation from feedbacks with dynamics would be desirable. Incorporating feedbacks, as done by Pimentel (2010) and Pimenetel and Flowers (2010), such as the effect of hydraulic jacking on subglacial drainage could lead to better representation.

Chapter 6: Conclusion

The relationship between temperature, melting and variations in the subglacial drainage system were modelled for the 2004 melt season on Petermann Glacier. The evolution of supraglacial lakes in 2012 was also investigated using satellite imagery. This allowed spatial and temporal variations in subglacial hydrology and lake evolution to be assessed, and the implications for the glacier's dynamics to be considered. The study also provided insight into application of a channelized subglacial model to a high-latitude, high-thickness, marine-terminating glacier. Four key findings were identified:

[1] Development and maintenance of a channelized drainage system is difficult in the high ice thickness, low-melt environment of Petermann Glacier. This is suggested by closure of conduits to minimum conduit diameter within seventeen hours of full model initiation under zero-melt conditions.

[2] The subglacial drainage system is most perturbed by rapid *variations* in melt. This is suggested by spikes in pressure accompanying warm periods and lake drainage events, though downglacier conduits were more stable due to more consistent high flow. This is further highlighted by the maintenance of steady pressures under constant in-flow after a period of fluctuating response. This suggests that the rapid supply of melt supplied by lake drainages is key to the behaviour of the subglacial hydrological system.

[3] The significance of lakes for the subglacial drainage system is presently limited by the short melt season causing many lakes to freeze-over in the upper ablation zone before they reach the critical

drainage volume. Evidence of lakes overspilling may also limit their role.

[4] The subglacial drainage system model developed by Arnold et al. (1998) and adapted by Banwell (2012) was successfully applied to Petermann Glacier for a channelized drainage system.

In conclusion, these findings lead the present study to propose the following:

- Petermann Glacier is characterised by an unstable channelized drainage system, as postulated by Cowton et al. (2013) for the early melt season in west Greenland. A small supply of basal melt is sufficient to maintain a channel, but high conduit closure rates mean the system is unable to accommodate quick and large variations in melt, and so subglacial pressure reaches ice overburden pressure.
- The subglacial drainage system is key to the dynamics of Petermann Glacier, and likely also to analogous glaciers with unconstrained ice-fronts. Studies suggest meltwater at the base of the glacier is the main factor in ice motion on the glacier (Nick et al., 2012) and the rapid variations in pressure exhibited in the present study have been shown to produce velocity spikes at other sites (Bartholomew et al., 2012).
- Warming will likely increase the velocity of Petermann Glacier by causing more pressure spikes associated with warm periods and by extending lake drainage events towards the interior, extending the basal hydrological connection. The high ice thickness will make stable channel formation difficult, meaning Sundal et al. (2011)'s prediction of ice slow-down with

warming, due to efficient channels forming earlier, is unlikely to apply to Petermann Glacier. Consequently Petermann Glacier is expected to contribute more to sea-level rise as warming occurs.

- The subglacial drainage model would benefit from the inclusion of distributed and intermediate 'unstable channel' (as described by Cowton et al., 2013) configurations. The model should also be adapted to include a transition mechanism between system states, such as implementation of the 'Q_{crit}' and 'Q_m' thresholds described by Schoof (2010).

References

AMAP (2009), 'The Greenland Ice Sheet in a changing climate: Snow, Water, Ice and Permafrost in the Arctic (SWIPA)', Dahl-Jensen, D. et al., *Arctic Monitoring and Assessment Programme (AMAP)*, Oslo, 115pp

Ambach, W. (1988a), 'Heat balance characteristics and ice ablation, western EGIG- profile, Greenland, Seventh Northern Research Basins Symposium/Workshop: Applied Hydrology in the Development of Northern Basins, May 25-June 1, Copenhagen Danish society for Arctic Technology, Ilulissat, Greenland, pp. 59-70

Ambach, W. (1988b), 'Interpretation of the positive-degree-days factor by heat balance characteristics – West Greenland', *Nordic Hydrology*, 19, 217-224

Anderson, M.L. et al (2010), 'Spatial and temporal melt variability at Helheim Glacier, east Greenland and its effect on ice dynamics', *Journal of Geophysical Research*,115, doi:10.1029/2010JF001760

Arnold, N (2010), 'A new approach for dealing with depressions in digital elevation models when calculating flow accumulation values', *Progress in Physical Geography*, 34, 781-809

Arnold, N et al. (1996), 'A distributed energy balance model for a small valley glacier. 1 Development and testing for Haut Glacier d'Arolla, Valais, Switzerland, *Journal of Glaciology*, 42, 78-89

Arnold, N et al. (1998), 'Initial results from a distributed, physically based model of glacier hydrology'*, Hydrological Processes,* 12, 191-219

Bamber, J. et al (2001), 'A new ice thickness and bed data set for the Greenland ice sheet. 1. Measurement, data reduction and errors', *Journal of Geophysical Research – Atmos.*, 106, 33773-33780

Bamber, J.L. et al. (2013), 'A new bed elevation dataset for Greenland', *Cryosphere*, 7, 499-510

Banwell, A. (2012), 'Modelling the hydrology of the Greenland Ice Sheet', *PhD Thesis*, University of Cambridge

Banwell, A.F. et al. (2012), Modelling supraglacial water routing and lake filling on the Greenland Ice Sheet', *Journal of Geophysical Research*, 117, doi:10.1029/2012JF002393

Bartholomew, I. et al (2010), 'Seasonal evolution of subglacial drainage and acceleration in a Greenland outlet glacier', *Nature Geoscience, 3, 408-411*

Bartholomew, I. et al (2011a), 'Supraglacial forcing of subglacial drainage in the ablation zone of the Greenland Ice Sheet', *Geophysical Research Letters,*

doi:10.1029/2011GL047063

Bartholomew, I. et al. (2011b), 'Seasonal variations in Greenland Ice Sheet motion: Inland extent and behavior at higher elevations', *Earth and Planetary Science Letters,* 307, 271-278

Bartholomew, I. et al (2012), 'Short-term variability in Greenland Ice Sheet motion forced by time-varying meltwater drainage: Implications for the relationship between subglacial drainage system behavior and ice velocity', *Journal of Geophysical Research*, 117, doi:10.1029/2011JF002220

Blake, E.W. (1992), 'The deforming bed beneath a surge-type glacier: Measurements of mechanical and electrical properties', *PhD Thesis*, University of British Columbia*,* Vancouver, Canada

Bougamont, M.J. et al. (2005), 'A surface mass balance model for the Greenland ice sheet', *Journal of Geophysical Research*, 110, F04.018

Bougamont, M. and P. Christoffersen (2012), 'Hydrologic forcing of ice stream flow promotes rapid transport of sediment in basal ice', *Geology*, 40, 735-738

Box, J.E. et al. (2011), Greenland Ice Sheet, in *Arctic Report Card 2011*, pp 117-138, NOAA, Silver Spring Md [Available at www.arctic.noaa.gov/reportcard]

Box, J.E. and K. Ski (2007), 'Remote sounding of Greenland supraglacial melt lakes: Implications for subglacial hydraulics', *Journal of Glaciology*, 53, 257-265

Braithwaite, R.J. (1995), 'Positive degree-day factors for ablation on the Greenland ice sheet studied by energy balance modelling', *Journal of Glaciology*, 41, 153-160

Braithwaite, R.J. and O.B. Olesen (1989), 'Calculation of glacier ablation from air temperature, West Greenland' In: Oerlemans, J. (Ed) Glacier Fluctuations and Climatic Change, glaciology and Quaternary Geology, Dordrecht, pp. 219-233

Braithwaite, R.J. and O.B. Olesen (1993), 'Seasonal variation of ice ablation at the margin of the Greenland ice sheet and its sensitivity to clima

Braithwaite, R.J. et al (1998), 'Errors in daily ablation measurements in northern Greenland, 1993-94, and their implications for glacier climate studies', *Journal of Glaciology*, 44, 583-588

Catania, G.A. et al. (2008), 'Characterizing englacial drainage in the ablation zone of the Greenland ice sheet', *Journal of Glaciology*, 54, 567-578

Cawkell, F.G.L and J.L. Bamber (2002), 'The impact of cloud cover on the net radiation budget of the Greenland ice sheet', *Annals of Glaciology*, 34, 141-149

Chandler, D.M. et al. (2013), 'Evolution of the subglacial drainage system

beneath the Greenland Ice Sheet revealed by tracers', *Nature Geoscience*, 6, 195-198
Chow, V.T. et al. (1988), 'Applied Hydrology, McGraw-Hill International Editions, Civil Engineering Series, *McGraw-Hill Book Company*, Singapore

Church, J., et al. (2001), Changes in sea level, in Climate Change 2001: The Scientific Basis, edited by J. T. Houghton et al., pp. 639 – 693, Cam- bridge Univ. Press, New York.

Clarke, G.K.C. (1996), 'Lumped-element analysis of subglacial hydraulic circuits', *Journal of Geophysical Research,*101, 17547-17599

Clason, C. et al. (2012), 'Modelling the delivery of supraglacial meltwater to the ice/bed interface: application to southwest Devon Ice Cap, Nunavut, Canada', *Journal of Glaciology*, 58, 361-374

Colgan, W. et al. (2011), 'The annual glaciohydrology cycle in the ablation zone of the Greenland ice sheet: Part 1. Hydrology model', *Journal of Glaciology*, 57, 697-709

Cowton, T. et al. (2013), 'Evolution of drainage system morphology at a land-terminating Greenlandic outlet glacier', *Journal of Geophysical Research: Earth Surface*, 118, doi:10.1029/2012JF002540

Das, S. B. et al (2008), 'Fracture propagation to the base of the Greenland Ice Sheet during supraglacial lake drainage', *Science*, 320(5877), 778-781

Echelmeyer, K. et al. (1991), 'Surficial glaciology of Jakobshavn Isbrae, West Greenland: Part 1. Surface morphology', *Journal of Glaciology*, 37, 368-382

Falkner, K.K. et al (2011), 'Context for the recent massive Petermann Glacier calving event', *Eos*, 92, 117

Fettweis, X. (2007), Reconstruction oft he 1979-2006 Greenland ice sheet surface mass balance using the regional climate model MAR',*Cryosphere,*1, 21-40

Fettweis, X. et al. (2011), ,The 1958-2009 Greenland ice sheet surface melt andthe mid-tropospheric atmospheric circulation', *Climate Dynamics*,36, 139-159
Finsterwalder, S. and H. Schunk (1887), 'Der Suldenferner. Zeitschfrift des Deutschen und Oesterreichieschen Alpenvereins', 18, 72-89

Fischer, U.H. and G.K.C. Clarke (1994), 'Ploughing of subglacial sediment', *Journal of Glaciology*, 40, 97-106

Flowers, G.E. and G.K.C. Clarke (1999), 'Surface and bed topography of Trapridge Glacier, Yukon Territory, Canada: digital elevation models and derived hydraulic geometry', *Journal of Glaciology*,45, 165-167

Flowers, G.E. and G.K.C. Clarke (2002a), 'A multicomponent coupled model of glacier hydrology 1. Theory and synthetic examples', *Journal of Geophysical Research*, 107, doi:10.1029/2001JB001122

Flowers, G.E. and G.K.C. Clarke (2002b), 'A multicomponent coupled model of glacier hydrology 2. Application to Trapridge Glacier, Yukon, Canada', *Journal of Geophysical Research,* 107, doi:10.1029/2001JB001124

Flowers, G.E. et al. (2003), 'New insights into the subglacial and periglacial hydrology of Vatnajokull, Iceland, from a distributed physical model',*Journal of Glaciology*,49, 257-270

Fountain, A.G. (1993), 'Geometry and flow conditions of subglacial water at South Cascade Glacier, Washington State, USA – An analysis of tracer injections, *Journal of Glaciology*, 39, 143-156

Georgiou, S et al. (2009), 'Seasonal evolution of supraglacial lake volume from ASTER imagery', *Annals of Glaciology*, 50, 95-100

Gudmundsson, G.H. (2003), 'Transmission of basal variability to a glacier surface', *Journal of Geophysical Research-Solid Earth*, 108, 2253

Hakuba, M.Z. et al. (2012), 'Impact of Greenland's topographic height on precipitation and snow accumulation in idealized simulation', *Journal of Geophysical Research*, 117, doi:10.1029/2011JD017052

Hall, D.K. et al. (2008), 'Greenland ice sheet surface temperature, melt and mass loss: 2000-2006', *Journal of Glaciology, 54,* 81-93

Hanna, E. et al. (2008), 'Increased runoff from melt from the Greenland Ice Sheet: A response to global warming', *Journal of Climatology*, 21, 331-341

Hock, R. (2003), 'Temperature index melt modelling in mountain areas', *Journal of Hydrology*, 282, 104-115

Hooke, R, LeB. (1984), 'On the role of mechanical energy in maintaining subglacial water conduits at atmospheric pressure', *Journal of Glaciology*, 30, 180-187

Howat, I.H. et al (2005), 'Rapid retreat and acceleration of Helheim Glacier, east Greenland', *Geophysical Research Letters*, 32, doi:10.1029/2005GL024737

Howat, I.H. et al. (2010), 'Seasonal variability in the dynamics of marine-terminating outlet glaciers in Greenland', *Journal of Glaciology*, 56, 601-613

Hubbard, B. et al (1995), 'Borehole water-level variations and the structure of the subglacial drainage system of Haut Glacier d'Arolla, Valais, Switzerland, *Journal of Glaciology*, 41, 572-583

Iken, A. (1981), 'The effect of the subglacial water pressure on the sliding velocity of a glacier in an idealized numerical in an idealized numerical model', *Journal of Glaciology*, 27, 407-421

Iken, A. et al (1983), 'The uplift of unteraargletscher at the beginning of the melt season – a consequence of water storage at the bed?', *Journal of Glaciology*, 29, 28-47

Iken, A. and R. A. Bindschadler (1986), 'Combined measurements of subglacial water pressure and surface velocity of Findelengletscher, Switzerland: conclusions about drainage system and sliding mechanism', *Journal of Glaciology*, 32, 101-119

IPCC (2007): Summary for Policymakers. In: Climate Change 2007: The Physical Science Basis. Contribution of Working Group 1 to the Fourth Assessment Report of the Intergovernmental Panel on Climate Change [Solomon, S. D. et al (eds.)] Cambridge University Press, Cambridge, UK and New York, NY, USA

Johannessen, O.M. et al (2005), 'Recent ice-sheet growth in the interior of Greenland', *Science*, 310, 1013-1016

Johnson, H.L. et al. (2011), 'Ocean circulation and properties in Petermann Fjord, Greenland', *Journal of Geophysical Research*, 116, doi:10.1029/2010JC006519

Joughin, I. et al. (1996), 'A mini surge on the Ruder Glacier, Greenland, observed by satellite radar interferometry', *Science*, 274, 228-230

Joughin, I. et al. (2004), 'Large fluctuations in speed of Greenland's Jakobshavn Isbrae glacier', *Nature,* 432, 608-610

Joughin, I. et al. (2008a), 'Continued evolution of Jakobshavn Isbrae following its rapid speedup', *Journal of Geophysical Research,* 113, doi:10.1029/2008JF001023

Kamb, B. (1987), 'Glacier surge mechanism based on linked cavity configuration of the basal water conduit system', *Journal of Geophysical Research*, 92, 983-100

Katz, R.F. and M.G. Worster (2010), 'Stability of ice-sheet grounding lines', *Proceedings of the Royal Society of London Ser A*, 466, 1597-1620

Kollmeyer, R.C. (1980), 'West Greenland outlet glaciers: an inventory of the major iceberg producers', *Internaional Association of Hydrological Science Publication 126*, 57-65

Krabill, W. et al (2004), 'Greenland ice sheet: increased coastal thinning', *Geophysical Research Letters*, 31, doi:10.1029/2004GL021533

Krawczynski, M. J., et al. (2009), 'Constrains on the lake volume required for

hydro-fracture through ice sheets', *Geophysical Research Letters*, 36,

Lampkin, D.J. (2011), 'Supraglacial lake spatial structure in western Greenland during the 2007 ablation season', *Journal of Geophysical Research,*, 116, doi:10.1029/2010JF001725.

Lampkin, D.J. and J. Vanderberg (2011), 'A preliminary investigation of the influence of basal and surface topography on supraglacial lake distribution near Jakobshavn Isbrae', *Hydrological Processes*, 25, 3347-3355

Lane, S.N. and J.H. Chandler (2003) 'Editorial: The generation of high quality topographic data for hydrology and geomorphology: New data sources, new applications and new problems', *Earth Surface Processes and Landforms*,28, 229-230.

Leeson, A.A. et al. (2012), 'Simulating the growth of supraglacial lakes at the western margin of the Greenland ice sheet', *The Cryosphere,* 6, 1077-1086

Lefebre, F. et al. (1991), 'Modelling of large-scale melt parameters with a regional climate model in south Greenland during the 1991 melt season', *Annals of Glaciology*,32, 391-397

Lindsay, J.B. and I.F. Creed (2006), 'Simulating the growth of supraglacial lakes at the western margin of the Greenland ice sheet', *The Cryosphere*, 6, 1077-1086

Luckman, A. and T. Murray (2005), 'Seasonal variation in velocity before retreat of Jakobshavn Isbrae, Greenland', *Geophysical Research Letters*, 32, doi:10.1029/2005GL022519

Luthje, M et al. (2006), 'Modelling the evolution of supraglacial lakes on the West Greenland ice-sheet margin', *Journal of Glaciology*, 52, 608-618

Mair, D. et al (2002), 'Influence of subglacial drainage system evolution on glacier surface motion: Haut Glacier d'Arolla, Switzerland', *Journal of Geophysical Research,* 107, 10.1029/2001JB000514

Manning, R. (1891), 'On the flow of water in open channels and pipes', *Transactions, Institution of Civil Engineers of Ireland*, 20, 161-207

Mayaud, J. (2012), 'Modelling meltwater drainage in the Paakitsoq region, western Greenland, and its response to 21st century climate change', *MPhil Thesis*, University of Cambridge, Cambridge

McMillan, M. et al. (2007), 'Seasonal evolution of supra-glacial lakes on the Greenland Ice Sheet', *Earth and Planetary Science Letters*, 262, 484-492

Mernild, S.H. et al (2010), 'Meltwater flux and runoff modelling the ablation area of Jakobshavn Isbrae, West Greenland', *Journal of Glaciology,* 56, 20-32

Moon, T. et al. (2012), '21st Century Evolution of Greenland Outlet Glacier Velocities', *Science*, 336, 576-578

Mote, T.L. (1998), 'Mid-tropospheric circulation and surface melt on the Greenland ice sheet. Part I: Atmospheric teleconnections', *International Journal of Climatology*,18, 111-129

Motyka, R.J. et al. (2003), 'Submarine melting at the terminus of a temperatet idewater glacier, LeConte Glacier, Alaska, U.S.A', *Annals of Glaciology, 36, 57-65*

Murray et al. (2010), 'Ocean regulation hypothesis for glacier dynamics in southeast Greenland and implications for ice sheet mass changes', *Journal of Geophysical Research*, 115, doi: 10.1029/2009JF001522

Nick, F.M. et al. (2012), 'The response of Petermann Glacier, Greenland, to large calving events and its future stability in the context of atmospheric and oceanic warming', *Journal of Glaciology*, 58, 229-239

Nienow, P.W. (1993), 'Dye tracer investigations of glacier hydrological systems', *PhD Thesis*, University of Cambridge, Cambridge

Nienow, P.W. et al. (1998), 'Seasonal changes in the morphology of the subglacial drainage system, Haut Glacier d'Arolla, Switzerland', *Earth Surface Processes-Landforms*, 23, 825-843

Nienow, P.W and B. Hubbard (2005), 'HSA172 – surface and englacial drainage of glaciers and ice sheets. In: Anderson, M. (Ed.), The Encyclopedia of Hydrological Sciences. John Wiley and Sons, London

Nye, J.F. (1953), 'The flow law of ice from measurements in glacier tunnels, laboratory experiments and the Jungfraufirn borehole experiment' *Prac. R. Sac. London – ser A*, 219, 477-489

Ohmura, A. (2001), 'Physical basis for the temperature-based melt-index method', *Journal of Applied Meteorology,* 40, 753-761

Parizek, B. R. and R. B. Alley (2004), 'Implications of increased Greenland surface melt under global-warming scenarios: ice-sheet simulations', *Quaternary Science Reviews,* 23, 1013-1027

Pfeffer, W. et al, (1991), 'Retention of Greenland runoff by refreezing: implications for projected future sea level change', *Journal of Geophysical Research*, 96(C12), 22, 117

Pimentel, S. and G. E. Flowers (2010), 'A numerical study of hydrologically driven glacier dynamics and subglacial flooding', *Proceedings of the Royal Society*, doi: 10.1098/rspa.2010.0211

Pimentel, S. et al. (2010), 'A hydrologically coupled higher-order flow-band

model of ice dynamics with a Coulomb friction sliding law', *Journal of Geophysical Research*, 115, doi:10.1029/2009JF001621

Pfeffer, W.T. (2007), 'A simple mechanism for irreversible tidewater glacier retreat', *Journal of Geophysical Research*, 112, doi:10.1029/2006JF000590

Radic, V and R. Hock (2011), 'Regionally differentiated contribution of mountain glaciers and ice caps to future sea-level rise', *Nature Geoscience*,4, 91-94

Rignot, E. (2001), 'Tidal motion, ice velocity and melt rate of Petermann Glacier, Greenland, measured from radar interferometry', *Journal of Glaciology*, 42, 476-485

Rignot, E. et al (2011), 'Acceleration of the contribution of the Greenland and Antarctic ice sheet to sea level rise', *Geophysical Research Letters*, 38, doi:10.1029/2011GL046583,

Rignot, E. and P. Kanagaratnam (2006), 'Changes in the velocity structure of the Greenland Ice Sheet', *Science*, 311, 986-990

Rignot, E. and K. Steffen (2008), 'Channelized bottom melting and stability of floating ice shelves', *Geophysical Research Letters*,35, doi:10.1029/2007GL031765

Rippin, D.I. et al. (2003), 'Changes in geometry and subglacial drainage of Midre Lovenbreen, Svalbard, determined from digital elevation models', *Earth Surface Processes – Landforms*, 28, 273-298

Roesner, L.A. et al. (1988), 'Storm Water Management Model User's Manual version 4: EXTRAN addendum. US Environmental Protection Agency, Athens, Geordia, 188pp

Rothlisberger, H. (1972), 'Water in intra- and subglacial channels', *Journal of Glaciology*, 11, 177-203

Rothlisberger, H. and H. Lang (1987), 'Glacial Hydrology in Glacio-fluvial Sediment Transfer', edited by A.M. Gurnell and M.J. Clarke, John Wiley & Sons, New York

Rye, C. J. et al. (2010), 'Modelling the surface mass balance of a high Arctic glacier using the ERA-40 renalaysis', *Journal of Geophysical Research,* 115, doi:10.1029/2009JF001364

Scambos, T.A. and T. Haran (2002), 'An image-enhanced DEM of the Greenland ice sheet', *Annals of Glaciology*, 34, 291-298

Schoof, C. (2007), 'Ice sheet grounding line dynamics: steady states, stability and hysteresis', *Journal of Geophysical Research*, *112,* doi:10.1029/2006JF000664

Schoof, C. (2010), 'Ice-sheet acceleration driven by melt supply variability', *Nature*, 468, 803-806

Seaberg, S.Z. et al. (1988), 'Character of the englacial and subglacial drainage system in the lower part of the ablation area of Storglaciaren, Sweden, as revealed by dye-trace studies', *Journal of Glaciology*, 34, 217-227

Selmes, N. et al. (2011), 'Fast draining lakes on the Greenland Ice sheet', *Geophysical Research Letters*, 38, doi:10.1029/2011GL047872,
Sharp, M. (2005), 'Subglacial Drainage', In Anderson, M.G. (Ed.), *Encyclopedia of Hydrological Sciences'*

Sharp, M.J. et al. (1993), 'Geometry, bed, topography and drainage system structure of the Haut Glacier d'Arolla, Switzerland', *Earth Surface Processes – landforms*, 18, 557-571

Shepherd, A. et al (2009), 'Greenland ice sheet motion coupled with daily melting in late summer'. *Geophysical Research Letters,* 36, doi: 10.1209/2008GL035758

Shreve, R.L (1972), 'Movement of water in glaciers', *Journal of Glaciology*, 11, 205-214

Sing, P. and N. Kumar (1996), 'Determination of snowmelt factor in the Himalayan region', *Hydrological Science Journal*, 41, 301-310

Simmons, A.J. and J.K. Gibson (2000), 'The ERA-40 project plan, project report' *European Centre for Medium-Range Weather Forecasting*, Reading, U.K.

Skidmore, M and M. Sharp (1999), 'Drainage system behavior of a high-Arctic polythermal glacier', *Annals of Glaciology*,28, 209-215

Smith, B.E. (2005), 'Cbaracterization of the small scale topography of Antarctic and Greenland', (PhD. Thesis, University of Washington) *in Lampkin and Vanderberg (2011)*

Sneed, W.A. and G.S. Hamilton (2007), 'Evolution of melt pond volume on the surface of the Greenland ice sheet', *Geophysical Research Letters*, 34, doi:10.1029/2006GL028697

Sneed, W.A. and G.S. Hamilton (2011), 'Validation of a method for determining the depth of glacial melt ponds using satellite imagery', *Annals of Glaciology*, 52, 15-22

Sole, A.J. et al. (2011), ' Seasonal speedup of a Greenland marine-terminating outlet glacier forced by surface melt-induced changes in subglacial hydrology', *Journal of Geophysical Research*, 116, doi:10.1029/2010JF001948

Spring, U. and K. Hutter (1981), 'Numerical studies of Jokullhlaups', *Cold Region Science & Technology*, 4, 227-244
Steffen, K et al. (1996), 'Greenland Climate Network: GC-Net', *in Colbeck, S.C. Ed. CRREL 96-27 Special Report on Glaciers Ice Sheets and volcanoes*, *trib to M Meier, pp, 98-103*

Steffen, K. and J. Box (2001), 'Surface climatology of the Greenland ice sheet: Greenland Climate Network 1995-1999', *Journal of Geophysical Research*, 106, 33951-33964

Sundal, A.V. et al (2009), 'Evolution of supra-glacial lakes across the Greenland Ice Sheet', *Remote Sensing of Environment*, 113, 2164-2171

Sundal, A. V. et al (2011), 'Melt-induced speed-up of Greenland ice sheet offset by efficient subglacial drainage', *Nature*, 469, 521-524

Tedesco, M. et al. (2012), 'Measurement and modelling of ablation of the bottom of supraglacial lakes in western Greenland', *Geophysical Research Letters*, 39, doi:10.1029/2011GL049882, 2

Thomsen, H.H. et al. (1988), 'Glacier-hydrological condition on the inland Ice north-east of Jakobshavn/Illulisat, west Greenland', *Rep. 13*, Groenl. Geol. Underst., Copenhagen

Thomas, R.B. et al. (2003), 'Investigation of surface melting and dynamic thinning on Jakobshavn Isbrae, Greenland', *Journal of Glaciology,* 49, 231-239

Thomas, R.B. (2004), 'Force-perturbation analysis of recent thinning and acceleration of Jakobshavn Isbrae, Greenland', *Journal of Glaciology*, 50, 57-66

Thomsen, H.H. and O.B. Olesen (1990), 'Continued glaciological investigations with respect to hydropower and ice-climate relationships, at Paakitsoq, Jakobshavn, West Greenland. *Rapport Gronlands Geologiske Undersogelse*,148, 83-86

Van den Broeke, M. et al (2009), 'Partitioning recent Greenland mass loss', *Science*, 326, 984-986

van der Veen, C. J. (2007), 'Fracture propagation as means of rapidly transferring surface meltwater to the base of glaciers', *Geophysical Research Letters*, 34, L01501, doi:10.1029/2006GL028385

Van der Veen, C.J. et al. (2011), 'Controls on the recent speed-up of Jakobshavn Isbrae, West Greenland', *Journal of Glaciology*, 57, 770-782

van Pelt, W. et al. (2012), 'Simulating melt, runoff and refreezing on Nordenskioldbreen, Svalbard, using a coupled snow and energy balance model', *The Cryosphere Discussions',* 6, 211-266

Velicogna, I. (2009), 'Increasing rates of ice mass loss from the Greenland and Antarctic ice sheets revealed by GRACE', *Geophysical Research Letters,*36, doi:10.1029/2009GL040222

Velicogna, I. and J. Wahr (2006), 'Acceleration of Greenland ice mass loss in spring 2004', *Nature,* 443, 329-331

Vieli, A. et al (2000), 'Tidewater glaciers: frontal flow acceleration and basal sliding', *Annals of Glaciology*, 31, 217-221

Vieli, A. and F. Nick (2011), 'Understand and Modelling Rapid Dynamic Changes of Tidewater Outlet Glaciers: Issues and Implications', *Survey Geophysics*, 32, 437-458

Walder, J.S. and A.C. Fowler (1994), 'Channelized subglacial drainage over a deformable bed', *Journal of Glaciology*, 40, 3-15

Walder, J.S. and B. Hallet (1979), 'Geometry of former subglacial water channels and cavities', *Journal of Glaciology*, 23, 335-346

Weertman, J. (1973), 'Can a water-filled crevasse reach the bottom surface of a glacier?', *IAHS Publishing*, 95, 185-188

Willis, I et al. (2009), Subglacial drainage system structure and morphology of Brewster Glacier, New Zealand', *Hydrological Processes*,23, 384-396

Wright, A.P. et al. (2007), 'Modelling the refreezing of meltwater as superimposed ice on a high Arctic glacier: A comparison of approaches', *Journal of Geophysical Research,* 112, doi:10.1029/2007JF000818

Zwally, H. J et al (2002), 'Surface melt-induced acceleration of Greenland ice-sheet flow', *Science*, 297, 218-222

Appendix A: Example SWMM Input File

Input file for the eastern channel (k=0.95) under conditions of background melt. Only a sample of input is provided, showing initial background melt and initial measured drainage.

```
SW 1 0 0
MM 1 11
*
*
*0.3m initial diam for conduits under 500m ice
*
$EXTRAN
A1 'Test data' !!
A1 'IB Channel 2'
*
*  RUN CONTROL
B0 1 0                                          !DO NOT ADJUST
*
B1 5760000 1.0 0.0 0 5760000 3600 0                     ! currently running for 360000 timesteps (=2500 hrs)
*
B2 1 0 1.0 30 0.05                              !DO NOT ADJUST
* Last number is number of input hydrograph junctions.
B3 11 9 11 9 4
*
B4 1 42 99 121 48 62 63 123 67 69 101                   !Printed Heads
*
B5 301 341 398 421 348 362 423 367 401          !Printed Flows
*
B6 1 42 99 121 48 62 63 123 67 69 101                   !Plotted Heads
*
B7 301 341 398 421 348 362 423 367 401          !Plotted Flows
*
*************************************************************
*  CONDUIT DATA
*************************************************************
*C1 block prepared for full model.
*       num     up      dn      inq     tp      area    deep    wide    len     inv     inv     rough   n/r     n/rr
*       System 1
C1      301     1       2       0       1       0       2       0       1061    0       0       0.05    0       0
C1      302     2       3       0       1       0       2       0       1118    0       0       0.05    0       0
C1      303     3       4       0       1       0       2       0       1000    0       0       0.05    0       0
C1      304     4       5       0       1       0       2       0       791     0       0       0.05    0       0
C1      305     5       6       0       1       0       2       0       1031    0       0       0.05    0       0
C1      306     6       7       0       1       0       2       0       1250    0       0       0.05    0       0
C1      307     7       8       0       1       0       2       0       1031    0       0       0.05    0       0
C1      308     8       9       0       1       0       2       0       791     0       0       0.05    0       0
C1      309     9       10      0       1       0       2       0       901     0       0       0.05    0       0
C1      310     10      11      0       1       0       2       0       901     0       0       0.05    0       0
C1      311     11      12      0       1       0       2       0       1061    0       0       0.05    0       0
C1      312     12      13      0       1       0       2       0       1031    0       0       0.05    0       0
C1      313     13      14      0       1       0       2       0       901     0       0       0.05    0       0
C1      314     14      15      0       1       0       2       0       791     0       0       0.05    0       0
C1      315     15      16      0       1       0       2       0       901     0       0       0.05    0       0
C1      316     16      17      0       1       0       2       0       1000    0       0       0.05    0       0
C1      317     17      18      0       1       0       2       0       791     0       0       0.05    0       0
C1      318     18      19      0       1       0       2       0       1061    0       0       0.05    0       0
C1      319     19      20      0       1       0       2       0       1000    0       0       0.05    0       0
C1      320     20      21      0       1       0       2       0       791     0       0       0.05    0       0
C1      321     21      22      0       1       0       2       0       1000    0       0       0.05    0       0
C1      322     22      23      0       1       0       2       0       750     0       0       0.05    0       0
C1      323     23      24      0       1       0       2       0       901     0       0       0.05    0       0
C1      324     24      25      0       1       0       2       0       1250    0       0       0.05    0       0
C1      326     26      27      0       1       0       2       0       1061    0       0       0.05    0       0
C1      327     27      28      0       1       0       2       0       1061    0       0       0.05    0       0
C1      328     28      29      0       1       0       2       0       1061    0       0       0.05    0       0
C1      329     29      30      0       1       0       2       0       1000    0       0       0.05    0       0
C1      330     30      31      0       1       0       2       0       791     0       0       0.05    0       0
C1      331     31      32      0       1       0       2       0       901     0       0       0.05    0       0
C1      332     32      33      0       1       0       2       0       1118    0       0       0.05    0       0
C1      333     33      34      0       1       0       2       0       901     0       0       0.05    0       0
C1      334     34      35      0       1       0       2       0       901     0       0       0.05    0       0
C1      335     35      36      0       1       0       2       0       1000    0       0       0.05    0       0
C1      336     36      37      0       1       0       2       0       901     0       0       0.05    0       0
C1      337     37      38      0       1       0       2       0       791     0       0       0.05    0       0
C1      338     38      39      0       1       0       2       0       1000    0       0       0.05    0       0
C1      339     39      40      0       1       0       2       0       791     0       0       0.05    0       0
C1      340     40      41      0       1       0       2       0       750     0       0       0.05    0       0
C1      341     41      42      0       1       0       2       0       901     0       0       0.05    0       0
C1      342     42      43      0       1       0       2       0       901     0       0       0.05    0       0
C1      343     43      44      0       1       0       2       0       1061    0       0       0.05    0       0
C1      344     44      45      0       1       0       2       0       1061    0       0       0.05    0       0
C1      345     45      46      0       1       0       2       0       791     0       0       0.05    0       0
C1      346     46      47      0       1       0       2       0       901     0       0       0.05    0       0
C1      347     47      48      0       1       0       2       0       791     0       0       0.05    0       0
C1      348     48      49      0       1       0       2       0       1000    0       0       0.05    0       0
C1      349     49      50      0       1       0       2       0       791     0       0       0.05    0       0
C1      350     50      51      0       1       0       2       0       1061    0       0       0.05    0       0
C1      351     51      52      0       1       0       2       0       791     0       0       0.05    0       0
C1      352     52      53      0       1       0       2       0       1000    0       0       0.05    0       0
C1      353     53      54      0       1       0       2       0       791     0       0       0.05    0       0
C1      354     54      55      0       1       0       2       0       1000    0       0       0.05    0       0
C1      355     55      56      0       1       0       2       0       750     0       0       0.05    0       0
C1      356     56      57      0       1       0       2       0       791     0       0       0.05    0       0
C1      357     57      58      0       1       0       2       0       1061    0       0       0.05    0       0
C1      358     58      59      0       1       0       2       0       1061    0       0       0.05    0       0
C1      359     59      60      0       1       0       2       0       707     0       0       0.05    0       0
C1      360     60      61      0       1       0       2       0       791     0       0       0.05    0       0
C1      361     61      62      0       1       0       2       0       1000    0       0       0.05    0       0
C1      362     62      63      0       1       0       2       0       791     0       0       0.05    0       0
C1      363     63      64      0       1       0       2       0       1414    0       0       0.05    0       0
C1      364     64      65      0       1       0       2       0       791     0       0       0.05    0       0
C1      365     65      66      0       1       0       2       0       901     0       0       0.05    0       0
C1      366     66      67      0       1       0       2       0       1000    0       0       0.05    0       0
C1      367     67      68      0       1       0       2       0       1000    0       0       0.05    0       0
C1      368     68      69      0       1       0       2       0       791     0       0       0.05    0       0
C1      369     69      70      0       1       0       2       0       750     0       0       0.05    0       0
C1      398     41      99      0       1       0       2       0       791     0       0       0.05    0       0
C1      399     99      100     0       1       0       2       0       901     0       0       0.05    0       0
C1      400     100     101     0       1       0       2       0       510     0       0       0.05    0       0
C1      401     101     102     0       1       0       2       0       791     0       0       0.05    0       0
C1      402     102     103     0       1       0       2       0       1000    0       0       0.05    0       0
C1      403     103     104     0       1       0       2       0       791     0       0       0.05    0       0
C1      404     104     105     0       1       0       2       0       791     0       0       0.05    0       0
C1      405     105     106     0       1       0       2       0       901     0       0       0.05    0       0
C1      406     106     107     0       1       0       2       0       791     0       0       0.05    0       0
C1      407     107     108     0       1       0       2       0       901     0       0       0.05    0       0
C1      408     108     109     0       1       0       2       0       1000    0       0       0.05    0       0
C1      409     109     110     0       1       0       2       0       791     0       0       0.05    0       0
```

```
C1      416     116     117     0       1       0       2       0       1061    0       0       0.05    0       0
C1      417     117     118     0       1       0       2       0       1061    0       0       0.05    0       0
C1      418     118     119     0       1       0       2       0       1061    0       0       0.05    0       0
C1      419     119     120     0       1       0       2       0       750     0       0       0.05    0       0
C1      420     120     62      0       1       0       2       0       750     0       0       0.05    0       0
C1      421     121     122     0       1       0       2       0       791     0       0       0.05    0       0
C1      422     122     48      0       1       0       2       0       901     0       0       0.05    0       0
C1      423     62      123     0       1       0       2       0       791     0       0       0.05    0       0
C1      424     123     124     0       1       0       2       0       1031    0       0       0.05    0       0
C1      425     124     125     0       1       0       2       0       1000    0       0       0.05    0       0
C1      426     125     126     0       1       0       2       0       1061    0       0       0.05    0       0
C1      427     126     67      0       1       0       2       0       901     0       0       0.05    0       0
C1      428     67      127     0       1       0       2       0       1061    0       0       0.05    0       0

*
*****************************************************************
*  JUNCTION DATA
*****************************************************************
* Block D1 prepared for full model.
*  Moulins
*      num      surf    base    Qin     initD
* System 1
D1      1       1739    683     0       0
D1      2       1734    682     0       0
D1      3       1735    680     0       0
D1      4       1729    679     0       0
D1      5       1721    676     0       0
D1      6       1708    675     0       0
D1      7       1692    673     0       0
D1      8       1686    672     0       0
D1      9       1687    670     0       0
D1      10      1687    669     0       0
D1      11      1683    667     0       0
D1      12      1674    666     0       0
D1      13      1673    664     0       0
D1      14      1674    663     0       0
D1      15      1670    661     0       0
D1      16      1660    659     0       0
D1      17      1635    657     0       0
D1      18      1617    657     0       0
D1      19      1604    636     0       0
D1      20      1597    629     0       0
D1      21      1584    624     0       0
D1      22      1566    622     0       0
D1      23      1554    619     0       0
D1      24      1536    616     0       0
D1      25      1533    612     0       0
D1      26      1532    609     0       0
D1      27      1524    606     0       0
D1      28      1501    602     0       0
D1      29      1479    599     0       0
D1      30      1468    596     0       0
D1      31      1461    593     0       0
D1      32      1441    590     0       0
D1      33      1420    587     0       0
D1      34      1418    582     0       0
D1      35      1414    569     0       0
```

```
D1      36      1399    552     0       0
D1      37      1370    541     0       0
D1      38      1356    529     0       0
D1      39      1336    510     0       0
D1      40      1323    451     0       0
D1      41      1309    391     0       0
D1      42      1303    377     0       0
D1      43      1295    362     0       0
D1      44      1281    346     0       0
D1      45      1228    331     0       0
D1      46      1197    315     0       0
D1      47      1177    314     0       0
D1      48      1174    314     0       0
D1      49      1179    313     0       0
D1      50      1181    312     0       0
D1      51      1175    311     0       0
D1      52      1148    311     0       0
D1      53      1123    310     0       0
D1      54      1113    309     0       0
D1      55      1111    309     0       0
D1      56      1108    308     0       0
D1      57      1101    305     0       0
D1      58      1084    302     0       0
D1      59      1053    300     0       0
D1      60      1026    300     0       0
D1      61      1003    299     0       0
D1      62      995     299     0       0
D1      63      995     298     0       0
D1      64      991     298     0       0
D1      65      974     297     0       0
D1      66      953     297     0       0
D1      67      934     296     0       0
D1      68      929     296     0       0
D1      69      925     295     0       0
D1      70      921     295     0       0
D1      99      1304    383     0       0
D1      100     1295    370     0       0
D1      101     1293    367     0       0
D1      102     1295    354     0       0
D1      103     1294    347     0       0
D1      104     1282    346     0       0
D1      105     1254    346     0       0
D1      106     1233    345     0       0
D1      107     1222    345     0       0
D1      108     1212    344     0       0
D1      109     1196    343     0       0
D1      110     1186    341     0       0
D1      111     1167    340     0       0
D1      112     1153    339     0       0
D1      113     1148    338     0       0
D1      114     1131    336     0       0
D1      115     1097    335     0       0
D1      116     1070    334     0       0
D1      117     1050    311     0       0
D1      118     1024    308     0       0
D1      119     1001    305     0       0
D1      120     996     302     0       0
D1      121     1172    426     0       0
D1      122     1181    372     0       0
D1      123     995     298.5   0       0
D1      124     978     298     0       0
D1      125     970     297.5   0       0
D1      126     952     297     0       0
D1      127     928     274     0       0
*
************************************************************************
*  STORAGE JUNCTIONS
************************************************************************
*Block E1 prepared for full model.
*   num surf    Area        NumSt
* System 1
*
E1      1       1739    2       0
E1      2       1734    0.1     0
E1      3       1735    0.1     0
E1      4       1729    0.1     0
E1      5       1721    0.1     0
E1      6       1708    0.1     0
E1      7       1692    0.1     0
E1      8       1686    0.1     0
E1      9       1687    0.1     0
E1      10      1687    0.1     0
E1      11      1683    0.1     0
E1      12      1674    0.1     0
E1      13      1673    0.1     0
E1      14      1674    0.1     0
E1      15      1670    0.1     0
E1      16      1660    0.1     0
E1      17      1635    0.1     0
E1      18      1617    0.1     0
E1      19      1604    0.1     0
E1      20      1597    0.1     0
E1      21      1584    0.1     0
E1      22      1566    0.1     0
E1      23      1554    0.1     0
E1      24      1536    0.1     0
E1      25      1533    0.1     0
E1      26      1532    0.1     0
E1      27      1524    0.1     0
E1      28      1501    0.1     0
E1      29      1479    0.1     0
E1      30      1468    0.1     0
E1      31      1461    0.1     0
E1      32      1441    0.1     0
E1      33      1420    0.1     0
E1      34      1418    0.1     0
E1      35      1414    0.1     0
E1      36      1399    0.1     0
E1      37      1378    0.1     0
E1      38      1356    0.1     0
E1      39      1336    0.1     0
E1      40      1323    0.1     0
E1      41      1309    0.1     0
E1      42      1303    0.1     0
```

```
E1      43      1295    0.1     0
E1      44      1281    0.1     0
E1      45      1228    0.1     0
E1      46      1197    0.1     0
E1      47      1177    0.1     0
E1      48      1174    2       0
E1      49      1179    0.1     0
E1      50      1181    0.1     0
E1      51      1175    0.1     0
E1      52      1148    0.1     0
E1      53      1123    0.1     0
E1      54      1113    0.1     0
E1      55      1111    0.1     0
E1      56      1108    0.1     0
E1      57      1101    0.1     0
E1      58      1084    0.1     0
E1      59      1053    0.1     0
E1      60      1026    0.1     0
E1      61      1003    0.1     0
E1      62      995     0.1     0
E1      63      995     0.1     0
E1      64      991     0.1     0
E1      65      974     0.1     0
E1      66      953     0.1     0
E1      67      934     0.1     0
E1      68      929     0.1     0
E1      69      925     0.1     0
E1      70      921     0.1     0
E1      99      1304    0.1     0
E1      100     1295    0.1     0
E1      101     1293    2       0
E1      102     1295    0.1     0
E1      103     1294    0.1     0
E1      104     1282    0.1     0
E1      105     1254    0.1     0
E1      106     1233    0.1     0
E1      107     1222    0.1     0
E1      108     1212    0.1     0
E1      109     1196    0.1     0
E1      110     1186    0.1     0
E1      111     1167    0.1     0
E1      112     1153    0.1     0
E1      113     1148    0.1     0
E1      114     1131    0.1     0
E1      115     1097    0.1     0
E1      116     1078    0.1     0
E1      117     1050    0.1     0
E1      118     1024    0.1     0
E1      119     1001    0.1     0
E1      120     996     0.1     0
E1      121     1172    2       0
E1      122     1181    0.1     0
E1      123     995     0.1     0
E1      124     978     0.1     0
E1      125     970     0.1     0
E1      126     952     0.1     0
E1      127     928     0.1     0
.
*****************************************************************
*  OUTLET DATA
* Blocks I1 and J1 prepared for full model.
*System 1
I1 70 1
I1 127 1
*
J1 1
*****************************************************************
*
* Block K complete for full model.
* Number of input locations (i.e. moulins)
K1  4
*
* Input location numbers
K2  121 48 101 1
*
* Inputs by time period                                         !each input moulin has it's own column of inputs
K3      0       2       2       2       2
K3      24      2       2       2       2
K3      48      2       2       2       2
K3      49      2       2       2       2
K3      50..    2       2       2       2
K3      1601    2       21.70672535     2       2
K3      1602    2       67.69386226     20.04040122     2
K3      1603    2       55.03779201     70.3445968      2
K3      1604    2       39.32466958     59.00140666     2
K3      1605    2       23.72658719     44.34997246     2
K3      1606    2       16.67032859     29.70269316     2
K3      1607    16.12612957     17.35503514     22.7966798      2
K3      1608    44.96795323     17.86648714     23.08558005     2
K3      1609    35.51512968     18.29283034     23.13728825     2
K3      1610    23.69762103     18.70166405     23.06104939     2
```